



A vorticity-based mixed formulation for the unsteady Brinkman–Forchheimer equations[☆]

Verónica Anaya^{a,b}, Ruben Caraballo^a, Sergio Caucao^{c,*}, Luis F. Gatica^{c,b},
Ricardo Ruiz-Baier^{d,e,f}, Ivan Yotov^g

^a GIMNAP, Departamento de Matemática, Universidad del Bío-Bío, Concepción, Chile

^b CI²MA, Universidad de Concepción, Casilla 160-C, Concepción, Chile

^c Departamento de Matemática y Física Aplicadas, Universidad Católica de la Santísima Concepción, Casilla 297, Concepción, Chile

^d School of Mathematical Sciences, Monash University, 9 Rainforest Walk, Melbourne VIC 3800, Australia

^e World-Class Research Center “Digital biodesign and personalized healthcare”, Sechenov First Moscow State Medical University, Moscow, Russia

^f Universidad Adventista de Chile, Casilla 7-D, Chillán, Chile

^g Department of Mathematics, University of Pittsburgh, Pittsburgh, PA 15260, USA

Received 17 August 2022; received in revised form 24 November 2022; accepted 24 November 2022

Available online xxx

Abstract

We propose and analyze an augmented mixed formulation for the time-dependent Brinkman–Forchheimer equations written in terms of vorticity, velocity and pressure. The weak formulation is based on the introduction of suitable least squares terms arising from the incompressibility condition and the constitutive equation relating the vorticity and velocity. We establish existence and uniqueness of a solution to the weak formulation, and derive the corresponding stability bounds, employing classical results on nonlinear monotone operators. We then propose a semidiscrete continuous-in-time approximation based on stable Stokes elements for the velocity and pressure, and continuous or discontinuous piecewise polynomial spaces for the vorticity. In addition, by means of the backward Euler time discretization, we introduce a fully discrete finite element scheme. We prove well-posedness and derive the stability bounds for both schemes, and establish the corresponding error estimates. We provide several numerical results verifying the theoretical rates of convergence and illustrating the performance and flexibility of the method for a range of domain configurations and model parameters.

© 2022 Elsevier B.V. All rights reserved.

MSC: 65N30; 65N12; 65N15; 35Q79; 80A20; 76R05; 76D07

Keywords: Unsteady Brinkman–Forchheimer equations; Mixed finite element methods; Velocity–vorticity–pressure formulation

[☆] This work has been partially supported by DICREA-UBB 2120173 GI/C; by ANID-Chile through the projects CENTRO DE MODELAMIENTO MATEMÁTICO (FB210005), ANILLO OF COMPUTATIONAL MATHEMATICS FOR DESALINATION PROCESSES (ACT210087), Fondecyt projects 11220393, 1211265 and 1181748, and Becas/Doctorado Nacional 21210945; by the Ministry of Science and Higher Education of the Russian Federation within the framework of state support for the creation and development of World-Class Research Centres DIGITAL BIODESIGN AND PERSONALIZED HEALTHCARE No. 075-15-2022-304; by ARC, Australia grant DP220103160; and by NSF grant DMS 2111129.

* Corresponding author.

E-mail addresses: vanaya@ubiobio.cl (V. Anaya), ruben.caraballo1801@alumnos.ubiobio.cl (R. Caraballo), scauciao@ucsc.cl (S. Caucao), lgatica@ucsc.cl (L.F. Gatica), ricardo.ruizbaier@monash.edu (R. Ruiz-Baier), yotov@math.pitt.edu (I. Yotov).

1. Introduction

Fluid flows through porous media with high Reynolds numbers occur in many industrial applications, such as environmental, chemical, and petroleum engineering. For instance, in groundwater remediation and oil and gas extraction, the flow may be fast near injection or production wells or if the aquifer/reservoir is highly porous. Many of the investigations in porous media have focused on the use of Darcy's law. Nevertheless, this fundamental equation may be inaccurate for modeling fluid flow through porous media with high Reynolds numbers or through media with high porosity. To overcome this deficiency, it is possible to consider the Brinkman–Forchheimer equations (see for instance [1,2]), where terms are added to Darcy's law in order to take into account high velocity flow and high porosity.

Several numerical methods for the Brinkman–Forchheimer problem have been developed previously. In [3] the authors propose and study a perturbed compressible system that approximates the Brinkman–Forchheimer equations. A numerical method for the perturbed system based on a semi-implicit Euler scheme for time discretization and the lowest-order Raviart–Thomas element for spatial discretization is developed. In [4] the authors propose and analyze a pressure-stabilization method, where the incompressibility constraint is perturbed as $\text{div}(\mathbf{u}) - \epsilon \Delta p = 0$. Then, a first-order time discretization and a finite element method based on piecewise continuous polynomials for the spatial discretization are considered. Second order error estimates in time are also obtained. In [5] the coupling of the unsteady Brinkman–Forchheimer model with a variable porosity Darcy model is developed and applied for simulating wormhole propagation. A semi-analytic time stepping scheme is employed to handle the variable porosity. An error analysis for the spatial and temporal discretization errors is performed. In [6] a mixed formulation based on the pseudostress tensor and the velocity field is presented. By employing classical results on nonlinear monotone operators and a suitable regularization technique in Banach spaces, existence and uniqueness are proved. A finite element method for space discretization based on the Raviart–Thomas spaces for the pseudostress tensor and discontinuous piecewise polynomial elements for the velocity, combined with a backward Euler time discretization, is proposed and sub-optimal error estimates are derived. More recently, a three-field Banach spaces-based mixed variational formulation is analyzed in [7], where the velocity, velocity gradient, and pseudostress tensor are the main unknowns of the system. Existence and uniqueness of a solution to the weak formulation, as well as stability bounds are derived by employing classical results on nonlinear monotone operators. A semidiscrete continuous-in-time mixed finite element approximation and a fully discrete scheme are introduced and sub-optimal rates of convergence improving the ones obtained in [6] are established. A staggered DG method for a velocity–velocity gradient–pressure formulation of the unsteady Brinkman–Forchheimer problem is developed in [8]. Well-posedness and error analysis are presented for the semi-discrete and fully discrete schemes. The method is robust with respect to the Brinkman parameter. In [9] the steady state Darcy–Brinkman–Forchheimer problem with mixed boundary condition is studied. The authors prove existence of a unique solution under small data conditions. Then, the convergence of a Taylor–Hood finite element approximation using a finite element interpolation of the porosity is proved under similar smallness assumptions. In addition, optimal error estimates are obtained. In turn, in [10], the steady Brinkman–Forchheimer model is coupled with a double-diffusion equation. The velocity gradient, the pseudostress tensor, the temperature and concentration gradients, and a pair of flux vectors are introduced as additional unknowns. Well-posedness for the resulting fully mixed continuous and discrete problems is established in a Banach space setting, and error analysis is carried out.

On the other hand, there is another approach that is increasingly studied to solve fluid flow problems, which incorporates the vorticity field as a new unknown in the system and results in different weak formulations, see [11–15]. This new strategy exhibits the advantage that the vorticity (which is a sought quantity of practical interest in industrial applications) can be approximated directly with the same accuracy as the velocity, see [13]. Vorticity plays a fundamental role in fluid flow problems as well as in their mathematical analysis; in many cases it is advantageous to describe the flow dynamics in terms of the evolution of the vorticity. In particular, for a vorticity–velocity–pressure formulation, since no postprocessing of the velocity is needed to compute the additional field, boundary conditions for external flows can be treated in a natural way, and non-inertial effects can be readily included by simply modifying initial and boundary data [14]. Moreover, the formulation allows for smooth vorticity approximations using continuous finite element spaces, in contrast to the discontinuous approximation obtained by postprocessing the velocity.

The purpose of the present work is to develop and analyze a new vorticity-based mixed formulation of the unsteady Brinkman–Forchheimer problem and study a suitable conforming numerical discretization. To that end,

unlike previous Brinkman–Forchheimer works and motivated by [11,12], we introduce the vorticity as an additional unknown besides the fluid velocity and pressure. In the addition to the advantage of a direct, accurate, and smooth approximation of the vorticity, our approach improves the suboptimal theoretical rates of convergence obtained in [6,7] for the pseudostress–velocity and velocity–velocity gradient–pseudostress formulations, respectively. In particular, optimal rates of convergence are obtained without any quasi-uniformity assumption on the mesh.

We remark that our formulation is based on the natural \mathbf{H}^1 – L^2 spaces for the velocity–pressure pair, thus allowing for classical stable Stokes elements to be used. Since the three-field formulation does not provide control of the velocity in the \mathbf{H}^1 -norm, it is augmented with two terms to control the curl and the divergence of the velocity. It is illustrated in Example 1 in the numerical section that these terms may improve the robustness in the convergence of the velocity and vorticity for small values of the viscosity, as well as its divergence-free property.

We establish existence and uniqueness of a solution to the continuous weak formulation by employing techniques from [10,16], combined with the classical monotone operator theory in a Hilbert space setting. Stability for the weak solution is established by means of an energy estimate. We further develop semidiscrete continuous-in-time and fully discrete finite element approximations. The velocity and pressure are approximated by stable Stokes elements, whereas, continuous or discontinuous piecewise polynomial spaces are employed to approximate the vorticity. We make use of the backward Euler method for the discretization in time. Adapting the tools employed for the analysis of the continuous problem, we prove well-posedness of the discrete schemes and derive the corresponding stability estimates. We further perform error analysis for the semidiscrete and fully discrete schemes, establishing optimal rates of convergence in space and time.

Outline. We have organized the contents of this paper as follows. In the remainder of this section we introduce some standard notation and needed functional spaces, and describe the model problem of interest. In Section 2 we develop the velocity–vorticity–pressure variational formulation. In Section 3 we show that it is well posed using classical results on nonlinear monotone operators. Next, in Section 4 we present the semidiscrete continuous-in-time approximation, provide particular families of stable finite elements, and obtain error estimates for the proposed methods. Section 5 is devoted to the fully discrete approximation. Finally, the performance of the method is studied in Section 6 with several numerical examples in 2D and 3D, verifying the aforementioned rates of convergence, as well as illustrating its flexibility to handle spatially varying parameters in complex geometries.

Preliminary notations. Let $\Omega \subset \mathbb{R}^d$, $d \in \{2, 3\}$, denote a domain with Lipschitz boundary Γ . For $s \geq 0$ and $p \in [1, +\infty]$, we denote by $L^p(\Omega)$ and $W^{s,p}(\Omega)$ the usual Lebesgue and Sobolev spaces endowed with the norms $\|\cdot\|_{L^p(\Omega)}$ and $\|\cdot\|_{W^{s,p}(\Omega)}$, respectively. Note that $W^{0,p}(\Omega) = L^p(\Omega)$. If $p = 2$, we write $H^s(\Omega)$ in place of $W^{s,2}(\Omega)$, and denote the corresponding norm by $\|\cdot\|_{H^s(\Omega)}$. By \mathbf{H} and \mathbb{H} we will denote the corresponding vectorial and tensorial counterparts of a generic scalar functional space H . The $L^2(\Omega)$ inner product for scalar, vector, or tensor valued functions is denoted by $(\cdot, \cdot)_\Omega$. The $L^2(\Gamma)$ inner product or duality pairing is denoted by $\langle \cdot, \cdot \rangle_\Gamma$. Moreover, given a separable Banach space V endowed with the norm $\|\cdot\|_V$, we introduce the Bochner spaces $L^p(0, T; V)$, $L^\infty(0, T; V)$, $W^{1,1}(0, T; V)$, and $W^{1,\infty}(0, T; V)$, endowed with the norms

$$\begin{aligned} \|f\|_{L^p(0,T;V)}^p &:= \int_0^T \|f(t)\|_V^p dt, & \|f\|_{L^\infty(0,T;V)} &:= \operatorname{ess\,sup}_{t \in [0,T]} \|f(t)\|_V, \\ \|f\|_{W^{1,1}(0,T;V)} &:= \int_0^T (\|f(t)\|_V + \|\partial_t f(t)\|_V) dt, & \|f\|_{W^{1,\infty}(0,T;V)} &:= \operatorname{ess\,sup}_{t \in [0,T]} \{ \|f(t)\|_V, \|\partial_t f(t)\|_V \}. \end{aligned}$$

In turn, for any vector field $\mathbf{v} := (v_i)_{i=1,d}$, we set the gradient and divergence operators, as

$$\nabla \mathbf{v} := \left(\frac{\partial v_i}{\partial x_j} \right)_{i,j=1,d} \quad \text{and} \quad \operatorname{div}(\mathbf{v}) := \sum_{j=1}^d \frac{\partial v_j}{\partial x_j}.$$

In addition, in the sequel we will make use of the well-known Hölder inequality given by

$$\int_\Omega |f g| \leq \|f\|_{L^p(\Omega)} \|g\|_{L^q(\Omega)} \quad \forall f \in L^p(\Omega), \forall g \in L^q(\Omega), \quad \text{with} \quad \frac{1}{p} + \frac{1}{q} = 1,$$

and the Young inequality, for $a, b \geq 0$, $1/p + 1/q = 1$, and $\delta > 0$,

$$a b \leq \frac{\delta^{p/2}}{p} a^p + \frac{1}{q \delta^{q/2}} b^q. \tag{1.1}$$

Finally, we recall that $H^1(\Omega)$ is continuously embedded into $L^p(\Omega)$ for $p \geq 1$ if $d = 2$ or $p \in [1, 6]$ if $d = 3$. More precisely, we have the following inequality

$$\|w\|_{L^p(\Omega)} \leq \|i_p\| \|w\|_{H^1(\Omega)} \quad \forall w \in H^1(\Omega), \tag{1.2}$$

with $\|i_p\| > 0$ depending only on $|\Omega|$ and p (see [17, Theorem 1.3.4]).

The model problem. Our model of interest is given by the unsteady Brinkman–Forchheimer equations (see for instance [1,3,6,7,18]). More precisely, given the body force term \mathbf{f} and a suitable initial data \mathbf{u}_0 , the aforementioned system of equations is given by

$$\begin{aligned} \frac{\partial \mathbf{u}}{\partial t} - \nu \Delta \mathbf{u} + \alpha \mathbf{u} + F |\mathbf{u}|^{p-2} \mathbf{u} + \nabla p &= \mathbf{f}, \quad \text{div}(\mathbf{u}) = 0 \quad \text{in } \Omega \times (0, T], \\ \mathbf{u} &= \mathbf{0} \quad \text{on } \Gamma \times (0, T], \quad \mathbf{u}(0) = \mathbf{u}_0 \quad \text{in } \Omega, \quad (p, 1)_\Omega = 0 \quad \text{in } (0, T], \end{aligned} \tag{1.3}$$

where the unknowns are the velocity field \mathbf{u} and the scalar pressure p . In addition, the constant $\nu > 0$ is the Brinkman coefficient, $\alpha > 0$ is the Darcy coefficient, $F > 0$ is the Forchheimer coefficient and $p \in [3, 4]$ is a given number.

2. The velocity–vorticity-pressure formulation

In this section we introduce a new velocity–vorticity-pressure formulation for (1.3). To that end, we proceed as in [11] (see similar approaches in [12,15]) and introduce as a further unknown the vorticity ω , which is defined by

$$\omega := \mathbf{curl}(\mathbf{u}) = \begin{cases} \frac{\partial u_2}{\partial x_1} - \frac{\partial u_1}{\partial x_2} & , \text{ for } d = 2, \\ \nabla \times \mathbf{u} & , \text{ for } d = 3. \end{cases}$$

Note that the **curl** of a two-dimensional vector field is a scalar, whereas for a three-dimensional one it is a vector. In order to avoid a multiplicity of notation, we agree nevertheless to denote it like a vector, provided there is no confusion. In addition, in 2-D the **curl** of a scalar field q is a vector given by $\mathbf{curl}(q) = \left(\frac{\partial q}{\partial x_2}, -\frac{\partial q}{\partial x_1} \right)^t$. Then, employing the well-known identity [19, Section I.2.3]:

$$\mathbf{curl}(\mathbf{curl}(\mathbf{v})) = -\Delta \mathbf{v} + \nabla(\text{div}(\mathbf{v})) \tag{2.1}$$

in combination with the incompressibility condition $\text{div}(\mathbf{u}) = 0$ in $\Omega \times (0, T]$, we find that (1.3) can be rewritten, equivalently, as follows: Find (\mathbf{u}, ω, p) in suitable spaces to be indicated below such that

$$\begin{aligned} \frac{\partial \mathbf{u}}{\partial t} + \alpha \mathbf{u} + F |\mathbf{u}|^{p-2} \mathbf{u} + \nu \mathbf{curl}(\omega) + \nabla p &= \mathbf{f}, \quad \omega = \mathbf{curl}(\mathbf{u}), \quad \text{div}(\mathbf{u}) = 0 \quad \text{in } \Omega \times (0, T], \\ \mathbf{u} &= \mathbf{0} \quad \text{on } \Gamma \times (0, T], \quad \mathbf{u}(0) = \mathbf{u}_0 \quad \text{in } \Omega, \quad (p, 1)_\Omega = 0 \quad \text{in } (0, T]. \end{aligned} \tag{2.2}$$

Next, multiplying the first equation of (2.2) by a suitable test function \mathbf{v} , we obtain

$$(\partial_t \mathbf{u}, \mathbf{v})_\Omega + \alpha (\mathbf{u}, \mathbf{v})_\Omega + F (|\mathbf{u}|^{p-2} \mathbf{u}, \mathbf{v})_\Omega + \nu (\mathbf{curl}(\omega), \mathbf{v})_\Omega + (\nabla p, \mathbf{v})_\Omega = (\mathbf{f}, \mathbf{v})_\Omega, \tag{2.3}$$

where we use the notation $\partial_t := \frac{\partial}{\partial t}$. Notice that the third term in the left-hand side of (2.3) requires \mathbf{u} to live in a smaller space than $L^2(\Omega)$. In fact, by applying Cauchy–Schwarz and Hölder’s inequalities and then the continuous injection i_p of $H^1(\Omega)$ into $L^p(\Omega)$, with $p \in [3, 4]$ (cf. (1.2)), we find that

$$|(|\mathbf{u}|^{p-2} \mathbf{u}, \mathbf{v})_\Omega| \leq \|\mathbf{u}\|_{L^p(\Omega)}^{p-1} \|\mathbf{v}\|_{L^p(\Omega)} \leq \|i_p\|^p \|\mathbf{u}\|_{H^1(\Omega)}^{p-1} \|\mathbf{v}\|_{H^1(\Omega)} \quad \forall \mathbf{u}, \mathbf{v} \in H^1(\Omega), \tag{2.4}$$

which together with the Dirichlet boundary condition $\mathbf{u} = \mathbf{0}$ on Γ (cf. (2.2)) suggest to look for the unknown \mathbf{u} in $H_0^1(\Omega)$ and to restrict the set of corresponding test functions \mathbf{v} to the same space. In addition, employing Green’s formula [19, Theorem I.2.11], the fourth term in the left-hand side in (2.3), can be rewritten as

$$(\mathbf{curl}(\omega), \mathbf{v})_\Omega = (\omega, \mathbf{curl}(\mathbf{v}))_\Omega - \langle \mathbf{v} \times \mathbf{n}, \omega \rangle_\Gamma = (\omega, \mathbf{curl}(\mathbf{v}))_\Omega \quad \forall \mathbf{v} \in H_0^1(\Omega). \tag{2.5}$$

Note that in 2-D the boundary term in (2.5) needs to be replaced by $\langle \mathbf{v} \cdot \mathbf{t}, \omega \rangle_\Gamma$. Thus, replacing back (2.5) into (2.3), integrating by parts the term $(\nabla p, \mathbf{v})_\Omega$, and incorporating the second and third equations of (2.2) in a weak

sense, we obtain the system

$$\begin{aligned} (\partial_t \mathbf{u}, \mathbf{v})_\Omega + \alpha (\mathbf{u}, \mathbf{v})_\Omega + F(|\mathbf{u}|^{p-2} \mathbf{u}, \mathbf{v})_\Omega + \nu (\boldsymbol{\omega}, \mathbf{curl}(\mathbf{v}))_\Omega - (p, \text{div}(\mathbf{v}))_\Omega &= (\mathbf{f}, \mathbf{v})_\Omega, \\ \nu (\boldsymbol{\omega}, \boldsymbol{\psi})_\Omega - \nu (\boldsymbol{\psi}, \mathbf{curl}(\mathbf{u}))_\Omega &= 0, \\ (q, \text{div}(\mathbf{u}))_\Omega &= 0, \end{aligned} \tag{2.6}$$

for all $(\mathbf{v}, \boldsymbol{\psi}, q) \in \mathbf{H}_0^1(\Omega) \times \mathbf{L}^2(\Omega) \times L_0^2(\Omega)$, where $L_0^2(\Omega) := \{q \in L^2(\Omega) : (q, 1)_\Omega = 0\}$.

The formulation (2.6) provides control of the velocity \mathbf{u} in $\mathbf{L}^2(\Omega)$, but not in $\mathbf{H}_0^1(\Omega)$, which is needed for the well-posedness analysis. In order to obtain such control, motivated by the well-known identity

$$\|\nabla \mathbf{v}\|_{\mathbf{L}^2(\Omega)}^2 = \|\mathbf{curl}(\mathbf{v})\|_{\mathbf{L}^2(\Omega)}^2 + \|\text{div}(\mathbf{v})\|_{L^2(\Omega)}^2 \quad \forall \mathbf{v} \in \mathbf{H}_0^1(\Omega), \tag{2.7}$$

which follows from (2.1), we proceed to augment the system (2.6) by adding the following residual terms arising from the second and third equations in (2.2):

$$\kappa_1 (\mathbf{curl}(\mathbf{u}) - \boldsymbol{\omega}, \mathbf{curl}(\mathbf{v}) + \boldsymbol{\psi})_\Omega \quad \text{and} \quad \kappa_2 (\text{div}(\mathbf{u}), \text{div}(\mathbf{v}))_\Omega, \tag{2.8}$$

where κ_1 and κ_2 are positive parameters to be specified later on. The inclusion of these terms allows us to establish strong monotonicity in the variable \mathbf{u} in the $\mathbf{H}_0^1(\Omega)$ -norm, cf. Lemma 3.4.

Remark 2.1. We note that the first term in (2.8) is chosen to be skew-symmetric. While the symmetric version of the term also results in a monotone operator, it leads to complications in the stability bound for $\|\partial_t \mathbf{u}\|_{\mathbf{L}^2(0,T;\mathbf{L}^2(\Omega))}$ (cf. (3.36)). In particular, the identity stated in (3.37) for the skew-symmetric scheme cannot be derived for the symmetric version, which is needed for the derivation of the pressure stability bound. On the other hand, there are no significant differences between the two schemes in terms of their numerical performance, including for small values of ν .

Next, in order to write the above formulation in a more suitable way for the analysis to be developed below, we now set

$$\underline{\mathbf{u}} := (\mathbf{u}, \boldsymbol{\omega}) \in \mathbf{H}_0^1(\Omega) \times \mathbf{L}^2(\Omega),$$

with corresponding norm given by

$$\|\underline{\mathbf{v}}\| = \|(\mathbf{v}, \boldsymbol{\psi})\| := \left(\|\mathbf{v}\|_{\mathbf{H}^1(\Omega)}^2 + \|\boldsymbol{\psi}\|_{\mathbf{L}^2(\Omega)}^2 \right)^{1/2} \quad \forall \underline{\mathbf{v}} := (\mathbf{v}, \boldsymbol{\psi}) \in \mathbf{H}_0^1(\Omega) \times \mathbf{L}^2(\Omega).$$

Hence, the weak form associated with the Brinkman–Forchheimer Eq. (2.6)–(2.8) reads: Given $\mathbf{f} : [0, T] \rightarrow \mathbf{L}^2(\Omega)$ and $\mathbf{u}_0 \in \mathbf{H}_0^1(\Omega)$, find $(\underline{\mathbf{u}}, p) : [0, T] \rightarrow (\mathbf{H}_0^1(\Omega) \times \mathbf{L}^2(\Omega)) \times L_0^2(\Omega)$ such that $\mathbf{u}(0) = \mathbf{u}_0$ and, for a.e. $t \in (0, T)$,

$$\begin{aligned} \frac{\partial}{\partial t} [\mathcal{E}(\underline{\mathbf{u}}(t)), \underline{\mathbf{v}}] + [\mathcal{A}(\underline{\mathbf{u}}(t)), \underline{\mathbf{v}}] + [\mathcal{B}'(p(t)), \underline{\mathbf{v}}] &= [\mathbf{F}(t), \underline{\mathbf{v}}] \quad \forall \underline{\mathbf{v}} \in \mathbf{H}_0^1(\Omega) \times \mathbf{L}^2(\Omega), \\ -[\mathcal{B}(\underline{\mathbf{u}}(t)), q] &= 0 \quad \forall q \in L_0^2(\Omega), \end{aligned} \tag{2.9}$$

where, the operators $\mathcal{E}, \mathcal{A} : (\mathbf{H}_0^1(\Omega) \times \mathbf{L}^2(\Omega)) \rightarrow (\mathbf{H}_0^1(\Omega) \times \mathbf{L}^2(\Omega))'$, and $\mathcal{B} : (\mathbf{H}_0^1(\Omega) \times \mathbf{L}^2(\Omega)) \rightarrow L_0^2(\Omega)'$ are defined, respectively, as

$$[\mathcal{E}(\underline{\mathbf{u}}), \underline{\mathbf{v}}] := (\mathbf{u}, \mathbf{v})_\Omega, \tag{2.10}$$

$$\begin{aligned} [\mathcal{A}(\underline{\mathbf{u}}), \underline{\mathbf{v}}] &:= \alpha (\mathbf{u}, \mathbf{v})_\Omega + F(|\mathbf{u}|^{p-2} \mathbf{u}, \mathbf{v})_\Omega + \nu (\boldsymbol{\omega}, \boldsymbol{\psi})_\Omega + \nu (\boldsymbol{\omega}, \mathbf{curl}(\mathbf{v}))_\Omega - \nu (\boldsymbol{\psi}, \mathbf{curl}(\mathbf{u}))_\Omega \\ &\quad + \kappa_1 (\mathbf{curl}(\mathbf{u}) - \boldsymbol{\omega}, \mathbf{curl}(\mathbf{v}) + \boldsymbol{\psi})_\Omega + \kappa_2 (\text{div}(\mathbf{u}), \text{div}(\mathbf{v}))_\Omega, \end{aligned} \tag{2.11}$$

$$[\mathcal{B}(\underline{\mathbf{v}}), q] := -(q, \text{div}(\mathbf{v}))_\Omega, \tag{2.12}$$

and $\mathbf{F} \in (\mathbf{H}_0^1(\Omega) \times \mathbf{L}^2(\Omega))'$ is the bounded linear functional given by

$$[\mathbf{F}, \underline{\mathbf{v}}] := (\mathbf{f}, \mathbf{v})_\Omega. \tag{2.13}$$

In all the terms above, $[\cdot, \cdot]$ denotes the duality pairing induced by the corresponding operators. In addition, we let $\mathcal{B}' : L_0^2(\Omega) \rightarrow (\mathbf{H}_0^1(\Omega) \times \mathbf{L}^2(\Omega))'$ be the adjoint of \mathcal{B} , which satisfy $[\mathcal{B}'(q), \underline{\mathbf{v}}] = [\mathcal{B}(\underline{\mathbf{v}}), q]$ for all $\underline{\mathbf{v}} = (\mathbf{v}, \boldsymbol{\psi}) \in \mathbf{H}_0^1(\Omega) \times \mathbf{L}^2(\Omega)$ and $q \in L_0^2(\Omega)$.

Note that the seminorm identity (2.7) is stated for the case of Dirichlet boundary conditions for velocity everywhere on Γ . As indicated in [19, Section 3.2], the requirement can be relaxed to imposing either $\mathbf{u} \cdot \mathbf{n} = 0$ or $\mathbf{u} \times \mathbf{n} = \mathbf{0}$ (where \mathbf{n} denotes the outward unit normal on the boundary) whenever Γ is of class $C^{1,1}$ or if it is piecewise smooth without reentrant corners.

3. Well-posedness of the model

In this section we establish the solvability of (2.9). To that end we first collect some previous results that will be used in the forthcoming analysis.

3.1. Preliminary results

We begin by recalling the key result [16, Theorem IV.6.1(b)], which will be used to establish the existence of a solution to (2.9). In what follows, $Rg(\mathcal{A})$ denotes the range of \mathcal{A} .

Theorem 3.1. *Let the linear, symmetric and monotone operator \mathcal{N} be given for the real vector space E to its algebraic dual E^* , and let E'_b be the Hilbert space which is the dual of E with the seminorm*

$$|x|_b = (\mathcal{N}x(x))^{1/2} \quad x \in E.$$

Let $\mathcal{M} \subset E \times E'_b$ be a relation with domain $\mathcal{D} = \{x \in E : \mathcal{M}(x) \neq \emptyset\}$.

Assume \mathcal{M} is monotone and $Rg(\mathcal{N} + \mathcal{M}) = E'_b$. Then, for each $f \in W^{1,1}(0, T; E'_b)$ and for each $u_0 \in \mathcal{D}$, there is a solution u of

$$\frac{\partial}{\partial t}(\mathcal{N}u(t)) + \mathcal{M}(u(t)) \ni f(t) \quad \text{a.e. } 0 < t < T, \tag{3.1}$$

with

$$\mathcal{N}u \in W^{1,\infty}(0, T; E'_b), \quad u(t) \in \mathcal{D}, \quad \text{for all } 0 \leq t \leq T, \quad \text{and } \mathcal{N}u(0) = \mathcal{N}u_0.$$

In addition, in order to provide the range condition in Theorem 3.1 we will require the following abstract result [10, Theorem 3.1], which in turn, is a modification of [20, Theorem 3.1].

Theorem 3.2. *Let X_1, X_2 and Y be separable and reflexive Banach spaces, being X_1 and X_2 uniformly convex, and set $X := X_1 \times X_2$. Let $\mathcal{A} : X \rightarrow X'$ be a nonlinear operator, $\mathcal{B} \in \mathcal{L}(X, Y')$, and let V be the kernel of \mathcal{B} , that is,*

$$V := \{v = (v_1, v_2) \in X : \mathcal{B}(v) = \mathbf{0}\}.$$

Assume that

(i) there exist constants $L_{\mathcal{A}} > 0$ and $p_1, p_2 \geq 2$, such that

$$\|\mathcal{A}(u) - \mathcal{A}(v)\|_{X'} \leq L_{\mathcal{A}} \sum_{i=1}^2 \left\{ \|u_i - v_i\|_{X_i} + (\|u_i\|_{X_i} + \|v_i\|_{X_i})^{p_i-2} \|u_i - v_i\|_{X_i} \right\},$$

for all $u = (u_1, u_2), v = (v_1, v_2) \in X$.

(ii) the family of operators $\{\mathcal{A}(\cdot + z) : V \rightarrow V' : z \in X\}$ is uniformly strongly monotone, that is there exists $\gamma > 0$, such that

$$[\mathcal{A}(u + z) - \mathcal{A}(v + z), u - v] \geq \gamma \|u - v\|_X^2,$$

for all $z \in X$, and for all $u, v \in V$, and

(iii) there exists $\beta > 0$ such that

$$\sup_{\mathbf{0} \neq v \in X} \frac{[\mathcal{B}(v), q]}{\|v\|_X} \geq \beta \|q\|_{Y'} \quad \forall q \in Y.$$

Then, for each $(\mathcal{F}, \mathcal{G}) \in X' \times Y'$ there exists a unique $(u, p) \in X \times Y$ such that

$$\begin{aligned} [\mathcal{A}(u), v] + [\mathcal{B}(v), p] &= [\mathcal{F}, v] \quad \forall v \in X, \\ [\mathcal{B}(u), q] &= [\mathcal{G}, q] \quad \forall q \in Y. \end{aligned}$$

Next, we establish the stability properties of the operators involved in (2.9). We begin by observing that the operators \mathcal{E}, \mathcal{B} and the functional \mathbf{F} are linear. In turn, from (2.10), (2.12) and (2.13), and employing Hölder and Cauchy–Schwarz inequalities, there hold

$$|[\mathcal{B}(\underline{\mathbf{v}}), q]| \leq \|\underline{\mathbf{v}}\| \|q\|_{\mathbf{L}^2(\Omega)} \quad \forall (\underline{\mathbf{v}}, q) \in (\mathbf{H}_0^1(\Omega) \times \mathbf{L}^2(\Omega)) \times \mathbf{L}_0^2(\Omega), \tag{3.2}$$

$$|[\mathbf{F}, \underline{\mathbf{v}}]| \leq \|\mathbf{f}\|_{\mathbf{L}^2(\Omega)} \|\underline{\mathbf{v}}\|_{\mathbf{L}^2(\Omega)} \leq \|\mathbf{f}\|_{\mathbf{L}^2(\Omega)} \|\underline{\mathbf{v}}\| \quad \forall \underline{\mathbf{v}} \in \mathbf{H}_0^1(\Omega) \times \mathbf{L}^2(\Omega), \tag{3.3}$$

and

$$|[\mathcal{E}(\underline{\mathbf{u}}), \underline{\mathbf{v}}]| \leq \|\underline{\mathbf{u}}\| \|\underline{\mathbf{v}}\|, \quad [\mathcal{E}(\underline{\mathbf{v}}), \underline{\mathbf{v}}] = \|\underline{\mathbf{v}}\|_{\mathbf{L}^2(\Omega)}^2 \quad \forall \underline{\mathbf{u}}, \underline{\mathbf{v}} \in \mathbf{H}_0^1(\Omega) \times \mathbf{L}^2(\Omega), \tag{3.4}$$

which implies that \mathcal{B} and \mathbf{F} are bounded and continuous, and \mathcal{E} is bounded, continuous, and monotone. In addition, employing the Cauchy–Schwarz and Hölder inequalities, the continuous injection of $\mathbf{H}^1(\Omega)$ into $\mathbf{L}^p(\Omega)$, with $p \in [3, 4]$, it is readily seen that, the nonlinear operator \mathcal{A} (cf. (2.11)) is bounded, that is

$$|[\mathcal{A}(\underline{\mathbf{u}}), \underline{\mathbf{v}}]| \leq C_{\mathcal{A}} \left\{ \|\underline{\mathbf{u}}\|_{\mathbf{H}^1(\Omega)} + \|\underline{\mathbf{u}}\|_{\mathbf{H}^1(\Omega)}^{p-1} + \|\omega\|_{\mathbf{L}^2(\Omega)} \right\} \|\underline{\mathbf{v}}\|, \tag{3.5}$$

with $C_{\mathcal{A}} > 0$ depending on $\|\mathbf{i}_p\|, \alpha, F, \nu, \kappa_1$, and κ_2 . On the other hand, for later use, we deduce from [21, Lemma 2.1, Eqs. (2.1a) and (2.1b)], and using the Hölder inequality, that for all $\mathbf{u}, \mathbf{v} \in \mathbf{L}^p(\Omega)$ there exist constants $c_p, C_p > 0$ depending only on $|\Omega|$ and p , such that

$$\| |\mathbf{u}|^{p-2}\mathbf{u} - |\mathbf{v}|^{p-2}\mathbf{v} \|_{\mathbf{L}^q(\Omega)} \leq c_p \left(\|\mathbf{u}\|_{\mathbf{L}^p(\Omega)} + \|\mathbf{v}\|_{\mathbf{L}^p(\Omega)} \right)^{p-2} \|\mathbf{u} - \mathbf{v}\|_{\mathbf{L}^p(\Omega)}, \tag{3.6}$$

with $1/p + 1/q = 1$, and

$$\left(|\mathbf{u}|^{p-2}\mathbf{u} - |\mathbf{v}|^{p-2}\mathbf{v}, \mathbf{u} - \mathbf{v} \right)_{\Omega} \geq C_p \|\mathbf{u} - \mathbf{v}\|_{\mathbf{L}^p(\Omega)}^p. \tag{3.7}$$

In addition, it can be shown in a way similar to (3.6) that for all $\mathbf{u}, \mathbf{v} \in \mathbf{L}^{2(p-1)}(\Omega)$ there exists a constant $\tilde{c}_p > 0$ depending only on $|\Omega|$ and p , such that

$$\| |\mathbf{u}|^{p-2}\mathbf{u} - |\mathbf{v}|^{p-2}\mathbf{v} \|_{\mathbf{L}^2(\Omega)} \leq \tilde{c}_p \left(\|\mathbf{u}\|_{\mathbf{L}^{2(p-1)}(\Omega)} + \|\mathbf{v}\|_{\mathbf{L}^{2(p-1)}(\Omega)} \right)^{p-2} \|\mathbf{u} - \mathbf{v}\|_{\mathbf{L}^{2(p-1)}(\Omega)}. \tag{3.8}$$

Finally, recalling the definition of the operators \mathcal{E}, \mathcal{A} , and \mathcal{B} (cf. (2.10), (2.11), (2.12)), we stress that problem (2.9) can be written in the form of (3.1) with

$$E := (\mathbf{H}_0^1(\Omega) \times \mathbf{L}^2(\Omega)) \times \mathbf{L}_0^2(\Omega), \quad u := \begin{pmatrix} \underline{\mathbf{u}} \\ p \end{pmatrix}, \quad \mathcal{N} := \begin{pmatrix} \mathcal{E} & \mathbf{0} \\ \mathbf{0} & \mathbf{0} \end{pmatrix}, \quad \mathcal{M} := \begin{pmatrix} \mathcal{A} & \mathcal{B}' \\ -\mathcal{B} & \mathbf{0} \end{pmatrix}. \tag{3.9}$$

Let \mathbf{E}'_2 be the Hilbert space that is the dual of $\mathbf{H}_0^1(\Omega) \times \mathbf{L}^2(\Omega)$ with the seminorm induced by the operator $\mathcal{E} := \begin{pmatrix} \mathcal{E} & \mathbf{0} \\ \mathbf{0} & \mathbf{0} \end{pmatrix}$ (cf. (2.10)), which is $\|\underline{\mathbf{v}}\|_{\mathcal{E}} = (\mathbf{v}, \mathbf{v})_{\Omega}^{1/2} = \|\mathbf{v}\|_{\mathbf{L}^2(\Omega)} \quad \forall \underline{\mathbf{v}} \in \mathbf{H}_0^1(\Omega) \times \mathbf{L}^2(\Omega)$. Note that $\mathbf{E}'_2 = \mathbf{L}^2(\Omega) \times \{\mathbf{0}\}$. Then we define the spaces

$$E'_b := (\mathbf{L}^2(\Omega) \times \{\mathbf{0}\}) \times \{\mathbf{0}\}, \quad \mathcal{D} := \left\{ (\underline{\mathbf{u}}, p) \in (\mathbf{H}_0^1(\Omega) \times \mathbf{L}^2(\Omega)) \times \mathbf{L}_0^2(\Omega) : \mathcal{M}(\underline{\mathbf{u}}, p) \in E'_b \right\}. \tag{3.10}$$

In the next section we prove the hypotheses of Theorem 3.1 to establish the well-posedness of (2.9).

3.2. Range condition and initial data

We begin with the verification of the range condition in Theorem 3.1. Let us consider the resolvent system associated with (2.9): Find $(\underline{\mathbf{u}}, p) \in (\mathbf{H}_0^1(\Omega) \times \mathbf{L}^2(\Omega)) \times \mathbf{L}_0^2(\Omega)$ such that

$$\begin{aligned} [(\mathcal{E} + \mathcal{A})(\underline{\mathbf{u}}), \underline{\mathbf{v}}] + [\mathcal{B}'(p), \underline{\mathbf{v}}] &= [\widehat{\mathbf{F}}, \underline{\mathbf{v}}] \quad \forall \underline{\mathbf{v}} \in \mathbf{H}_0^1(\Omega) \times \mathbf{L}^2(\Omega), \\ [\mathcal{B}(\underline{\mathbf{u}}), q] &= 0 \quad \forall q \in \mathbf{L}_0^2(\Omega), \end{aligned} \tag{3.11}$$

where $\widehat{\mathbf{F}} \in \mathbf{L}^2(\Omega) \times \{\mathbf{0}\} \subset (\mathbf{H}_0^1(\Omega))' \times \{\mathbf{0}\}$ is a functional given by $\widehat{\mathbf{F}}(\mathbf{v}) := (\widehat{\mathbf{f}}, \mathbf{v})_\Omega$ for some $\widehat{\mathbf{f}} \in \mathbf{L}^2(\Omega)$. Next, a solution to (3.11) is established by employing Theorem 3.2. We begin by observing that, thanks to the uniform convexity and separability of $L^p(\Omega)$ for $p \in (1, +\infty)$, the spaces $\mathbf{H}_0^1(\Omega)$, $\mathbf{L}^2(\Omega)$, and $L_0^2(\Omega)$ are uniformly convex and separable as well.

We continue our analysis by proving that the nonlinear operator $\mathcal{E} + \mathcal{A}$ satisfies hypothesis (i) of Theorem 3.2 with $p_1 = p \in [3, 4]$ and $p_2 = 2$.

Lemma 3.3. *Let $p \in [3, 4]$. Then, there exists $L_{\text{BF}} > 0$, depending on $\|\mathbf{i}_p\|$, $|\Omega|$, ν , F , α , κ_1 , and κ_2 such that*

$$\begin{aligned} & \|(\mathcal{E} + \mathcal{A})(\underline{\mathbf{u}}) - (\mathcal{E} + \mathcal{A})(\underline{\mathbf{v}})\| \\ & \leq L_{\text{BF}} \left\{ \|\underline{\mathbf{u}} - \underline{\mathbf{v}}\|_{\mathbf{H}^1(\Omega)} + \|\underline{\boldsymbol{\omega}} - \underline{\boldsymbol{\psi}}\|_{\mathbf{L}^2(\Omega)} + (\|\underline{\mathbf{u}}\|_{\mathbf{H}^1(\Omega)} + \|\underline{\mathbf{v}}\|_{\mathbf{H}^1(\Omega)})^{p-2} \|\underline{\mathbf{u}} - \underline{\mathbf{v}}\|_{\mathbf{H}^1(\Omega)} \right\}, \end{aligned} \tag{3.12}$$

for all $\underline{\mathbf{u}} = (\mathbf{u}, \boldsymbol{\omega})$, $\underline{\mathbf{v}} = (\mathbf{v}, \boldsymbol{\psi}) \in \mathbf{H}_0^1(\Omega) \times \mathbf{L}^2(\Omega)$.

Proof. Let $\underline{\mathbf{u}} = (\mathbf{u}, \boldsymbol{\omega})$, $\underline{\mathbf{v}} = (\mathbf{v}, \boldsymbol{\psi})$, $\underline{\mathbf{w}} = (\mathbf{w}, \boldsymbol{\phi}) \in \mathbf{H}_0^1(\Omega) \times \mathbf{L}^2(\Omega)$. From the definition of the operators \mathcal{E} , \mathcal{A} (cf. (2.10), (2.11)), and using the Cauchy–Schwarz and Hölder inequalities, we deduce that

$$\begin{aligned} & \|(\mathcal{E} + \mathcal{A})(\underline{\mathbf{u}}) - (\mathcal{E} + \mathcal{A})(\underline{\mathbf{v}}), \underline{\mathbf{w}}\| \leq F \left\| |\mathbf{u}|^{p-2}\mathbf{u} - |\mathbf{v}|^{p-2}\mathbf{v} \right\|_{\mathbf{L}^q(\Omega)} \|\mathbf{w}\|_{\mathbf{L}^p(\Omega)} \\ & + 2(\nu + \max\{1 + \alpha, \kappa_1, \kappa_2\}) (\|\underline{\mathbf{u}} - \underline{\mathbf{v}}\|_{\mathbf{H}^1(\Omega)} + \|\underline{\boldsymbol{\omega}} - \underline{\boldsymbol{\psi}}\|_{\mathbf{L}^2(\Omega)}) \|(\mathbf{w}, \boldsymbol{\phi})\|. \end{aligned} \tag{3.13}$$

Then, using (3.6) to bound the first term on the right-hand side of (3.13), and using the continuous injection \mathbf{i}_p of $\mathbf{H}^1(\Omega)$ into $\mathbf{L}^p(\Omega)$ (cf. (1.2)), we obtain

$$\begin{aligned} & \|(\mathcal{E} + \mathcal{A})(\underline{\mathbf{u}}) - (\mathcal{E} + \mathcal{A})(\underline{\mathbf{v}})\| \leq F \|\mathbf{i}_p\|^p c_p (\|\underline{\mathbf{u}}\|_{\mathbf{H}^1(\Omega)} + \|\underline{\mathbf{v}}\|_{\mathbf{H}^1(\Omega)})^{p-2} \|\underline{\mathbf{u}} - \underline{\mathbf{v}}\|_{\mathbf{H}^1(\Omega)} \\ & + 2(\nu + \max\{1 + \alpha, \kappa_1, \kappa_2\}) (\|\underline{\mathbf{u}} - \underline{\mathbf{v}}\|_{\mathbf{H}^1(\Omega)} + \|\underline{\boldsymbol{\omega}} - \underline{\boldsymbol{\psi}}\|_{\mathbf{L}^2(\Omega)}), \end{aligned}$$

which implies (3.12) with $L_{\text{BF}} = \max\left\{2(\nu + \max\{1 + \alpha, \kappa_1, \kappa_2\}), F \|\mathbf{i}_p\|^p c_p\right\}$. \square

Next, the following lemma shows that the operator $\mathcal{E} + \mathcal{A}$ satisfies hypothesis (ii) of Theorem 3.2 with $p_1 = p \in [3, 4]$ and $p_2 = 2$.

Lemma 3.4. *Assume that $\kappa_1 \in (0, \nu)$ and $\kappa_2 \in (0, +\infty)$. Then, the family of operators $\{(\mathcal{E} + \mathcal{A})(\cdot + \underline{\mathbf{z}}) : \mathbf{H}_0^1(\Omega) \times \mathbf{L}^2(\Omega) \rightarrow (\mathbf{H}_0^1(\Omega) \times \mathbf{L}^2(\Omega))' : \underline{\mathbf{z}} \in \mathbf{H}_0^1(\Omega) \times \mathbf{L}^2(\Omega)\}$ is uniformly strongly monotone, that is, there exists $\gamma_{\text{BF}} > 0$, such that*

$$[(\mathcal{E} + \mathcal{A})(\underline{\mathbf{u}} + \underline{\mathbf{z}}) - (\mathcal{E} + \mathcal{A})(\underline{\mathbf{v}} + \underline{\mathbf{z}}), \underline{\mathbf{u}} - \underline{\mathbf{v}}] \geq \gamma_{\text{BF}} \|\underline{\mathbf{u}} - \underline{\mathbf{v}}\|^2 \quad \forall \underline{\mathbf{u}}, \underline{\mathbf{v}} \in \mathbf{H}_0^1(\Omega) \times \mathbf{L}^2(\Omega). \tag{3.14}$$

Proof. Let $\underline{\mathbf{u}} = (\mathbf{u}, \boldsymbol{\omega})$, $\underline{\mathbf{v}} = (\mathbf{v}, \boldsymbol{\psi})$, $\underline{\mathbf{z}} = (\mathbf{z}, \boldsymbol{\phi}) \in \mathbf{H}_0^1(\Omega) \times \mathbf{L}^2(\Omega)$. Then, from the definition of the operators \mathcal{E} , \mathcal{A} (cf. (2.10), (2.11)), we get

$$\begin{aligned} & [(\mathcal{E} + \mathcal{A})(\underline{\mathbf{u}} + \underline{\mathbf{z}}) - (\mathcal{E} + \mathcal{A})(\underline{\mathbf{v}} + \underline{\mathbf{z}}), \underline{\mathbf{u}} - \underline{\mathbf{v}}] \\ & = (1 + \alpha) \|\underline{\mathbf{u}} - \underline{\mathbf{v}}\|_{\mathbf{L}^2(\Omega)}^2 + F (|\mathbf{u} + \mathbf{z}|^{p-2}(\mathbf{u} + \mathbf{z}) - |\mathbf{v} + \mathbf{z}|^{p-2}(\mathbf{v} + \mathbf{z}), \mathbf{u} - \mathbf{v})_\Omega \\ & + \kappa_1 \|\mathbf{curl}(\mathbf{u} - \mathbf{v})\|_{\mathbf{L}^2(\Omega)}^2 + \kappa_2 \|\mathbf{div}(\mathbf{u} - \mathbf{v})\|_{\mathbf{L}^2(\Omega)}^2 + (\nu - \kappa_1) \|\underline{\boldsymbol{\omega}} - \underline{\boldsymbol{\psi}}\|_{\mathbf{L}^2(\Omega)}^2. \end{aligned} \tag{3.15}$$

Hence, using (3.7) to bound the second term on the right-hand side of (3.15), and using the Cauchy–Schwarz and Young inequalities we find that for all $\underline{\mathbf{u}} = (\mathbf{u}, \boldsymbol{\omega})$, $\underline{\mathbf{v}} = (\mathbf{v}, \boldsymbol{\psi}) \in \mathbf{H}_0^1(\Omega) \times \mathbf{L}^2(\Omega)$, there holds

$$\begin{aligned} & [(\mathcal{E} + \mathcal{A})(\underline{\mathbf{u}} + \underline{\mathbf{z}}) - (\mathcal{E} + \mathcal{A})(\underline{\mathbf{v}} + \underline{\mathbf{z}}), \underline{\mathbf{u}} - \underline{\mathbf{v}}] \\ & \geq (1 + \alpha) \|\underline{\mathbf{u}} - \underline{\mathbf{v}}\|_{\mathbf{L}^2(\Omega)}^2 + \kappa_1 \|\mathbf{curl}(\mathbf{u} - \mathbf{v})\|_{\mathbf{L}^2(\Omega)}^2 + \kappa_2 \|\mathbf{div}(\mathbf{u} - \mathbf{v})\|_{\mathbf{L}^2(\Omega)}^2 \\ & + F C_p \|\underline{\mathbf{u}} - \underline{\mathbf{v}}\|_{\mathbf{L}^p(\Omega)}^p + (\nu - \kappa_1) \|\underline{\boldsymbol{\omega}} - \underline{\boldsymbol{\psi}}\|_{\mathbf{L}^2(\Omega)}^2. \end{aligned} \tag{3.16}$$

Then, assuming the stipulated ranges on κ_1 and κ_2 , we can define the positive constants

$$\gamma_1 := \min\{\kappa_1, \kappa_2\} \quad \text{and} \quad \gamma_2 := \nu - \kappa_1, \tag{3.17}$$

which together with the identity (2.7), and neglecting the $L^p(\Omega)$ -term in the right-hand side of (3.16), yields

$$[(\mathcal{E} + \mathcal{A})(\mathbf{u} + \mathbf{z}) - (\mathcal{E} + \mathcal{A})(\mathbf{v} + \mathbf{z}), \mathbf{u} - \mathbf{v}] \geq (1 + \alpha) \|\mathbf{u} - \mathbf{v}\|_{L^2(\Omega)}^2 + \gamma_1 \|\nabla(\mathbf{u} - \mathbf{v})\|_{L^2(\Omega)}^2 + \gamma_2 \|\boldsymbol{\omega} - \boldsymbol{\psi}\|_{L^2(\Omega)}^2, \quad (3.18)$$

which implies (3.14) with $\gamma_{BF} := \min\{(1 + \alpha), \gamma_1, \gamma_2\}$. \square

Remark 3.1. The terms $(1 + \alpha) \|\mathbf{u} - \mathbf{v}\|_{L^2(\Omega)}^2$ and $\gamma_1 \|\nabla(\mathbf{u} - \mathbf{v})\|_{L^2(\Omega)}^2$ in (3.18) and the definition of γ_1 in (3.17) imply that the control on the velocity \mathbf{u} in the $L^2(\Omega)$ -norm is independent of ν , κ_1 , and κ_2 , while control on $\nabla \mathbf{u}$ in the $L^2(\Omega)$ -norm can be maintained for small values of the viscosity ν by keeping κ_1 and κ_2 independent of ν . However, the condition $\kappa_1 \in (0, \nu)$ is needed for the control of the vorticity $\boldsymbol{\omega}$. In the case $\kappa_1 > \nu$, one can consider modification of the operator \mathcal{A} defined in (2.11), obtained by subtracting the terms with test function $\boldsymbol{\psi}$ in (2.6) and (2.8), resulting in

$$[\tilde{\mathcal{A}}(\mathbf{u}), \mathbf{v}] := \alpha (\mathbf{u}, \mathbf{v})_{\Omega} + F(|\mathbf{u}|^{p-2} \mathbf{u}, \mathbf{v})_{\Omega} - \nu (\boldsymbol{\omega}, \boldsymbol{\psi})_{\Omega} + \nu (\boldsymbol{\omega}, \mathbf{curl}(\mathbf{v}))_{\Omega} + \nu (\boldsymbol{\psi}, \mathbf{curl}(\mathbf{u}))_{\Omega} + \kappa_1 (\mathbf{curl}(\mathbf{u}) - \boldsymbol{\omega}, \mathbf{curl}(\mathbf{v}) - \boldsymbol{\psi})_{\Omega} + \kappa_2 (\text{div}(\mathbf{u}), \text{div}(\mathbf{v}))_{\Omega}.$$

The terms involving κ_1 and ν on the right-hand side of (3.15) then become

$$(\kappa_1 - \nu) \|\mathbf{curl}(\mathbf{u} - \mathbf{v}) - (\boldsymbol{\omega} - \boldsymbol{\psi})\|_{L^2(\Omega)}^2 + \nu \|\mathbf{curl}(\mathbf{u} - \mathbf{v})\|_{L^2(\Omega)}^2,$$

which, combined with $\|\boldsymbol{\omega} - \boldsymbol{\psi}\|_{L^2(\Omega)}^2 \leq 2 \|\mathbf{curl}(\mathbf{u} - \mathbf{v}) - (\boldsymbol{\omega} - \boldsymbol{\psi})\|_{L^2(\Omega)}^2 + 2 \|\mathbf{curl}(\mathbf{u} - \mathbf{v})\|_{L^2(\Omega)}^2$, results in control on

$$\frac{1}{2} \min\{\kappa_1 - \nu, \frac{\nu}{2}\} \|\boldsymbol{\omega} - \boldsymbol{\psi}\|_{L^2(\Omega)}^2 + \frac{\nu}{2} \|\mathbf{curl}(\mathbf{u} - \mathbf{v})\|_{L^2(\Omega)}^2.$$

Therefore the well-posedness analysis of the model can also be extended to the case $\kappa_1 > \nu$. Similar techniques can be used in the stability analysis of the continuous and discrete formulations, as well as in the error analysis. To keep the presentation simpler and easier to follow, we focus on the case $\kappa_1 \in (0, \nu)$. We note, however, that the numerical study in Example 1 in Section 6 indicates that the numerical method is stable and convergent in the case $\kappa_1 > \nu$, and in particular it converges optimally for the velocity in the $\mathbf{H}^1(\Omega)$ -norm in the regime of small viscosity when κ_1 is kept fixed.

Remark 3.2. The kernel of the operator \mathcal{B} (cf. (2.12)) can be written as $\mathbf{V} := \mathbf{K} \times L^2(\Omega)$, where

$$\mathbf{K} = \left\{ \mathbf{v} \in \mathbf{H}_0^1(\Omega) : \text{div}(\mathbf{v}) = 0 \text{ in } \Omega \right\}. \quad (3.19)$$

In turn, since the strong monotonicity bound (3.14) holds on $\mathbf{H}_0^1(\Omega) \times L^2(\Omega)$, it is clear that it also holds on \mathbf{V} . Notice also that $\mathbf{v} \in \mathbf{K}$ (cf. (3.19)) implies that the term $\kappa_2 (\text{div}(\mathbf{u}), \text{div}(\mathbf{v}))_{\Omega}$ is not longer required in (2.11) to prove that the operator \mathcal{A} is strongly monotone on \mathbf{V} but in order to consider classical conforming discrete spaces that are not divergence-free, we keep the κ_2 -term and state the result on the whole space $\mathbf{H}_0^1(\Omega) \times L^2(\Omega)$. Furthermore, the term $\kappa_2 \|\text{div}(\mathbf{u} - \mathbf{v})\|_{L^2(\Omega)}^2$ in (3.15) implies that increasing κ_2 improved the divergence-free property of the method. This is illustrated in Example 1 in Section 6.

Remark 3.3. We also note that for computational purposes, and in order to maximize the strong monotonicity constant γ_{BF} (cf. (3.17)), we can choose explicitly the parameter κ_1 and κ_2 by taking κ_1 as the middle point of its feasible range and $\kappa_2 \geq \min\{1 + \alpha, \kappa_1\}$. More precisely, we can simply take

$$\kappa_1 = \frac{\nu}{2} \quad \text{and} \quad \kappa_2 \geq \min\left\{1 + \alpha, \frac{\nu}{2}\right\}.$$

We end the verification of the hypotheses of Theorem 3.2, with the corresponding inf–sup condition for the operator \mathcal{B} (cf. (2.12)).

Lemma 3.5. *There exists a constant $\beta > 0$ such that*

$$\sup_{\mathbf{0} \neq \mathbf{v} \in \mathbf{H}_0^1(\Omega) \times L^2(\Omega)} \frac{[\mathcal{B}(\mathbf{v}), q]}{\|\mathbf{v}\|} \geq \beta \|q\|_{L^2(\Omega)} \quad \forall q \in L_0^2(\Omega). \quad (3.20)$$

Proof. First, we recall from [22, Corollary B.71] the inf–sup condition

$$\sup_{\mathbf{0} \neq \mathbf{v} \in \mathbf{H}_0^1(\Omega)} \frac{\int_{\Omega} q \operatorname{div}(\mathbf{v})}{\|\mathbf{v}\|_{\mathbf{H}^1(\Omega)}} \geq \beta \|q\|_{L^2(\Omega)} \quad \forall q \in L_0^2(\Omega). \tag{3.21}$$

Thus, (3.20) follows straightforwardly from (3.21) and the definition of the operator \mathcal{B} (cf. (2.12)). \square

The main result of this section is established now.

Lemma 3.6. Assume κ_1 and κ_2 as in Lemma 3.4. Then, given $\widehat{\mathbf{F}} = (\widehat{\mathbf{f}}, \mathbf{0}) \in \mathbf{L}^2(\Omega) \times \{\mathbf{0}\}$, there exists a unique solution $(\underline{\mathbf{u}}, p) \in (\mathbf{H}_0^1(\Omega) \times \mathbf{L}^2(\Omega)) \times L_0^2(\Omega)$ of the resolvent system (3.11).

Proof. First, we recall from (3.2) and (3.3) that \mathcal{B} and $\widehat{\mathbf{F}}$ are linear and bounded. Then, as a consequence of Lemmas 3.3, 3.4, and 3.5, and a straightforward application of Theorem 3.2 we conclude the result. \square

We end this section establishing a suitable initial condition result, which is necessary to apply Theorem 3.1 to our context.

Lemma 3.7. Assume the initial condition $\mathbf{u}_0 \in \mathbf{H}_{\Delta}$, where

$$\mathbf{H}_{\Delta} := \left\{ \mathbf{v} \in \mathbf{H}_0^1(\Omega) : \Delta \mathbf{v} \in \mathbf{L}^2(\Omega) \text{ and } \operatorname{div}(\mathbf{v}) = 0 \text{ in } \Omega \right\}. \tag{3.22}$$

Then, there exists $(\boldsymbol{\omega}_0, p_0) \in \mathbf{L}^2(\Omega) \times L_0^2(\Omega)$ such that $\underline{\mathbf{u}}_0 = (\mathbf{u}_0, \boldsymbol{\omega}_0)$ and

$$\begin{pmatrix} \mathcal{A} & \mathcal{B}' \\ -\mathcal{B} & \mathbf{0} \end{pmatrix} \begin{pmatrix} \underline{\mathbf{u}}_0 \\ p_0 \end{pmatrix} \in (\mathbf{L}^2(\Omega) \times \{\mathbf{0}\}) \times \{\mathbf{0}\}. \tag{3.23}$$

Proof. We proceed as in [6, Lemma 3.6]. In fact, we define $\boldsymbol{\omega}_0 := \operatorname{curl}(\mathbf{u}_0)$ and choose $p_0 = 0$ in Ω , with $\mathbf{u}_0 \in \mathbf{H}_{\Delta}$ (cf. (3.22)). It follows that $\boldsymbol{\omega}_0 \in \mathbf{L}^2(\Omega)$ and $p_0 \in L_0^2(\Omega)$. In addition, using (2.1), we get

$$\nu \operatorname{curl}(\boldsymbol{\omega}_0) = -\nu \Delta \mathbf{u}_0 \quad \text{in } \Omega. \tag{3.24}$$

Next, multiplying the identities (3.24), $\nu(\boldsymbol{\omega}_0 - \operatorname{curl}(\mathbf{u}_0)) = \mathbf{0}$ and $\operatorname{div}(\mathbf{u}_0) = 0$ in Ω by $\mathbf{v} \in \mathbf{H}_0^1(\Omega)$, $\boldsymbol{\psi} \in \mathbf{L}^2(\Omega)$, and $q \in L_0^2(\Omega)$, respectively, integrating by parts as in (2.5), considering the fact that $\kappa_1(\operatorname{curl}(\mathbf{u}_0) - \boldsymbol{\omega}_0) = \mathbf{0}$ and $\kappa_2 \operatorname{div}(\mathbf{u}_0) = 0$ in Ω , and after a minor algebraic manipulation, we deduce

$$\begin{pmatrix} \mathcal{A} & \mathcal{B}' \\ -\mathcal{B} & \mathbf{0} \end{pmatrix} \begin{pmatrix} \underline{\mathbf{u}}_0 \\ p_0 \end{pmatrix} = \begin{pmatrix} \mathbf{F}_0 \\ \mathbf{0} \end{pmatrix}, \tag{3.25}$$

where, $\mathbf{F}_0 = (\mathbf{f}_0, \mathbf{0})$ and

$$(\mathbf{f}_0, \mathbf{v})_{\Omega} := (-\nu \Delta \mathbf{u}_0 + \alpha \mathbf{u}_0 + \mathbf{F} |\mathbf{u}_0|^{p-2} \mathbf{u}_0, \mathbf{v})_{\Omega},$$

which together with the additional regularity of \mathbf{u}_0 , and the continuous injection of $\mathbf{H}^1(\Omega)$ into $\mathbf{L}^{2(p-1)}(\Omega)$, with $2(p-1) \in [4, 6]$, cf. (1.2), implies that

$$\begin{aligned} |(\mathbf{f}_0, \mathbf{v})_{\Omega}| &\leq \left\{ \nu \|\Delta \mathbf{u}_0\|_{\mathbf{L}^2(\Omega)} + \alpha \|\mathbf{u}_0\|_{\mathbf{L}^2(\Omega)} + \mathbf{F} \|\mathbf{u}_0\|_{\mathbf{L}^{2(p-1)}(\Omega)}^{p-1} \right\} \|\mathbf{v}\|_{\mathbf{L}^2(\Omega)} \\ &\leq C \left\{ \|\Delta \mathbf{u}_0\|_{\mathbf{L}^2(\Omega)} + \|\mathbf{u}_0\|_{\mathbf{L}^2(\Omega)} + \|\mathbf{u}_0\|_{\mathbf{H}^1(\Omega)}^{p-1} \right\} \|\mathbf{v}\|_{\mathbf{L}^2(\Omega)}. \end{aligned} \tag{3.26}$$

Thus, $\mathbf{F}_0 \in \mathbf{L}^2(\Omega) \times \{\mathbf{0}\}$ so then (3.23) holds, completing the proof. \square

Remark 3.4. The assumption on the initial condition \mathbf{u}_0 in (3.22) is not necessary for all the results that follow but we shall assume it from now on for simplicity. A similar assumption to \mathbf{u}_0 is also made in [6, Lemma 3.6] (see also [7, Lemma 3.7] and [18, Eq. (2.2)]). Note also that $(\underline{\mathbf{u}}_0, p_0)$ satisfying (3.23) is not unique.

3.3. Main result

We now establish the well-posedness of problem (2.9).

Theorem 3.8. *Assume κ_1 and κ_2 as in Lemma 3.4. Then, for each $\mathbf{f} \in W^{1,1}(0, T; L^2(\Omega))$ and $\mathbf{u}_0 \in \mathbf{H}_\Delta$ (cf. (3.22)), there exists a unique $(\underline{\mathbf{u}}, p) = ((\mathbf{u}, \boldsymbol{\omega}), p) : [0, T] \rightarrow (\mathbf{H}_0^1(\Omega) \times \mathbf{L}^2(\Omega)) \times L_0^2(\Omega)$ solution to (2.9), such that $\mathbf{u} \in W^{1,\infty}(0, T; L^2(\Omega))$ and $\mathbf{u}(0) = \mathbf{u}_0$. In addition, $\boldsymbol{\omega}(0) = \boldsymbol{\omega}_0 = \text{curl}(\mathbf{u}_0)$.*

Proof. We recall that (2.9) fits the problem in Theorem 3.1 with the definitions (3.9) and (3.10). Note that \mathcal{N} is linear, symmetric and monotone since \mathcal{E} is (cf. (3.4)). In addition, since \mathcal{A} is strongly monotone, it is not difficult to see that \mathcal{M} is monotone. On the other hand, from Lemma 3.6 we know that for some $(\widehat{\mathbf{F}}, \mathbf{0}) \in E'_b$ with $\widehat{\mathbf{F}} = (\widehat{\mathbf{f}}, \mathbf{0})$, there is a $(\underline{\mathbf{u}}, p) = ((\mathbf{u}, \boldsymbol{\omega}), p) \in (\mathbf{H}_0^1(\Omega) \times \mathbf{L}^2(\Omega)) \times L_0^2(\Omega)$, such that $(\widehat{\mathbf{F}}, \mathbf{0}) = (\mathcal{N} + \mathcal{M})(\underline{\mathbf{u}}, p)$ which implies $Rg(\mathcal{N} + \mathcal{M}) = E'_b$. Finally, considering $\mathbf{u}_0 \in \mathbf{H}_\Delta$ (cf. (3.22)), from a straightforward application of Lemma 3.7 we are able to find $(\boldsymbol{\omega}_0, p_0) \in \mathbf{L}^2(\Omega) \times L_0^2(\Omega)$ such that $(\underline{\mathbf{u}}_0, p_0) = ((\mathbf{u}_0, \boldsymbol{\omega}_0), p_0) \in \mathcal{D}$. Therefore, applying Theorem 3.1 to our context, we conclude the existence of a solution $(\underline{\mathbf{u}}, p) = ((\mathbf{u}, \boldsymbol{\omega}), p)$ to (2.9), with $\mathbf{u} \in W^{1,\infty}(0, T; L^2(\Omega))$ and $\mathbf{u}(0) = \mathbf{u}_0$.

We next show that the solution of (2.9) is unique. To that end, let $(\underline{\mathbf{u}}_i, p_i) = ((\mathbf{u}_i, \boldsymbol{\omega}_i), p_i)$, with $i \in \{1, 2\}$, be two solutions corresponding to the same data. Then, taking (2.9) with $(\underline{\mathbf{v}}, q) = (\underline{\mathbf{u}}_1 - \underline{\mathbf{u}}_2, p_1 - p_2) \in (\mathbf{H}_0^1(\Omega) \times \mathbf{L}^2(\Omega)) \times L_0^2(\Omega)$, subtracting the problems, we deduce that

$$\frac{1}{2} \partial_t \|\mathbf{u}_1 - \mathbf{u}_2\|_{L^2(\Omega)}^2 + [\mathcal{A}(\underline{\mathbf{u}}_1) - \mathcal{A}(\underline{\mathbf{u}}_2), \underline{\mathbf{u}}_1 - \underline{\mathbf{u}}_2] = 0,$$

which together with the strong monotonicity bound of \mathcal{A} (cf. (3.16)–(3.17)), yields

$$\frac{1}{2} \partial_t \|\mathbf{u}_1 - \mathbf{u}_2\|_{L^2(\Omega)}^2 + \widehat{\gamma}_1 \|\mathbf{u}_1 - \mathbf{u}_2\|_{\mathbf{H}^1(\Omega)}^2 + \gamma_2 \|\boldsymbol{\omega}_1 - \boldsymbol{\omega}_2\|_{L^2(\Omega)}^2 \leq 0, \tag{3.27}$$

where $\widehat{\gamma}_1 := \min\{\alpha, \kappa_1, \kappa_2\}$ and γ_2 is defined in (3.17). Integrating in time (3.27) from 0 to $t \in (0, T]$, and using that $\mathbf{u}_1(0) = \mathbf{u}_2(0)$, we obtain

$$\|\mathbf{u}_1(t) - \mathbf{u}_2(t)\|_{L^2(\Omega)}^2 + \int_0^t \left(\|\mathbf{u}_1 - \mathbf{u}_2\|_{\mathbf{H}^1(\Omega)}^2 + \|\boldsymbol{\omega}_1 - \boldsymbol{\omega}_2\|_{L^2(\Omega)}^2 \right) ds \leq 0. \tag{3.28}$$

Therefore, it follows from (3.28) that $\mathbf{u}_1(t) = \mathbf{u}_2(t)$ and $\boldsymbol{\omega}_1(t) = \boldsymbol{\omega}_2(t)$ for all $t \in (0, T]$. Next, from the inf–sup condition of the operator \mathcal{B} (cf. (3.20)) and the first equation of (2.9), we get

$$\beta \|p_1 - p_2\|_{L^2(\Omega)} \leq \sup_{\mathbf{0} \neq \underline{\mathbf{v}} \in \mathbf{H}_0^1(\Omega) \times \mathbf{L}^2(\Omega)} \frac{-([\partial_t \mathcal{E}(\underline{\mathbf{u}}_1 - \underline{\mathbf{u}}_2), \underline{\mathbf{v}}] + [\mathcal{A}(\underline{\mathbf{u}}_1) - \mathcal{A}(\underline{\mathbf{u}}_2), \underline{\mathbf{v}}])}{\|\underline{\mathbf{v}}\|} = 0,$$

which implies that $p_1(t) = p_2(t)$ for all $t \in (0, T]$, and therefore (2.9) has a unique solution.

Finally, since Theorem 3.1 implies that $\mathcal{M}(u) \in L^\infty(0, T; E'_b)$, we can take $t \rightarrow 0$ in all equations without time derivatives in (2.9). Using that the initial data $(\underline{\mathbf{u}}_0, p_0) = ((\mathbf{u}_0, \boldsymbol{\omega}_0), p_0)$ satisfies the same equations at $t = 0$ (cf. (3.23)), and that $\mathbf{u}(0) = \mathbf{u}_0$, we obtain

$$(v - \kappa_1)(\boldsymbol{\omega}(0) - \boldsymbol{\omega}_0, \boldsymbol{\psi})_\Omega = 0 \quad \forall \boldsymbol{\psi} \in \mathbf{L}^2(\Omega). \tag{3.29}$$

Thus, taking $\boldsymbol{\psi} = \boldsymbol{\omega}(0) - \boldsymbol{\omega}_0$ in (3.29) we deduce that $\boldsymbol{\omega}(0) = \boldsymbol{\omega}_0$, completing the proof. \square

We conclude this section with stability bounds for the solution of (2.9).

Theorem 3.9. *Let $p \in [3, 4]$. Suppose that the stabilization parameters κ_1 and κ_2 are taken as in Lemma 3.4. Assume further that $\mathbf{f} \in W^{1,1}(0, T; L^2(\Omega)) \cap L^2(0, T; L^2(\Omega))$ and $\mathbf{u}_0 \in \mathbf{H}_\Delta$ satisfying (3.23). Then, there exist constants $C_{BF,1}, C_{BF,2} > 0$ only depending on $\|\mathbf{i}_p\|, |\Omega|, v, \alpha, F, \beta, \kappa_1$, and κ_2 such that*

$$\begin{aligned} & \|\mathbf{u}\|_{L^\infty(0,T;L^2(\Omega))} + \|\mathbf{u}\|_{L^2(0,T;\mathbf{H}^1(\Omega))} + \|\boldsymbol{\omega}\|_{L^2(0,T;L^2(\Omega))} + \|p\|_{L^2(0,T;L^2(\Omega))} \\ & \leq C_{BF,1} \left\{ \|\mathbf{f}\|_{L^2(0,T;L^2(\Omega))}^{2(p-1)/p} + \|\mathbf{f}\|_{L^2(0,T;L^2(\Omega))} + \|\mathbf{u}_0\|_{L^p(\Omega)}^{p-1} + \|\mathbf{u}_0\|_{L^p(\Omega)}^{p/2} + \|\mathbf{u}_0\|_{\mathbf{H}^1(\Omega)}^{2(p-1)/p} + \|\mathbf{u}_0\|_{\mathbf{H}^1(\Omega)} \right\}, \end{aligned} \tag{3.30}$$

and

$$\|\mathbf{u}\|_{L^\infty(0,T;\mathbf{H}^1(\Omega))} \leq C_{\text{BF},2} \left\{ \|\mathbf{f}\|_{L^2(0,T;L^2(\Omega))} + \|\mathbf{u}_0\|_{L^p(\Omega)}^{p/2} + \|\mathbf{u}_0\|_{\mathbf{H}^1(\Omega)} \right\}. \tag{3.31}$$

Proof. We proceed as in [6, Theorem 3.3]. In fact, we begin choosing $(\underline{\mathbf{v}}, q) = (\underline{\mathbf{u}}, p)$ in (2.9) to get

$$\frac{1}{2} \partial_t (\mathbf{u}, \mathbf{u})_\Omega + [\mathcal{A}(\underline{\mathbf{u}}), \underline{\mathbf{u}}] = (\mathbf{f}, \mathbf{u})_\Omega.$$

Next, from the definition of the operator \mathcal{A} (cf. (2.11)), employing similar arguments to (3.16) and using Cauchy–Schwarz and Young’s inequalities, we obtain

$$\begin{aligned} \frac{1}{2} \partial_t \|\mathbf{u}\|_{L^2(\Omega)}^2 + \alpha \|\mathbf{u}\|_{L^2(\Omega)}^2 + F \|\mathbf{u}\|_{L^p(\Omega)}^p + \kappa_1 \|\mathbf{curl}(\mathbf{u})\|_{L^2(\Omega)}^2 + \kappa_2 \|\text{div}(\mathbf{u})\|_{L^2(\Omega)}^2 \\ + \gamma_2 \|\boldsymbol{\omega}\|_{L^2(\Omega)}^2 \leq \frac{\delta}{2} \|\mathbf{f}\|_{L^2(\Omega)}^2 + \frac{1}{2\delta} \|\mathbf{u}\|_{L^2(\Omega)}^2, \end{aligned} \tag{3.32}$$

where γ_2 is defined in (3.17). Then, choosing $\delta = 1/\alpha$ and integrating (3.32) from 0 to $t \in (0, T]$, we obtain

$$\begin{aligned} \|\mathbf{u}(t)\|_{L^2(\Omega)}^2 + \int_0^t \left(\alpha \|\mathbf{u}\|_{L^2(\Omega)}^2 + 2\kappa_1 \|\mathbf{curl}(\mathbf{u})\|_{L^2(\Omega)}^2 + 2\kappa_2 \|\text{div}(\mathbf{u})\|_{L^2(\Omega)}^2 + 2\gamma_2 \|\boldsymbol{\omega}\|_{L^2(\Omega)}^2 \right) ds \\ \leq \frac{1}{\alpha} \int_0^t \|\mathbf{f}\|_{L^2(\Omega)}^2 ds + \|\mathbf{u}(0)\|_{L^2(\Omega)}^2. \end{aligned} \tag{3.33}$$

Notice that, in order to simplify the stability bound, we have neglected the term $\|\mathbf{u}\|_{L^p(\Omega)}^p$ in the left hand side of (3.32).

On the other hand, from the inf–sup condition of \mathcal{B} (cf. (3.21)), the first equation of (2.9) related to \mathbf{v} , the stability bounds of \mathbf{F} , \mathcal{E} (cf. (3.3), (3.4)), the definition of \mathcal{A} (cf. (2.11)), and the continuous injection of $\mathbf{H}^1(\Omega)$ into $L^p(\Omega)$, with $p \in [3, 4]$, we deduce that

$$\begin{aligned} \beta \|p\|_{L^2(\Omega)} \leq \sup_{\mathbf{0} \neq \mathbf{v} \in \mathbf{H}_0^1(\Omega)} \frac{[\mathbf{F}, (\mathbf{v}, \mathbf{0})] - [\partial_t \mathcal{E}(\underline{\mathbf{u}}), (\mathbf{v}, \mathbf{0})] - [\mathcal{A}(\underline{\mathbf{u}}), (\mathbf{v}, \mathbf{0})]}{\|\mathbf{v}\|_{\mathbf{H}^1(\Omega)}} \\ \leq \|\mathbf{f}\|_{L^2(\Omega)} + \alpha \|\mathbf{u}\|_{L^2(\Omega)} + F \|\mathbf{i}_p\| \|\mathbf{u}\|_{L^p(\Omega)}^{p-1} + \kappa_1 \|\mathbf{curl}(\mathbf{u})\|_{L^2(\Omega)} \\ + \kappa_2 \|\text{div}(\mathbf{u})\|_{L^2(\Omega)} + \gamma_2 \|\boldsymbol{\omega}\|_{L^2(\Omega)} + \|\partial_t \mathbf{u}\|_{L^2(\Omega)}. \end{aligned} \tag{3.34}$$

Then, taking square in (3.34), integrating from 0 to $t \in (0, T]$, and using (3.33), we get

$$\int_0^t \|p\|_{L^2(\Omega)}^2 ds \leq C_1 \left\{ \int_0^t \|\mathbf{f}\|_{L^2(\Omega)}^2 ds + \|\mathbf{u}(0)\|_{L^2(\Omega)}^2 + \int_0^t \left(F \|\mathbf{u}\|_{L^p(\Omega)}^{2(p-1)} + \|\partial_t \mathbf{u}\|_{L^2(\Omega)}^2 \right) ds \right\}, \tag{3.35}$$

with $C_1 > 0$ depending on $|\Omega|$, $\|\mathbf{i}_p\|$, ν , F , α , β , κ_1 and κ_2 . Next, in order to bound the last two terms in (3.35), we differentiate in time the equations of (2.9) related to $\boldsymbol{\psi}$ and q , choose $(\underline{\mathbf{v}}, q) = ((\partial_t \mathbf{u}, \boldsymbol{\omega}), p)$, and employ Cauchy–Schwarz and Young’s inequalities, to find that

$$\begin{aligned} \frac{1}{2} \partial_t \left(\alpha \|\mathbf{u}\|_{L^2(\Omega)}^2 + \frac{2F}{p} \|\mathbf{u}\|_{L^p(\Omega)}^p + \kappa_2 \|\text{div}(\mathbf{u})\|_{L^2(\Omega)}^2 + \nu \|\boldsymbol{\omega}\|_{L^2(\Omega)}^2 \right) + \|\partial_t \mathbf{u}\|_{L^2(\Omega)}^2 \\ + \kappa_1 (\mathbf{curl}(\mathbf{u}) - \boldsymbol{\omega}, \partial_t \mathbf{curl}(\mathbf{u}))_\Omega + \kappa_1 (\partial_t (\mathbf{curl}(\mathbf{u}) - \boldsymbol{\omega}), \boldsymbol{\omega})_\Omega \leq \frac{1}{2} \|\mathbf{f}\|_{L^2(\Omega)}^2 + \frac{1}{2} \|\partial_t \mathbf{u}\|_{L^2(\Omega)}^2. \end{aligned} \tag{3.36}$$

Using the linearity of the time derivative, it follows that

$$\kappa_1 (\mathbf{curl}(\mathbf{u}) - \boldsymbol{\omega}, \partial_t \mathbf{curl}(\mathbf{u}))_\Omega + \kappa_1 (\partial_t (\mathbf{curl}(\mathbf{u}) - \boldsymbol{\omega}), \boldsymbol{\omega})_\Omega = \frac{1}{2} \partial_t \left(\kappa_1 \|\mathbf{curl}(\mathbf{u})\|_{L^2(\Omega)}^2 - \kappa_1 \|\boldsymbol{\omega}\|_{L^2(\Omega)}^2 \right). \tag{3.37}$$

Thus, replacing back (3.37) into (3.36), integrating from 0 to $t \in (0, T]$ and using (2.7), we get

$$\begin{aligned} \alpha \|\mathbf{u}(t)\|_{L^2(\Omega)}^2 + \frac{2F}{p} \|\mathbf{u}(t)\|_{L^p(\Omega)}^p + \gamma_1 \|\nabla \mathbf{u}(t)\|_{L^2(\Omega)}^2 + \gamma_2 \|\boldsymbol{\omega}(t)\|_{L^2(\Omega)}^2 + \int_0^t \|\partial_t \mathbf{u}\|_{L^2(\Omega)}^2 ds \\ \leq \int_0^t \|\mathbf{f}\|_{L^2(\Omega)}^2 ds + \alpha \|\mathbf{u}(0)\|_{L^2(\Omega)}^2 + \frac{2F}{p} \|\mathbf{u}(0)\|_{L^p(\Omega)}^p + \gamma_1 \|\nabla \mathbf{u}(0)\|_{L^2(\Omega)}^2 + \gamma_2 \|\boldsymbol{\omega}(0)\|_{L^2(\Omega)}^2, \end{aligned} \tag{3.38}$$

with γ_1 and γ_2 defined in (3.17). Combining (3.38) with (3.35), yields

$$\int_0^t \|P\|_{L^2(\Omega)}^2 ds \leq C_2 \left\{ \left(\int_0^t \|\mathbf{f}\|_{L^2(\Omega)}^2 ds \right)^{2(p-1)/p} + \int_0^t \|\mathbf{f}\|_{L^2(\Omega)}^2 ds + \|\mathbf{u}(0)\|_{L^p(\Omega)}^{2(p-1)} + \|\mathbf{u}(0)\|_{L^p(\Omega)}^p + \|\mathbf{u}(0)\|_{\mathbf{H}^1(\Omega)}^{4(p-1)/p} + \|\mathbf{u}(0)\|_{\mathbf{H}^1(\Omega)}^2 + \|\boldsymbol{\omega}(0)\|_{L^2(\Omega)}^{4(p-1)/p} + \|\boldsymbol{\omega}(0)\|_{L^2(\Omega)}^2 \right\}, \tag{3.39}$$

with $C_2 > 0$ depending on $|\Omega|, \|\mathbf{i}_p\|, \nu, F, \alpha, \beta, \kappa_1$ and κ_2 , which, combined with (3.33) and the fact that $(\mathbf{u}(0), \boldsymbol{\omega}(0)) = (\mathbf{u}_0, \boldsymbol{\omega}_0)$ and $\boldsymbol{\omega}_0 = \mathbf{curl}(\mathbf{u}_0)$ in Ω (cf. Lemma 3.7), implies (3.30). In addition, the first and third terms in the left-hand side of (3.38) and some algebraic computations yields (3.31) concluding the proof. \square

Remark 3.5. We note that (3.31) can be expanded to include a bound on $\|\mathbf{u}\|_{\mathbf{H}^1(0,T;L^2(\Omega))}, \|\boldsymbol{\omega}\|_{L^\infty(0,T;L^2(\Omega))}$, and $\|P\|_{L^\infty(0,T;L^2(\Omega))}$, using (3.38) and (3.39). We state it in this simpler form, since the bound on $\|\mathbf{u}\|_{L^\infty(0,T;\mathbf{H}^1(\Omega))}$ will be employed in the next section to deal with the nonlinear term associated to the operator \mathcal{A} (cf. (2.11)), which is necessary to obtain the error estimate.

Remark 3.6. Bound (3.33) and the identity (2.7) show that the stability constant for $\|\nabla \mathbf{u}\|_{L^2(0,T;L^2(\Omega))}$ is linearly dependent on $\frac{1}{\sqrt{\gamma_1}}$, $\gamma_1 = \min\{\kappa_1, \kappa_2\}$, while the one for $\|\boldsymbol{\omega}\|_{L^2(0,T;L^2(\Omega))}$ is linearly dependent on $\frac{1}{\sqrt{\gamma_2}}$, $\gamma_2 = \nu - \kappa_1$. In addition, bounds (3.33) and (3.39) show that the stability constants for $\|\mathbf{u}\|_{L^2(0,T;L^2(\Omega))}$ and $\|P\|_{L^2(0,T;L^2(\Omega))}$ do not depend on $\frac{1}{\nu}, \frac{1}{\kappa_1}$, or $\frac{1}{\kappa_2}$.

4. Semidiscrete continuous-in-time approximation

In this section we introduce and analyze the semidiscrete continuous-in-time approximation of (2.9). We analyze its solvability by employing the strategy developed in Section 3. Finally, we derive the error estimates and obtain the corresponding rates of convergence.

4.1. Existence and uniqueness of a solution

Let \mathcal{T}_h be a shape-regular triangulation of Ω consisting of triangles K (when $d = 2$) or tetrahedra K (when $d = 3$) of diameter h_K , and define the mesh-size $h := \max\{h_K : K \in \mathcal{T}_h\}$. Let $(\mathbf{H}_h^u, \mathbf{H}_h^p)$ be a pair of stable Stokes elements satisfying the discrete inf-sup condition: there exists a constant $\tilde{\beta} > 0$, independent of h , such that

$$\sup_{\mathbf{0} \neq \mathbf{v}_h \in \mathbf{H}_h^u} \frac{\int_\Omega q_h \operatorname{div}(\mathbf{v}_h)}{\|\mathbf{v}_h\|_{\mathbf{H}^1(\Omega)}} \geq \tilde{\beta} \|q_h\|_{L^2(\Omega)} \quad \forall q_h \in \mathbf{H}_h^p. \tag{4.1}$$

We refer the reader to [23,24] for examples of stable Stokes elements. To simplify the presentation, we focus on Taylor–Hood [25] finite elements for velocity and pressure, and continuous piecewise polynomials spaces for vorticity. Given an integer $l \geq 0$ and a subset S of \mathbb{R}^d , we denote by $P_l(S)$ the space of polynomials of total degree at most l defined on S . For any $k \geq 1$, we consider:

$$\begin{aligned} \mathbf{H}_h^u &:= \left\{ \mathbf{v}_h \in [C(\overline{\Omega})]^d : \mathbf{v}_h|_K \in [P_{k+1}(K)]^d \quad \forall K \in \mathcal{T}_h \right\} \cap \mathbf{H}_0^1(\Omega), \\ \mathbf{H}_h^p &:= \left\{ q_h \in C(\overline{\Omega}) : q_h|_K \in P_k(K) \quad \forall K \in \mathcal{T}_h \right\} \cap L_0^2(\Omega), \\ \mathbf{H}_h^\omega &:= \left\{ \boldsymbol{\omega}_h \in [C(\overline{\Omega})]^{d(d-1)/2} : \boldsymbol{\omega}_h|_K \in [P_k(K)]^{d(d-1)/2} \quad \forall K \in \mathcal{T}_h \right\}. \end{aligned} \tag{4.2}$$

It is well known that the pair $(\mathbf{H}_h^u, \mathbf{H}_h^p)$ in (4.2) satisfies (4.1) [26]. We observe that similarly to [12,15], we can also consider discontinuous piecewise polynomials spaces for the vorticity, that is,

$$\mathbf{H}_h^\omega := \left\{ \boldsymbol{\omega}_h \in [L^2(\Omega)]^{d(d-1)/2} : \boldsymbol{\omega}_h|_K \in [P_k(K)]^{d(d-1)/2} \quad \forall K \in \mathcal{T}_h \right\}.$$

In addition to the Taylor–Hood elements for the velocity and pressure, in the numerical experiments in Section 6 we also consider the classical MINI-element [23, Sections 8.4.2, 8.6 and 8.7] and Crouzeix–Raviart elements with

tangential jump penalization (see [27] for the discrete inf–sup condition for the lowest-order case and, e.g., the recent paper [28] for cubic order).

Now, defining $\underline{\mathbf{u}}_h := (\mathbf{u}_h, \boldsymbol{\omega}_h)$, $\underline{\mathbf{v}}_h := (\mathbf{v}_h, \boldsymbol{\psi}_h) \in \mathbf{H}_h^{\mathbf{u}} \times \mathbf{H}_h^{\boldsymbol{\omega}}$, the semidiscrete continuous-in-time problem associated with (2.9) reads: Find $(\underline{\mathbf{u}}_h, p_h) : [0, T] \rightarrow (\mathbf{H}_h^{\mathbf{u}} \times \mathbf{H}_h^{\boldsymbol{\omega}}) \times \mathbf{H}_h^p$ such that, for a.e. $t \in (0, T)$,

$$\begin{aligned} \frac{\partial}{\partial t} [\mathcal{E}(\underline{\mathbf{u}}_h), \underline{\mathbf{v}}_h] + [\mathcal{A}(\underline{\mathbf{u}}_h), \underline{\mathbf{v}}_h] + [\mathcal{B}(\underline{\mathbf{v}}_h), p_h] &= [\mathbf{F}, \underline{\mathbf{v}}_h] \quad \forall \underline{\mathbf{v}}_h \in \mathbf{H}_h^{\mathbf{u}} \times \mathbf{H}_h^{\boldsymbol{\omega}}, \\ -[\mathcal{B}(\underline{\mathbf{u}}_h), q_h] &= 0 \quad \forall q_h \in \mathbf{H}_h^p. \end{aligned} \tag{4.3}$$

As initial condition we take $(\underline{\mathbf{u}}_{h,0}, p_{h,0}) = ((\mathbf{u}_{h,0}, \boldsymbol{\omega}_{h,0}), p_{h,0})$ to be a suitable approximations of $(\underline{\mathbf{u}}_0, p_0)$, the solution of (3.25), that is, we chose $(\underline{\mathbf{u}}_{h,0}, p_{h,0})$ solving

$$\begin{aligned} [\mathcal{A}(\underline{\mathbf{u}}_{h,0}), \underline{\mathbf{v}}_h] + [\mathcal{B}(\underline{\mathbf{v}}_h), p_{h,0}] &= [\mathbf{F}_0, \underline{\mathbf{v}}_h] \quad \forall \underline{\mathbf{v}}_h \in \mathbf{H}_h^{\mathbf{u}} \times \mathbf{H}_h^{\boldsymbol{\omega}}, \\ -[\mathcal{B}(\underline{\mathbf{u}}_{h,0}), q_h] &= 0 \quad \forall q_h \in \mathbf{H}_h^p, \end{aligned} \tag{4.4}$$

with $\mathbf{F}_0 \in \mathbf{L}^2(\Omega) \times \{\mathbf{0}\}$ being the right-hand side of (3.25). This choice is necessary to guarantee that the discrete initial data is compatible in the sense of Lemma 3.7, which is needed for the application of Theorem 3.1. Notice that the well-posedness of problem (4.4) follows from similar arguments to the proof of Lemma 3.6. In addition, taking $(\underline{\mathbf{v}}_h, q_h) = (\underline{\mathbf{u}}_{h,0}, p_{h,0})$ in (4.4), we deduce from the definition of the operator \mathcal{A} (cf. (2.11)), the identity (2.7), and the continuity bound of \mathbf{F}_0 (cf. (3.26)) that, there exists a constant $C_0 > 0$, depending only on $|\Omega|$, $\|\mathbf{i}_p\|$, ν , α , \mathbf{F} , κ_1 , and κ_2 , and hence independent of h , such that

$$\|\mathbf{u}_{h,0}\|_{\mathbf{L}^p(\Omega)}^p + \|\mathbf{u}_{h,0}\|_{\mathbf{H}^1(\Omega)}^2 + \|\boldsymbol{\omega}_{h,0}\|_{\mathbf{L}^2(\Omega)}^2 \leq C_0 \left\{ \|\mathbf{u}_0\|_{\mathbf{H}^1(\Omega)}^{2(p-1)} + \|\Delta \mathbf{u}_0\|_{\mathbf{L}^2(\Omega)}^2 + \|\mathbf{u}_0\|_{\mathbf{L}^2(\Omega)}^2 \right\}. \tag{4.5}$$

In this way, the well-posedness of (4.3) follows analogously to its continuous counterpart provided in Theorem 3.8. More precisely, we first address the discrete counterparts of Lemmas 3.3 and 3.4, whose proofs, being almost verbatim of the continuous ones, are omitted.

Lemma 4.1. *Let $p \in [3, 4]$. Assume κ_1 and κ_2 as in Lemma 3.4. Then, the family of operators $\{(\mathcal{E} + \mathcal{A})(\cdot) + \mathcal{z}_h\} : \mathbf{H}_h^{\mathbf{u}} \times \mathbf{H}_h^{\boldsymbol{\omega}} \rightarrow (\mathbf{H}_h^{\mathbf{u}} \times \mathbf{H}_h^{\boldsymbol{\omega}})'$: $\mathcal{z}_h \in \mathbf{H}_h^{\mathbf{u}} \times \mathbf{H}_h^{\boldsymbol{\omega}}\}$ is uniformly strongly monotone with the same constant $\gamma_{\text{BF}} > 0$ from (3.14), that is, there holds*

$$[(\mathcal{E} + \mathcal{A})(\underline{\mathbf{u}}_h + \mathcal{z}_h) - (\mathcal{E} + \mathcal{A})(\underline{\mathbf{v}}_h + \mathcal{z}_h), \underline{\mathbf{u}}_h - \underline{\mathbf{v}}_h] \geq \gamma_{\text{BF}} \|\underline{\mathbf{u}}_h - \underline{\mathbf{v}}_h\|^2,$$

for each $\mathcal{z}_h = (\mathcal{z}_h, \boldsymbol{\phi}_h) \in \mathbf{H}_h^{\mathbf{u}} \times \mathbf{H}_h^{\boldsymbol{\omega}}$, and for all $\underline{\mathbf{u}}_h = (\mathbf{u}_h, \boldsymbol{\omega}_h)$, $\underline{\mathbf{v}}_h = (\mathbf{v}_h, \boldsymbol{\psi}_h) \in \mathbf{H}_h^{\mathbf{u}} \times \mathbf{H}_h^{\boldsymbol{\omega}}$. In addition, the operator $\mathcal{E} + \mathcal{A} : (\mathbf{H}_h^{\mathbf{u}} \times \mathbf{H}_h^{\boldsymbol{\omega}}) \rightarrow (\mathbf{H}_h^{\mathbf{u}} \times \mathbf{H}_h^{\boldsymbol{\omega}})'$ is continuous in the sense of (3.12), with the same constant L_{BF} .

We continue with the discrete inf–sup condition of \mathcal{B} .

Lemma 4.2. *There exists a constant $\tilde{\beta} > 0$, such that*

$$\sup_{\mathbf{0} \neq \underline{\mathbf{v}}_h \in \mathbf{H}_h^{\mathbf{u}} \times \mathbf{H}_h^{\boldsymbol{\omega}}} \frac{[\mathcal{B}(\underline{\mathbf{v}}_h), q_h]}{\|\underline{\mathbf{v}}_h\|} \geq \tilde{\beta} \|q_h\|_{\mathbf{L}^2(\Omega)} \quad \forall q_h \in \mathbf{H}_h^p. \tag{4.6}$$

Proof. The statement follows directly from (4.1). \square

We are now in a position to establish the semi-discrete continuous in time analogue of Theorems 3.8 and 3.9.

Theorem 4.3. *Let $p \in [3, 4]$. Assume κ_1 and κ_2 as in Lemma 3.4. Then, for each compatible initial data $(\underline{\mathbf{u}}_{h,0}, p_{h,0}) := ((\mathbf{u}_{h,0}, \boldsymbol{\omega}_{h,0}), p_{h,0})$ satisfying (4.4) and $\mathbf{f} \in \mathbf{W}^{1,1}(0, T; \mathbf{L}^2(\Omega))$, there exists a unique $(\underline{\mathbf{u}}_h, p_h) = ((\mathbf{u}_h, \boldsymbol{\omega}_h), p_h) : [0, T] \rightarrow (\mathbf{H}_h^{\mathbf{u}} \times \mathbf{H}_h^{\boldsymbol{\omega}}) \times \mathbf{H}_h^p$ solution to (4.3), satisfying $\mathbf{u}_h \in \mathbf{W}^{1,\infty}(0, T; \mathbf{H}_h^{\mathbf{u}})$ and $(\mathbf{u}_h(0), \boldsymbol{\omega}_h(0)) = (\mathbf{u}_{h,0}, \boldsymbol{\omega}_{h,0})$. Moreover, assuming that $\mathbf{u}_0 \in \mathbf{H}_{\Delta}$ satisfies (3.23) and that $\mathbf{f} \in \mathbf{L}^2(0, T; \mathbf{L}^2(\Omega))$, there exist constants $\widehat{C}_{\text{BF},1}, \widehat{C}_{\text{BF},2} > 0$ depending only on $|\Omega|$, $\|\mathbf{i}_p\|$, ν , α , \mathbf{F} , $\tilde{\beta}$, κ_1 , and κ_2 such that*

$$\begin{aligned} &\|\mathbf{u}_h\|_{\mathbf{L}^{\infty}(0, T; \mathbf{L}^2(\Omega))} + \|\mathbf{u}_h\|_{\mathbf{L}^2(0, T; \mathbf{H}^1(\Omega))} + \|\boldsymbol{\omega}_h\|_{\mathbf{L}^2(0, T; \mathbf{L}^2(\Omega))} + \|p_h\|_{\mathbf{L}^2(0, T; \mathbf{L}^2(\Omega))} \\ &\leq \widehat{C}_{\text{BF},1} \left\{ \|\mathbf{f}\|_{\mathbf{L}^2(0, T; \mathbf{L}^2(\Omega))}^{2(p-1)/p} + \|\mathbf{f}\|_{\mathbf{L}^2(0, T; \mathbf{L}^2(\Omega))} + \|\mathbf{u}_0\|_{\mathbf{H}^1(\Omega)}^{2(p-1)^2/p} + \|\mathbf{u}_0\|_{\mathbf{H}^1(\Omega)}^{p-1} \right. \\ &\quad \left. + \|\Delta \mathbf{u}_0\|_{\mathbf{L}^2(\Omega)}^{2(p-1)/p} + \|\Delta \mathbf{u}_0\|_{\mathbf{L}^2(\Omega)} + \|\mathbf{u}_0\|_{\mathbf{L}^2(\Omega)}^{2(p-1)/p} + \|\mathbf{u}_0\|_{\mathbf{L}^2(\Omega)} \right\} \end{aligned} \tag{4.7}$$

and

$$\|\mathbf{u}_h\|_{L^\infty(0,T;\mathbf{H}^1(\Omega))} \leq \widehat{C}_{\text{BF},2} \left\{ \|\mathbf{f}\|_{L^2(0,T;L^2(\Omega))} + \|\mathbf{u}_0\|_{\mathbf{H}^1(\Omega)}^{p-1} + \|\Delta \mathbf{u}_0\|_{L^2(\Omega)} + \|\mathbf{u}_0\|_{L^2(\Omega)} \right\}. \tag{4.8}$$

Proof. According to Lemma 4.1, the discrete inf–sup condition for \mathcal{B} provided by (4.6) (cf. Lemma 4.2), and considering that $(\mathbf{u}_{h,0}, p_{h,0})$ satisfies (4.4), the proof of existence and uniqueness of solution of (4.3) with $\mathbf{u}_h \in \mathbf{W}^{1,\infty}(0, T; \mathbf{H}_h^{\mathbf{u}})$ and $\mathbf{u}_h(0) = \mathbf{u}_{h,0}$, follows similarly to the proof of Theorem 3.8 by applying Theorem 3.1. Moreover, from the discrete version of (3.29), we deduce that $\boldsymbol{\omega}_h(0) = \boldsymbol{\omega}_{h,0}$.

On the other hand, mimicking the steps followed in the proof of Theorem 3.9, we obtain the discrete versions of (3.33)–(3.39). Then, using the fact that $(\mathbf{u}_h(0), \boldsymbol{\omega}_h(0)) = (\mathbf{u}_{h,0}, \boldsymbol{\omega}_{h,0})$ and estimate (4.5), we derive (4.7) and (4.8), thus completing the proof. \square

4.2. Error analysis

Now we derive suitable error estimates for the semidiscrete scheme (4.3). To that end, we first introduce the discrete kernel of \mathcal{B} , that is, $\mathbf{V}_h := \mathbf{K}_h \times \mathbf{H}_h^\omega$, where

$$\mathbf{K}_h = \left\{ \mathbf{v}_h \in \mathbf{H}_h^{\mathbf{u}} : (q_h, \text{div}(\mathbf{v}_h))_\Omega = 0 \quad \forall q_h \in \mathbf{H}_h^p \right\}, \tag{4.9}$$

and recall that the discrete inf–sup condition of \mathcal{B} (cf. (4.6)), and a classical result on mixed methods (see, for instance [29, Eq. (2.89) in Theorem 2.6]) ensure the existence of a constant $C > 0$, independent of h , such that:

$$\inf_{\mathbf{v}_h \in \mathbf{V}_h} \|\underline{\mathbf{u}} - \mathbf{v}_h\| \leq C \inf_{\mathbf{v}_h \in \mathbf{H}_h^{\mathbf{u}} \times \mathbf{H}_h^\omega} \|\underline{\mathbf{u}} - \mathbf{v}_h\|. \tag{4.10}$$

Next, in order to obtain the theoretical rates of convergence for the discrete scheme (4.3), we recall the approximation properties of the finite element subspaces $\mathbf{H}_h^{\mathbf{u}}$, \mathbf{H}_h^ω , and \mathbf{H}_h^p (cf. (4.2)), that can be found in [23,24], and [22]. Assume that $\mathbf{u} \in \mathbf{H}^{1+s}(\Omega)$, $\boldsymbol{\omega} \in [\mathbf{H}^s(\Omega)]^{d(d-1)/2}$, and $p \in \mathbf{H}^s(\Omega)$, for some $s \in (1/2, k + 1]$. Then there exists $C > 0$, independent of h , such that

$$\inf_{\mathbf{v}_h \in \mathbf{H}_h^{\mathbf{u}}} \|\mathbf{u} - \mathbf{v}_h\|_{\mathbf{H}^1(\Omega)} \leq C h^s \|\mathbf{u}\|_{\mathbf{H}^{1+s}(\Omega)}, \tag{4.11}$$

$$\inf_{\boldsymbol{\psi}_h \in \mathbf{H}_h^\omega} \|\boldsymbol{\omega} - \boldsymbol{\psi}_h\|_{L^2(\Omega)} \leq C h^s \|\boldsymbol{\omega}\|_{\mathbf{H}^s(\Omega)}, \tag{4.12}$$

$$\inf_{q_h \in \mathbf{H}_h^p} \|p - q_h\|_{L^2(\Omega)} \leq C h^s \|p\|_{\mathbf{H}^s(\Omega)}. \tag{4.13}$$

Owing to (4.10) and (4.11)–(4.13), it follows that, under an extra regularity assumption on the exact solution, there exist positive constants $C(\underline{\mathbf{u}})$, $C(\partial_t \underline{\mathbf{u}})$, $C(p)$, and $C(\partial_t p)$, depending on \mathbf{u} , $\boldsymbol{\omega}$ and p , respectively, such that

$$\begin{aligned} \inf_{\mathbf{v}_h \in \mathbf{V}_h} \|\underline{\mathbf{u}} - \mathbf{v}_h\| &\leq C(\underline{\mathbf{u}}) h^s, & \inf_{\mathbf{v}_h \in \mathbf{V}_h} \|\partial_t \underline{\mathbf{u}} - \mathbf{v}_h\| &\leq C(\partial_t \underline{\mathbf{u}}) h^s, \\ \inf_{q_h \in \mathbf{H}_h^p} \|p - q_h\|_{L^2(\Omega)} &\leq C(p) h^s, & \inf_{q_h \in \mathbf{H}_h^p} \|\partial_t p - q_h\|_{L^2(\Omega)} &\leq C(\partial_t p) h^s. \end{aligned} \tag{4.14}$$

In turn, in order to simplify the subsequent analysis, we write $\mathbf{e}_{\underline{\mathbf{u}}} = (\mathbf{e}_{\mathbf{u}}, \mathbf{e}_{\boldsymbol{\omega}}) = (\mathbf{u} - \mathbf{u}_h, \boldsymbol{\omega} - \boldsymbol{\omega}_h)$, and $\mathbf{e}_p = p - p_h$. Next, given arbitrary $\widehat{\mathbf{v}}_h := (\widehat{\mathbf{v}}_h, \widehat{\boldsymbol{\omega}}_h) : [0, T] \rightarrow \mathbf{V}_h$ (cf. (4.9)) and $\widehat{q}_h : [0, T] \rightarrow \mathbf{H}_h^p$, as usual, we shall then decompose the errors into

$$\mathbf{e}_{\underline{\mathbf{u}}} = \boldsymbol{\delta}_{\underline{\mathbf{u}}} + \boldsymbol{\eta}_{\underline{\mathbf{u}}} = (\boldsymbol{\delta}_{\mathbf{u}}, \boldsymbol{\delta}_{\boldsymbol{\omega}}) + (\boldsymbol{\eta}_{\mathbf{u}}, \boldsymbol{\eta}_{\boldsymbol{\omega}}), \quad \mathbf{e}_p = \boldsymbol{\delta}_p + \boldsymbol{\eta}_p, \tag{4.15}$$

with

$$\boldsymbol{\delta}_{\mathbf{u}} = \mathbf{u} - \widehat{\mathbf{v}}_h, \quad \boldsymbol{\delta}_{\boldsymbol{\omega}} = \boldsymbol{\omega} - \widehat{\boldsymbol{\psi}}_h, \quad \boldsymbol{\delta}_p = p - \widehat{q}_h, \tag{4.16}$$

$$\boldsymbol{\eta}_{\mathbf{u}} = \widehat{\mathbf{v}}_h - \mathbf{u}_h, \quad \boldsymbol{\eta}_{\boldsymbol{\omega}} = \widehat{\boldsymbol{\psi}}_h - \boldsymbol{\omega}_h, \quad \boldsymbol{\eta}_p = \widehat{q}_h - p_h.$$

In addition, we stress for later use that $\partial_t \mathbf{v}_h : [0, T] \rightarrow \mathbf{V}_h$ for each $\mathbf{v}_h(t) \in \mathbf{V}_h$ (cf. (4.9)). In fact, given $(\mathbf{v}_h, q_h) : [0, T] \rightarrow \mathbf{V}_h \times \mathbf{H}_h^p$, after simple algebraic computations, we obtain

$$[\mathcal{B}(\partial_t \mathbf{v}_h), q_h] = \partial_t([\mathcal{B}(\mathbf{v}_h), q_h]) - [\mathcal{B}(\mathbf{v}_h), \partial_t q_h] = 0, \tag{4.17}$$

where, the latter is obtained by observing that $\partial_t q_h(t) \in \mathbf{H}_h^p$.

In this way, by subtracting the discrete and continuous problems (2.9) and (4.3), respectively, we obtain the following system:

$$\begin{aligned} \frac{\partial}{\partial t} [\mathcal{E}(\mathbf{e}_u), \mathbf{v}_h] + [\mathcal{A}(\mathbf{u}) - \mathcal{A}(\mathbf{u}_h), \mathbf{v}_h] + [\mathcal{B}(\mathbf{v}_h), \mathbf{e}_p] &= 0 \quad \forall \mathbf{v}_h \in \mathbf{H}_h^u \times \mathbf{H}_h^\omega, \\ [\mathcal{B}(\mathbf{e}_u), q_h] &= 0 \quad \forall q_h \in \mathbf{H}_h^p. \end{aligned} \tag{4.18}$$

We now establish the main result of this section, namely, the theoretical rate of convergence of the discrete scheme (4.3). Notice that, optimal rates of convergences are obtained for all the unknowns.

Theorem 4.4. *Let $p \in [3, 4]$. Assume κ_1 and κ_2 as in Lemma 3.4. Let $((\mathbf{u}, \boldsymbol{\omega}), p) : [0, T] \rightarrow (\mathbf{H}_0^1(\Omega) \times \mathbf{L}^2(\Omega)) \times \mathbf{L}_0^2(\Omega)$ with $\mathbf{u} \in \mathbf{W}^{1,\infty}(0, T; \mathbf{L}^2(\Omega))$ and $((\mathbf{u}_h, \boldsymbol{\omega}_h), p_h) : [0, T] \rightarrow (\mathbf{H}_h^u \times \mathbf{H}_h^\omega) \times \mathbf{H}_h^p$ with $\mathbf{u}_h \in \mathbf{W}^{1,\infty}(0, T; \mathbf{H}_h^u)$, be the unique solutions of the continuous and semidiscrete problems (2.9) and (4.3), respectively. Assume further that there exists $s \in (1/2, k + 1]$, such that $\mathbf{u} \in \mathbf{H}^{1+s}(\Omega)$, $\boldsymbol{\omega} \in [\mathbf{H}^s(\Omega)]^{d(d-1)/2}$, and $p \in \mathbf{H}^s(\Omega)$. Then, there exists $C(\mathbf{u}, p) > 0$ depending only on $C(\mathbf{u}), C(\partial_t \mathbf{u}), C(p), C(\partial_t p), |\Omega|, \|\mathbf{i}_p\|, \|\mathbf{i}_{2(p-1)}\|, \nu, \alpha, F, \tilde{\beta}, \kappa_1, \kappa_2$, and data, such that*

$$\begin{aligned} \|\mathbf{e}_u\|_{\mathbf{L}^\infty(0,T;\mathbf{L}^2(\Omega))} + \|\mathbf{e}_u\|_{\mathbf{L}^2(0,T;\mathbf{H}^1(\Omega))} \\ + \|\mathbf{e}_\omega\|_{\mathbf{L}^2(0,T;\mathbf{L}^2(\Omega))} + \|\mathbf{e}_p\|_{\mathbf{L}^2(0,T;\mathbf{L}^2(\Omega))} \leq C(\mathbf{u}, p) \left(h^s + h^{s(p-1)} \right). \end{aligned} \tag{4.19}$$

Proof. First, adding and subtracting suitable terms in the first equation of (4.18), with $\mathbf{v}_h = \boldsymbol{\eta}_u = (\boldsymbol{\eta}_u, \boldsymbol{\eta}_\omega) : [0, T] \rightarrow \mathbf{V}_h$ (cf. (4.9)), proceeding as in (3.16) and using the fact that $\boldsymbol{\eta}_u(t) \in \mathbf{V}_h$, thus $[\mathcal{B}(\boldsymbol{\eta}_u), \boldsymbol{\eta}_p] = 0$, we deduce that

$$\begin{aligned} \frac{1}{2} \partial_t \|\boldsymbol{\eta}_u\|_{\mathbf{L}^2(\Omega)}^2 + \alpha \|\boldsymbol{\eta}_u\|_{\mathbf{L}^2(\Omega)}^2 + F C_p \|\boldsymbol{\eta}_u\|_{\mathbf{L}^p(\Omega)}^p + \kappa_1 \|\mathbf{curl}(\boldsymbol{\eta}_u)\|_{\mathbf{L}^2(\Omega)}^2 \\ + \kappa_2 \|\mathbf{div}(\boldsymbol{\eta}_u)\|_{\mathbf{L}^2(\Omega)}^2 + \gamma_2 \|\boldsymbol{\eta}_\omega\|_{\mathbf{L}^2(\Omega)}^2 \\ \leq -(\partial_t \boldsymbol{\delta}_u, \boldsymbol{\eta}_u)_\Omega - \alpha (\boldsymbol{\delta}_u, \boldsymbol{\eta}_u)_\Omega - F(|\mathbf{u}|^{p-2} \mathbf{u} - |\widehat{\mathbf{v}}_h|^{p-2} \widehat{\mathbf{v}}_h, \boldsymbol{\eta}_u)_\Omega - \nu (\boldsymbol{\delta}_\omega, \boldsymbol{\eta}_\omega + \mathbf{curl}(\boldsymbol{\eta}_u))_\Omega \\ + \nu (\boldsymbol{\eta}_\omega, \mathbf{curl}(\boldsymbol{\delta}_u))_\Omega - \kappa_1 (\mathbf{curl}(\boldsymbol{\delta}_u) - \boldsymbol{\delta}_\omega, \mathbf{curl}(\boldsymbol{\eta}_u) + \boldsymbol{\eta}_\omega)_\Omega + (\boldsymbol{\delta}_p - \kappa_2 \mathbf{div}(\boldsymbol{\delta}_u), \mathbf{div}(\boldsymbol{\eta}_u))_\Omega, \end{aligned} \tag{4.20}$$

with γ_2 defined in (3.17). The terms on the right hand side can be bounded using the Cauchy–Schwarz and Young’s inequalities (cf. (1.1)), and (3.8), as follows:

$$-(\partial_t \boldsymbol{\delta}_u, \boldsymbol{\eta}_u)_\Omega - \alpha (\boldsymbol{\delta}_u, \boldsymbol{\eta}_u)_\Omega \leq \frac{1}{\alpha} \|\partial_t \boldsymbol{\delta}_u\|_{\mathbf{L}^2(\Omega)}^2 + \alpha \|\boldsymbol{\delta}_u\|_{\mathbf{L}^2(\Omega)}^2 + \frac{\alpha}{2} \|\boldsymbol{\eta}_u\|_{\mathbf{L}^2(\Omega)}^2, \tag{4.21}$$

$$\begin{aligned} -F(|\mathbf{u}|^{p-2} \mathbf{u} - |\widehat{\mathbf{v}}_h|^{p-2} \widehat{\mathbf{v}}_h, \boldsymbol{\eta}_u)_\Omega \\ \leq F \tilde{c}_p \left(\|\mathbf{u}\|_{\mathbf{L}^{2(p-1)}(\Omega)} + \|\widehat{\mathbf{v}}_h\|_{\mathbf{L}^{2(p-1)}(\Omega)} \right)^{p-2} \|\boldsymbol{\delta}_u\|_{\mathbf{L}^{2(p-1)}(\Omega)} \|\boldsymbol{\eta}_u\|_{\mathbf{L}^2(\Omega)} \\ \leq F \tilde{c}_p \left(2 \|\mathbf{u}\|_{\mathbf{L}^{2(p-1)}(\Omega)} + \|\boldsymbol{\delta}_u\|_{\mathbf{L}^{2(p-1)}(\Omega)} \right)^{p-2} \|\boldsymbol{\delta}_u\|_{\mathbf{L}^{2(p-1)}(\Omega)} \|\boldsymbol{\eta}_u\|_{\mathbf{L}^2(\Omega)} \\ \leq \tilde{C} \left(\|\mathbf{u}\|_{\mathbf{H}^1(\Omega)}^{p-2} + \|\boldsymbol{\delta}_u\|_{\mathbf{H}^1(\Omega)}^{p-2} \right) \|\boldsymbol{\delta}_u\|_{\mathbf{H}^1(\Omega)} \|\boldsymbol{\eta}_u\|_{\mathbf{L}^2(\Omega)} \\ \leq \frac{2\tilde{C}}{\alpha} \left(\|\mathbf{u}\|_{\mathbf{H}^1(\Omega)}^{2(p-2)} \|\boldsymbol{\delta}_u\|_{\mathbf{H}^1(\Omega)}^2 + \|\boldsymbol{\delta}_u\|_{\mathbf{H}^1(\Omega)}^{2(p-1)} \right) + \frac{\alpha}{4} \|\boldsymbol{\eta}_u\|_{\mathbf{L}^2(\Omega)}^2 \end{aligned} \tag{4.22}$$

$$\gamma_2 (\mathbf{curl}(\boldsymbol{\delta}_u) - \boldsymbol{\delta}_\omega, \boldsymbol{\eta}_\omega) \leq \frac{\gamma_2}{2} \|\mathbf{curl}(\boldsymbol{\delta}_u) - \boldsymbol{\delta}_\omega\|_{\mathbf{L}^2(\Omega)}^2 + \frac{\gamma_2}{2} \|\boldsymbol{\eta}_\omega\|_{\mathbf{L}^2(\Omega)}^2, \tag{4.23}$$

$$\begin{aligned} -\nu (\boldsymbol{\delta}_\omega, \mathbf{curl}(\boldsymbol{\eta}_u))_\Omega - \kappa_1 (\mathbf{curl}(\boldsymbol{\delta}_u) - \boldsymbol{\delta}_\omega, \mathbf{curl}(\boldsymbol{\eta}_u))_\Omega \\ \leq \frac{\nu^2}{\kappa_1} \|\boldsymbol{\delta}_\omega\|_{\mathbf{L}^2(\Omega)}^2 + \kappa_1 \|\mathbf{curl}(\boldsymbol{\delta}_u) - \boldsymbol{\delta}_\omega\|_{\mathbf{L}^2(\Omega)}^2 + \frac{\kappa_1}{2} \|\mathbf{curl}(\boldsymbol{\eta}_u)\|_{\mathbf{L}^2(\Omega)}^2, \end{aligned} \tag{4.24}$$

$$(\boldsymbol{\delta}_p - \kappa_2 \mathbf{div}(\boldsymbol{\delta}_u), \mathbf{div}(\boldsymbol{\eta}_u))_\Omega \leq \frac{1}{\kappa_2} \|\boldsymbol{\delta}_p\|_{\mathbf{L}^2(\Omega)}^2 + \kappa_2 \|\mathbf{div}(\boldsymbol{\delta}_u)\|_{\mathbf{L}^2(\Omega)}^2 + \frac{\kappa_2}{2} \|\mathbf{div}(\boldsymbol{\eta}_u)\|_{\mathbf{L}^2(\Omega)}^2, \tag{4.25}$$

where $\tilde{C} > 0$ depends on $|\Omega|, \|\mathbf{i}_{2(p-1)}\|$, and F . We note that in (4.22) we used the continuous injection of $\mathbf{H}^1(\Omega)$ into $\mathbf{L}^{2(p-1)}(\Omega)$, with $2(p-1) \in [4, 6]$, cf. (1.2). Combining (4.20)–(4.25), using the identity (2.7), and neglecting the term $\|\boldsymbol{\eta}_u\|_{\mathbf{L}^p(\Omega)}^p$ in (4.20) to obtain a simplified error estimate, we get

$$\begin{aligned} \partial_t \|\boldsymbol{\eta}_u\|_{\mathbf{L}^2(\Omega)}^2 + \alpha \|\boldsymbol{\eta}_u\|_{\mathbf{L}^2(\Omega)}^2 + \gamma_1 \|\nabla \boldsymbol{\eta}_u\|_{\mathbf{L}^2(\Omega)}^2 + \gamma_2 \|\boldsymbol{\eta}_\omega\|_{\mathbf{L}^2(\Omega)}^2 \\ \leq C_1 \left(\|\partial_t \boldsymbol{\delta}_u\|_{\mathbf{L}^2(\Omega)}^2 + \|\boldsymbol{\delta}_u\|_{\mathbf{H}^1(\Omega)}^{2(p-1)} + (1 + \|\mathbf{u}\|_{\mathbf{H}^1(\Omega)}^{2(p-2)}) \|\boldsymbol{\delta}_u\|_{\mathbf{H}^1(\Omega)}^2 + \|\boldsymbol{\delta}_\omega\|_{\mathbf{L}^2(\Omega)}^2 + \|\boldsymbol{\delta}_p\|_{\mathbf{L}^2(\Omega)}^2 \right), \end{aligned} \tag{4.26}$$

with γ_1 defined in (3.17) and C_1 is a positive constant depending on $|\Omega|$, $\|\mathbf{i}_{2(p-1)}\|$, ν , α , \mathbf{F} , κ_1 , and κ_2 . Integrating (4.26) from 0 to $t \in (0, T]$, recalling that $\|\mathbf{u}\|_{L^\infty(0,T;\mathbf{H}^1(\Omega))}$ is bounded by data (cf. (3.31)), we find that

$$\begin{aligned} & \|\boldsymbol{\eta}_{\mathbf{u}}(t)\|_{\mathbf{L}^2(\Omega)}^2 + \int_0^t \left(\alpha \|\boldsymbol{\eta}_{\mathbf{u}}\|_{\mathbf{L}^2(\Omega)}^2 + \gamma_1 \|\nabla \boldsymbol{\eta}_{\mathbf{u}}\|_{\mathbf{L}^2(\Omega)}^2 + \gamma_2 \|\boldsymbol{\eta}_{\boldsymbol{\omega}}\|_{\mathbf{L}^2(\Omega)}^2 \right) ds \\ & \leq C_2 \int_0^t \left(\|\partial_t \boldsymbol{\delta}_{\mathbf{u}}\|_{\mathbf{L}^2(\Omega)}^2 + \|\boldsymbol{\delta}_{\mathbf{u}}\|_{\mathbf{H}^1(\Omega)}^{2(p-1)} + \|\boldsymbol{\delta}_{\mathbf{u}}\|^2 + \|\boldsymbol{\delta}_p\|_{\mathbf{L}^2(\Omega)}^2 \right) ds + \|\boldsymbol{\eta}_{\mathbf{u}}(0)\|_{\mathbf{L}^2(\Omega)}^2, \end{aligned} \tag{4.27}$$

with $C_2 > 0$ depending on $|\Omega|$, $\|\mathbf{i}_{2(p-1)}\|$, ν , α , \mathbf{F} , κ_1 , κ_2 , and data.

Next, in order to bound the last term in (4.27), we subtract the continuous and discrete initial condition problems (3.25) and (4.4), to obtain the error system:

$$\begin{aligned} [\mathcal{A}(\underline{\mathbf{u}}_0) - \mathcal{A}(\underline{\mathbf{u}}_{h,0}), \underline{\mathbf{v}}_h] + [\mathcal{B}(\underline{\mathbf{v}}_h), p_0 - p_{h,0}] &= 0 \quad \forall \underline{\mathbf{v}}_h \in \mathbf{H}_h^{\mathbf{u}} \times \mathbf{H}_h^{\boldsymbol{\omega}}, \\ -[\mathcal{B}(\underline{\mathbf{u}}_0 - \underline{\mathbf{u}}_{h,0}), q_h] &= 0 \quad \forall q_h \in \mathbf{H}_h^p. \end{aligned}$$

Then, proceeding as in (4.26), recalling from Theorems 3.8 and 4.3 that $(\mathbf{u}(0), \boldsymbol{\omega}(0)) = (\mathbf{u}_0, \boldsymbol{\omega}_0)$ and $(\mathbf{u}_h(0), \boldsymbol{\omega}_h(0)) = (\mathbf{u}_{h,0}, \boldsymbol{\omega}_{h,0})$, respectively, we get

$$\alpha \|\boldsymbol{\eta}_{\mathbf{u}}(0)\|_{\mathbf{L}^2(\Omega)}^2 + \gamma_1 \|\nabla \boldsymbol{\eta}_{\mathbf{u}}(0)\|_{\mathbf{L}^2(\Omega)}^2 + \gamma_2 \|\boldsymbol{\eta}_{\boldsymbol{\omega}}(0)\|_{\mathbf{L}^2(\Omega)}^2 \leq \widehat{C}_0 \left(\|\boldsymbol{\delta}_{\mathbf{u}_0}\|_{\mathbf{H}^1(\Omega)}^{2(p-1)} + \|\boldsymbol{\delta}_{\mathbf{u}_0}\|^2 + \|\boldsymbol{\delta}_{p_0}\|_{\mathbf{L}^2(\Omega)}^2 \right), \tag{4.28}$$

where, similarly to (4.16), we denote $\boldsymbol{\delta}_{\mathbf{u}_0} = (\boldsymbol{\delta}_{\mathbf{u}_0}, \boldsymbol{\delta}_{\boldsymbol{\omega}_0}) = (\mathbf{u}_0 - \widehat{\mathbf{v}}_h(0), \boldsymbol{\omega}_0 - \widehat{\boldsymbol{\psi}}_h(0))$ and $\boldsymbol{\delta}_{p_0} = p_0 - \widehat{q}_h(0)$, with arbitrary $(\widehat{\mathbf{v}}_h(0), \widehat{\boldsymbol{\psi}}_h(0)) \in \mathbf{V}_h$ and $\widehat{q}_h(0) \in \mathbf{H}_h^p$, and \widehat{C}_0 is a positive constant depending on $|\Omega|$, $\|\mathbf{i}_{2(p-1)}\|$, ν , α , \mathbf{F} , κ_1 , and κ_2 . Thus, combining (4.27) and (4.28), and using the error decomposition (4.15), there holds

$$\|\mathbf{e}_{\mathbf{u}}(t)\|_{\mathbf{L}^2(\Omega)}^2 + \int_0^t \left(\alpha \|\mathbf{e}_{\mathbf{u}}\|_{\mathbf{L}^2(\Omega)}^2 + \gamma_1 \|\nabla \mathbf{e}_{\mathbf{u}}\|_{\mathbf{L}^2(\Omega)}^2 + \gamma_2 \|\mathbf{e}_{\boldsymbol{\omega}}\|_{\mathbf{L}^2(\Omega)}^2 \right) ds \leq C \Psi(\underline{\mathbf{u}}, p), \tag{4.29}$$

where

$$\begin{aligned} \Psi(\underline{\mathbf{u}}, p) &:= \|\boldsymbol{\delta}_{\mathbf{u}}(t)\|^2 + \int_0^t \left(\|\partial_t \boldsymbol{\delta}_{\mathbf{u}}\|^2 + \|\boldsymbol{\delta}_{\mathbf{u}}\|^{2(p-1)} + \|\boldsymbol{\delta}_{\mathbf{u}}\|^2 + \|\boldsymbol{\delta}_p\|_{\mathbf{L}^2(\Omega)}^2 \right) ds \\ &+ \|\boldsymbol{\delta}_{\mathbf{u}_0}\|^{2(p-1)} + \|\boldsymbol{\delta}_{\mathbf{u}_0}\|^2 + \|\boldsymbol{\delta}_{p_0}\|_{\mathbf{L}^2(\Omega)}^2. \end{aligned}$$

On the other hand, to estimate $\|\mathbf{e}_p\|_{L^2(0,T;L^2(\Omega))}$, we observe that from the discrete inf-sup condition of \mathcal{B} (cf. (4.6)), the first equation of (4.18), and the continuity bounds of \mathcal{E} , \mathcal{A} , \mathcal{B} (cf. (3.4), (3.12), (3.2)), there holds

$$\begin{aligned} \widetilde{\beta} \|\boldsymbol{\eta}_p\|_{\mathbf{L}^2(\Omega)} &\leq \sup_{\mathbf{0} \neq \underline{\mathbf{v}}_h \in \mathbf{H}_h^{\mathbf{u}} \times \mathbf{H}_h^{\boldsymbol{\omega}}} \frac{-([\partial_t \mathcal{E}(\mathbf{e}_{\mathbf{u}}), \underline{\mathbf{v}}_h] + [\mathcal{A}(\underline{\mathbf{u}}) - \mathcal{A}(\underline{\mathbf{u}}_h), \underline{\mathbf{v}}_h] + [\mathcal{B}(\underline{\mathbf{v}}_h), \boldsymbol{\delta}_p])}{\|\underline{\mathbf{v}}_h\|} \\ &\leq C_3 \left(\|\partial_t \mathbf{e}_{\mathbf{u}}\|_{\mathbf{L}^2(\Omega)} + \|\mathbf{e}_{\mathbf{u}}\|_{\mathbf{H}^1(\Omega)} + (\|\mathbf{u}\|_{\mathbf{H}^1(\Omega)} + \|\mathbf{u}_h\|_{\mathbf{H}^1(\Omega)})^{p-2} \|\mathbf{e}_{\mathbf{u}}\|_{\mathbf{H}^1(\Omega)} + \|\mathbf{e}_{\boldsymbol{\omega}}\|_{\mathbf{L}^2(\Omega)} + \|\boldsymbol{\delta}_p\|_{\mathbf{L}^2(\Omega)} \right), \end{aligned}$$

with $C_3 > 0$ depending linearly on $|\Omega|$, $\|\mathbf{i}_p\|$, ν , α , \mathbf{F} , κ_1 , and κ_2 . Then, taking square in the above inequality, integrating from 0 to $t \in (0, T]$, recalling that both $\|\mathbf{u}\|_{L^\infty(0,T;\mathbf{H}^1(\Omega))}$ and $\|\mathbf{u}_h\|_{L^\infty(0,T;\mathbf{H}^1(\Omega))}$ are bounded by data (cf. (3.31), (4.8)), and employing (4.29), we deduce that

$$\int_0^t \|\boldsymbol{\eta}_p\|_{\mathbf{L}^2(\Omega)}^2 ds \leq C_4 \left\{ \Psi(\underline{\mathbf{u}}, p) + \int_0^t \|\partial_t \boldsymbol{\eta}_{\mathbf{u}}\|_{\mathbf{L}^2(\Omega)}^2 ds \right\}, \tag{4.30}$$

with $C_4 > 0$ depending on $|\Omega|$, $\|\mathbf{i}_p\|$, $\|\mathbf{i}_{2(p-1)}\|$, ν , α , \mathbf{F} , $\widetilde{\beta}$, κ_1 , κ_2 , and data. Next, in order to bound the last term in (4.30), we differentiate in time the equation of (4.18) related to $\boldsymbol{\psi}_h$, choose $\underline{\mathbf{v}}_h = (\partial_t \boldsymbol{\eta}_{\mathbf{u}}, \boldsymbol{\eta}_{\boldsymbol{\omega}})$, and use the identity (3.37), to find that

$$\begin{aligned} & \|\partial_t \boldsymbol{\eta}_{\mathbf{u}}\|_{\mathbf{L}^2(\Omega)}^2 + \frac{1}{2} \partial_t \left(\alpha \|\boldsymbol{\eta}_{\mathbf{u}}\|_{\mathbf{L}^2(\Omega)}^2 + \kappa_1 \|\mathbf{curl}(\boldsymbol{\eta}_{\mathbf{u}})\|_{\mathbf{L}^2(\Omega)}^2 + \kappa_2 \|\mathbf{div}(\boldsymbol{\eta}_{\mathbf{u}})\|_{\mathbf{L}^2(\Omega)}^2 + (\nu - \kappa_1) \|\boldsymbol{\eta}_{\boldsymbol{\omega}}\|_{\mathbf{L}^2(\Omega)}^2 \right) \\ &= -(\partial_t \boldsymbol{\delta}_{\mathbf{u}}, \partial_t \boldsymbol{\eta}_{\mathbf{u}})_{\Omega} - \alpha (\boldsymbol{\delta}_{\mathbf{u}}, \partial_t \boldsymbol{\eta}_{\mathbf{u}})_{\Omega} - \mathbf{F} (|\mathbf{u}|^{p-2} \mathbf{u} - |\mathbf{u}_h|^{p-2} \mathbf{u}_h, \partial_t \boldsymbol{\eta}_{\mathbf{u}})_{\Omega} - \nu (\partial_t \boldsymbol{\delta}_{\boldsymbol{\omega}}, \boldsymbol{\eta}_{\boldsymbol{\omega}})_{\Omega} \\ &\quad - \nu (\boldsymbol{\delta}_{\boldsymbol{\omega}}, \mathbf{curl}(\partial_t \boldsymbol{\eta}_{\mathbf{u}}))_{\Omega} + \nu (\boldsymbol{\eta}_{\boldsymbol{\omega}}, \mathbf{curl}(\partial_t \boldsymbol{\delta}_{\mathbf{u}}))_{\Omega} - \kappa_1 (\mathbf{curl}(\boldsymbol{\delta}_{\mathbf{u}}) - \boldsymbol{\delta}_{\boldsymbol{\omega}}, \mathbf{curl}(\partial_t \boldsymbol{\eta}_{\mathbf{u}}) - \partial_t \boldsymbol{\eta}_{\boldsymbol{\omega}})_{\Omega} \\ &\quad - \kappa_1 \partial_t (\mathbf{curl}(\boldsymbol{\delta}_{\mathbf{u}}) - \boldsymbol{\delta}_{\boldsymbol{\omega}}, \boldsymbol{\eta}_{\boldsymbol{\omega}})_{\Omega} - \kappa_2 (\mathbf{div}(\boldsymbol{\delta}_{\mathbf{u}}), \mathbf{div}(\partial_t \boldsymbol{\eta}_{\mathbf{u}}))_{\Omega} + (\boldsymbol{\delta}_p, \mathbf{div}(\partial_t \boldsymbol{\eta}_{\mathbf{u}}))_{\Omega}. \end{aligned} \tag{4.31}$$

Notice that $(\boldsymbol{\eta}_p, \operatorname{div}(\partial_t \boldsymbol{\eta}_u))_\Omega = 0$ since $(\boldsymbol{\eta}_u(t), \mathbf{0}) \in \mathbf{V}_h$ (cf. (4.9) and (4.17)). Then, using the identities

$$\begin{aligned} (\boldsymbol{\delta}_\omega, \operatorname{curl}(\partial_t \boldsymbol{\eta}_u))_\Omega &= \partial_t (\boldsymbol{\delta}_\omega, \operatorname{curl}(\boldsymbol{\eta}_u))_\Omega - (\partial_t \boldsymbol{\delta}_\omega, \operatorname{curl}(\boldsymbol{\eta}_u))_\Omega, \\ (\operatorname{curl}(\boldsymbol{\delta}_u) - \boldsymbol{\delta}_\omega, \operatorname{curl}(\partial_t \boldsymbol{\eta}_u) - \partial_t \boldsymbol{\eta}_\omega)_\Omega &= \partial_t (\operatorname{curl}(\boldsymbol{\delta}_u) - \boldsymbol{\delta}_\omega, \operatorname{curl}(\boldsymbol{\eta}_u) - \boldsymbol{\eta}_\omega)_\Omega \\ &\quad - (\operatorname{curl}(\partial_t \boldsymbol{\delta}_u) - \partial_t \boldsymbol{\delta}_\omega, \operatorname{curl}(\boldsymbol{\eta}_u) - \boldsymbol{\eta}_\omega)_\Omega, \\ (\operatorname{div}(\boldsymbol{\delta}_u), \operatorname{div}(\partial_t \boldsymbol{\eta}_u))_\Omega &= \partial_t (\operatorname{div}(\boldsymbol{\delta}_u), \operatorname{div}(\boldsymbol{\eta}_u))_\Omega - (\operatorname{div}(\partial_t \boldsymbol{\delta}_u), \operatorname{div}(\boldsymbol{\eta}_u))_\Omega, \\ (\boldsymbol{\delta}_p, \operatorname{div}(\partial_t \boldsymbol{\eta}_u))_\Omega &= \partial_t (\boldsymbol{\delta}_p, \operatorname{div}(\boldsymbol{\eta}_u))_\Omega - (\partial_t \boldsymbol{\delta}_p, \operatorname{div}(\boldsymbol{\eta}_u))_\Omega. \end{aligned} \tag{4.32}$$

In turn, using the Cauchy–Schwarz inequality, (3.8), and the continuous injection of $\mathbf{H}^1(\Omega)$ into $\mathbf{L}^{2(p-1)}(\Omega)$ we deduce that there exists a constant $C_5 > 0$ depending on $|\Omega|$ and $\|\mathbf{i}_{2(p-1)}\|$ such that

$$\begin{aligned} (|\mathbf{u}|^{p-2} \mathbf{u} - |\mathbf{u}_h|^{p-2} \mathbf{u}_h, \partial_t \boldsymbol{\eta}_u)_\Omega &\leq \tilde{c}_p (\|\mathbf{u}\|_{\mathbf{L}^{2(p-1)}(\Omega)} + \|\mathbf{u}_h\|_{\mathbf{L}^{2(p-1)}(\Omega)})^{p-2} \|\mathbf{e}_u\|_{\mathbf{L}^{2(p-1)}(\Omega)} \|\partial_t \boldsymbol{\eta}_u\|_{\mathbf{L}^2(\Omega)} \\ &\leq C_5 (\|\mathbf{u}\|_{\mathbf{H}^1(\Omega)} + \|\mathbf{u}_h\|_{\mathbf{H}^1(\Omega)})^{p-2} \|\mathbf{e}_u\|_{\mathbf{H}^1(\Omega)} \|\partial_t \boldsymbol{\eta}_u\|_{\mathbf{L}^2(\Omega)}. \end{aligned} \tag{4.33}$$

Thus, integrating (4.31) from 0 to $t \in (0, T]$, using the identities (2.7) and (4.32), the estimate (4.33), and the Cauchy–Schwarz and Young’s inequalities, in a way similar to (4.21)–(4.25), we find that

$$\begin{aligned} \alpha \|\boldsymbol{\eta}_u(t)\|_{\mathbf{L}^2(\Omega)}^2 + \gamma_1 \|\nabla \boldsymbol{\eta}_u(t)\|_{\mathbb{L}^2(\Omega)}^2 + \gamma_2 \|\boldsymbol{\eta}_\omega(t)\|_{\mathbf{L}^2(\Omega)}^2 + \int_0^t \|\partial_t \boldsymbol{\eta}_u\|_{\mathbf{L}^2(\Omega)}^2 ds \\ \leq C_6 \left(\int_0^t (\|\partial_t \boldsymbol{\delta}_u\|^2 + \|\partial_t \boldsymbol{\delta}_p\|_{\mathbf{L}^2(\Omega)}^2 + \|\boldsymbol{\delta}_u\|_{\mathbf{L}^2(\Omega)}^2 + (\|\mathbf{u}\|_{\mathbf{H}^1(\Omega)} + \|\mathbf{u}_h\|_{\mathbf{H}^1(\Omega)})^{2(p-2)} \|\mathbf{e}_u\|_{\mathbf{H}^1(\Omega)}^2) ds \right. \\ \left. + \|\boldsymbol{\delta}_u(t)\|^2 + \|\boldsymbol{\delta}_p(t)\|_{\mathbf{L}^2(\Omega)}^2 + \|\boldsymbol{\delta}_{u_0}\|^2 + \|\boldsymbol{\delta}_{p_0}\|_{\mathbf{L}^2(\Omega)}^2 + \int_0^t \|\boldsymbol{\eta}_u\|^2 ds + \|\boldsymbol{\eta}_u(0)\|^2 \right) \\ + \frac{\alpha}{2} \|\boldsymbol{\eta}_u(t)\|_{\mathbf{L}^2(\Omega)}^2 + \frac{\gamma_1}{2} \|\nabla \boldsymbol{\eta}_u(t)\|_{\mathbb{L}^2(\Omega)}^2 + \frac{\gamma_2}{2} \|\boldsymbol{\eta}_\omega(t)\|_{\mathbf{L}^2(\Omega)}^2 + \frac{1}{2} \int_0^t \|\partial_t \boldsymbol{\eta}_u\|_{\mathbf{L}^2(\Omega)}^2 ds, \end{aligned}$$

where $C_6 > 0$ depends on $|\Omega|$, $\|\mathbf{i}_{2(p-1)}\|$, ν , α , F , κ_1 , and κ_2 . Then, recalling that $\|\mathbf{u}\|_{\mathbf{L}^\infty(0,T;\mathbf{H}^1(\Omega))}$ and $\|\mathbf{u}_h\|_{\mathbf{L}^\infty(0,T;\mathbf{H}^1(\Omega))}$ are bounded by data (cf. (3.31) and (4.8)), employing estimates (4.27) and (4.28), and some algebraic manipulations, we deduce that

$$\begin{aligned} \alpha \|\boldsymbol{\eta}_u(t)\|_{\mathbf{L}^2(\Omega)}^2 + \gamma_1 \|\nabla \boldsymbol{\eta}_u(t)\|_{\mathbb{L}^2(\Omega)}^2 + \gamma_2 \|\boldsymbol{\eta}_\omega(t)\|_{\mathbf{L}^2(\Omega)}^2 + \int_0^t \|\partial_t \boldsymbol{\eta}_u\|_{\mathbf{L}^2(\Omega)}^2 ds \\ \leq C_7 \left(\int_0^t (\|\partial_t \boldsymbol{\delta}_u\|^2 + \|\partial_t \boldsymbol{\delta}_p\|_{\mathbf{L}^2(\Omega)}^2 + \|\boldsymbol{\delta}_u\|_{\mathbf{H}^1(\Omega)}^{2(p-1)} + \|\boldsymbol{\delta}_u\|^2 + \|\boldsymbol{\delta}_p\|_{\mathbf{L}^2(\Omega)}^2) ds \right. \\ \left. + \|\boldsymbol{\delta}_u(t)\|^2 + \|\boldsymbol{\delta}_p(t)\|_{\mathbf{L}^2(\Omega)}^2 + \|\boldsymbol{\delta}_{u_0}\|_{\mathbf{H}^1(\Omega)}^{2(p-1)} + \|\boldsymbol{\delta}_{u_0}\|^2 + \|\boldsymbol{\delta}_{p_0}\|_{\mathbf{L}^2(\Omega)}^2 \right), \end{aligned} \tag{4.34}$$

with $C_7 > 0$ depending on $|\Omega|$, $\|\mathbf{i}_p\|$, $\|\mathbf{i}_{2(p-1)}\|$, ν , α , F , $\tilde{\beta}$, κ_1 , κ_2 , and data. Thus, combining (4.30) with (4.34), and using the error decomposition (4.15), yields

$$\int_0^t \|\mathbf{e}_p\|_{\mathbf{L}^2(\Omega)}^2 ds \leq C_8 \left\{ \Psi(\mathbf{u}, p) + \|\boldsymbol{\delta}_p(t)\|_{\mathbf{L}^2(\Omega)}^2 + \int_0^t \|\partial_t \boldsymbol{\delta}_p\|_{\mathbf{L}^2(\Omega)}^2 ds \right\}, \tag{4.35}$$

with $C_8 > 0$ depending on $|\Omega|$, $\|\mathbf{i}_p\|$, $\|\mathbf{i}_{2(p-1)}\|$, ν , α , F , $\tilde{\beta}$, κ_1 , κ_2 , and data. Finally, using the fact that $\widehat{\mathbf{v}}_h : [0, T] \rightarrow \mathbf{V}_h$ and $\widehat{\boldsymbol{q}}_h : [0, T] \rightarrow \mathbf{H}_h^p$ are arbitrary, taking infimum in (4.29) and (4.35) over the corresponding discrete subspaces \mathbf{V}_h and \mathbf{H}_h^p , and applying the approximation properties (4.14), we derive (4.19) and conclude the proof. \square

Remark 4.1. Bounds (4.21)–(4.25) imply that the constant C on the right-hand side of (4.29) is linearly dependent on $\frac{\nu^2}{\kappa_1}$ and $\frac{1}{\kappa_2}$. Combined with the constants on the left-hand side of (4.29), this shows that the convergence constant for $\|\mathbf{e}_u\|_{\mathbf{L}^2(0,T;\mathbf{L}^2(\Omega))}$ is linearly dependent on $\frac{\nu}{\sqrt{\kappa_1}}$ and $\frac{1}{\sqrt{\kappa_2}}$, the one for $\|\nabla \mathbf{e}_u\|_{\mathbb{L}^2(0,T;\mathbf{L}^2(\Omega))}$ is linearly dependent on $\frac{1}{\sqrt{\gamma_1}}$, $\frac{\nu}{\sqrt{\gamma_1 \kappa_1}}$, and $\frac{1}{\sqrt{\gamma_1 \kappa_2}}$, $\gamma_1 = \min\{\kappa_1, \kappa_2\}$, and the one for $\|\mathbf{e}_\omega\|_{\mathbf{L}^2(0,T;\mathbf{L}^2(\Omega))}$ is linearly dependent on $\frac{1}{\sqrt{\gamma_2}}$, $\frac{\nu}{\sqrt{\gamma_2 \kappa_1}}$, and $\frac{1}{\sqrt{\gamma_2 \kappa_2}}$, $\gamma_2 = \nu - \kappa_1$.

5. Fully discrete approximation

In this section we introduce and analyze a fully discrete approximation of (2.9) (cf. (4.3)). To that end, for the time discretization we employ the backward Euler method. Let Δt be the time step, $T = N \Delta t$, and let $t_n = n \Delta t$,

$n = 0, \dots, N$. More precisely, we let $d_t u^n = (\Delta t)^{-1}(u^n - u^{n-1})$ be the first order (backward) discrete time derivative, where $u^n := u(t_n)$. Then the fully discrete method reads: given $\mathbf{f}^n \in \mathbf{L}^2(\Omega)$ and $(\mathbf{u}_h^0, p_h^0) = ((\mathbf{u}_{h,0}, \boldsymbol{\omega}_{h,0}), p_{h,0})$ satisfying (4.4) find $(\mathbf{u}_h^n, p_h^n) := ((\mathbf{u}_h^n, \boldsymbol{\omega}_h^n), p_h^n) \in (\mathbf{H}_h^{\mathbf{u}} \times \mathbf{H}_h^{\boldsymbol{\omega}}) \times H_h^p$, $n = 1, \dots, N$, such that

$$\begin{aligned} d_t[\mathcal{E}(\mathbf{u}_h^n), \mathbf{v}_h] + [\mathcal{A}(\mathbf{u}_h^n), \mathbf{v}_h] + [\mathcal{B}(\mathbf{v}_h), p_h^n] &= [\mathbf{F}^n, \mathbf{v}_h] \quad \forall \mathbf{v}_h \in \mathbf{H}_h^{\mathbf{u}} \times \mathbf{H}_h^{\boldsymbol{\omega}}, \\ -[\mathcal{B}(\mathbf{u}_h^n), q_h] &= 0 \quad \forall q_h \in H_h^p, \end{aligned} \tag{5.1}$$

where $[\mathbf{F}^n, \mathbf{v}_h] := (\mathbf{f}^n, \mathbf{v}_h)_{\Omega}$.

In what follows, given a separable Banach space V endowed with the norm $\|\cdot\|_V$, we make use of the following discrete in time norms

$$\|u\|_{\ell^p(0,T;V)}^p := \Delta t \sum_{n=1}^N \|u^n\|_V^p \quad \text{and} \quad \|u\|_{\ell^\infty(0,T;V)} := \max_{0 \leq n \leq N} \|u^n\|_V. \tag{5.2}$$

Next, we state the main results for method (5.1).

Theorem 5.1. *Let $p \in [3, 4]$. Assume κ_1 and κ_2 as in Lemma 3.4. Then, for each $(\mathbf{u}_h^0, p_h^0) := ((\mathbf{u}_{h,0}, \boldsymbol{\omega}_{h,0}), p_{h,0})$ satisfying (4.4) and $\mathbf{f}^n \in \mathbf{L}^2(\Omega)$, $n = 1, \dots, N$, there exists a unique solution $(\mathbf{u}_h^n, p_h^n) := ((\mathbf{u}_h^n, \boldsymbol{\omega}_h^n), p_h^n) \in (\mathbf{H}_h^{\mathbf{u}} \times \mathbf{H}_h^{\boldsymbol{\omega}}) \times H_h^p$ to (5.1). Moreover, under a suitable extra regularity assumption on the data, there exist constants $\tilde{C}_{\text{BF},1}, \tilde{C}_{\text{BF},2} > 0$ depending only on $|\Omega|, \|\mathbf{i}_p\|, \nu, \alpha, F, \beta, \kappa_1$, and κ_2 , such that*

$$\begin{aligned} &\|\mathbf{u}_h\|_{\ell^\infty(0,T;\mathbf{L}^2(\Omega))} + \Delta t \|d_t \mathbf{u}_h\|_{\ell^2(0,T;\mathbf{L}^2(\Omega))} + \|\mathbf{u}_h\|_{\ell^2(0,T;\mathbf{H}^1(\Omega))} + \|\boldsymbol{\omega}_h\|_{\ell^2(0,T;\mathbf{L}^2(\Omega))} + \|p_h\|_{\ell^2(0,T;\mathbf{L}^2(\Omega))} \\ &\leq \tilde{C}_{\text{BF},1} \left\{ \|\mathbf{f}\|_{\mathbf{L}^2(0,T;\mathbf{L}^2(\Omega))}^{2(p-1)/p} + \|\mathbf{f}\|_{\mathbf{L}^2(0,T;\mathbf{L}^2(\Omega))} + \|\mathbf{u}_0\|_{\mathbf{H}^1(\Omega)}^{2(p-1)^2/p} + \|\mathbf{u}_0\|_{\mathbf{H}^1(\Omega)}^{p-1} \right. \\ &\quad \left. + \|\Delta \mathbf{u}_0\|_{\mathbf{L}^2(\Omega)}^{2(p-1)/p} + \|\Delta \mathbf{u}_0\|_{\mathbf{L}^2(\Omega)} + \|\mathbf{u}_0\|_{\mathbf{L}^2(\Omega)}^{2(p-1)/p} + \|\mathbf{u}_0\|_{\mathbf{L}^2(\Omega)} \right\}, \end{aligned} \tag{5.3}$$

and

$$\|\mathbf{u}_h\|_{\ell^\infty(0,T;\mathbf{H}^1(\Omega))} \leq \tilde{C}_{\text{BF},2} \left\{ \|\mathbf{f}\|_{\mathbf{L}^2(0,T;\mathbf{L}^2(\Omega))} + \|\mathbf{u}_0\|_{\mathbf{H}^1(\Omega)}^{p-1} + \|\Delta \mathbf{u}_0\|_{\mathbf{L}^2(\Omega)} + \|\mathbf{u}_0\|_{\mathbf{L}^2(\Omega)} \right\}. \tag{5.4}$$

Proof. First, we note that at each time step the well-posedness of the fully discrete problem (5.1), with $n = 1, \dots, N$, follows from similar arguments to the proof of Lemma 3.6.

On the other hand, the derivation of (5.3) and (5.4) can be obtained similarly as in the proof of Theorem 3.9. In fact, we choose $(\mathbf{v}_h, q_h) = (\mathbf{u}_h^n, p_h^n)$ in (5.1), use the identity

$$(d_t \mathbf{u}_h^n, \mathbf{u}_h^n)_{\Omega} = \frac{1}{2} d_t \|\mathbf{u}_h^n\|_{\mathbf{L}^2(\Omega)}^2 + \frac{1}{2} \Delta t \|d_t \mathbf{u}_h^n\|_{\mathbf{L}^2(\Omega)}^2, \tag{5.5}$$

the definition of the operator \mathcal{A} (cf. (2.11)), the identity (2.7), and the Cauchy–Schwarz and Young’s inequalities (cf. (1.1)), to obtain

$$\begin{aligned} &\frac{1}{2} d_t \|\mathbf{u}_h^n\|_{\mathbf{L}^2(\Omega)}^2 + \frac{1}{2} \Delta t \|d_t \mathbf{u}_h^n\|_{\mathbf{L}^2(\Omega)}^2 + \alpha \|\mathbf{u}_h^n\|_{\mathbf{L}^2(\Omega)}^2 + F \|\mathbf{u}_h^n\|_{\mathbf{L}^p(\Omega)}^p \\ &\quad + \kappa_1 \|\mathbf{curl}(\mathbf{u}_h^n)\|_{\mathbf{L}^2(\Omega)}^2 + \kappa_2 \|\mathbf{div}(\mathbf{u}_h^n)\|_{\mathbf{L}^2(\Omega)}^2 + \gamma_2 \|\boldsymbol{\omega}_h^n\|_{\mathbf{L}^2(\Omega)}^2 \leq \frac{\delta}{2} \|\mathbf{f}^n\|_{\mathbf{L}^2(\Omega)}^2 + \frac{1}{2\delta} \|\mathbf{u}_h^n\|_{\mathbf{L}^2(\Omega)}^2, \end{aligned} \tag{5.6}$$

where γ_2 is defined in (3.17). Then, choosing $\delta = 1/\alpha$ and summing up over the time index $n = 1, \dots, m$, with $m = 1, \dots, N$, in (5.6) and multiplying by Δt , we get

$$\begin{aligned} &\|\mathbf{u}_h^m\|_{\mathbf{L}^2(\Omega)}^2 + (\Delta t)^2 \sum_{n=1}^m \|d_t \mathbf{u}_h^n\|_{\mathbf{L}^2(\Omega)}^2 + \Delta t \sum_{n=1}^m \left(\alpha \|\mathbf{u}_h^n\|_{\mathbf{L}^2(\Omega)}^2 + 2\kappa_1 \|\mathbf{curl}(\mathbf{u}_h^n)\|_{\mathbf{L}^2(\Omega)}^2 \right) \\ &\quad + \Delta t \sum_{n=1}^m \left(2\kappa_2 \|\mathbf{div}(\mathbf{u}_h^n)\|_{\mathbf{L}^2(\Omega)}^2 + 2\gamma_2 \|\boldsymbol{\omega}_h^n\|_{\mathbf{L}^2(\Omega)}^2 \right) \leq \frac{\Delta t}{\alpha} \sum_{n=1}^m \|\mathbf{f}^n\|_{\mathbf{L}^2(\Omega)}^2 + \|\mathbf{u}_h^0\|_{\mathbf{L}^2(\Omega)}^2. \end{aligned} \tag{5.7}$$

Notice that, in order to simplify the stability bound, we have neglected the term $\|\mathbf{u}_h^n\|_{\mathbf{L}^p(\Omega)}^p$ in the left-hand side of (5.6).

On the other hand, from the discrete inf–sup condition of \mathcal{B} (cf. (4.1)) and the first equation of (5.1) related to \mathbf{v}_h , we deduce that

$$\begin{aligned} \tilde{\beta} \|p_h^n\|_{\mathbf{L}^2(\Omega)} &\leq \|\mathbf{f}^n\|_{\mathbf{L}^2(\Omega)} + \alpha \|\mathbf{u}_h^n\|_{\mathbf{L}^2(\Omega)} + F \|\mathbf{i}_p\| \|\mathbf{u}_h^n\|_{\mathbf{L}^p(\Omega)}^{p-1} \\ &\quad + \kappa_1 \|\mathbf{curl}(\mathbf{u}_h^n)\|_{\mathbf{L}^2(\Omega)} + \kappa_2 \|\mathbf{div}(\mathbf{u}_h^n)\|_{\mathbf{L}^2(\Omega)} + \gamma_2 \|\boldsymbol{\omega}_h^n\|_{\mathbf{L}^2(\Omega)} + \|d_t \mathbf{u}_h^n\|_{\mathbf{L}^2(\Omega)}. \end{aligned} \tag{5.8}$$

Then, taking square in (5.8), using (5.7), we deduce the analogous estimate of (3.35), that is

$$\Delta t \sum_{n=1}^m \|p_h^n\|_{L^2(\Omega)}^2 \leq C_1 \left\{ \Delta t \sum_{n=1}^m \|\mathbf{f}^n\|_{L^2(\Omega)}^2 + \|\mathbf{u}_h^0\|_{L^2(\Omega)}^2 + \Delta t \sum_{n=1}^m \left(F \|\mathbf{u}_h^n\|_{L^p(\Omega)}^{2(p-1)} + \|d_t \mathbf{u}_h^n\|_{L^2(\Omega)}^2 \right) \right\}, \text{ with } m = 1, \dots, N, \tag{5.9}$$

with $C_1 > 0$ depending on $|\Omega|, \|\mathbf{i}_p\|, \nu, \alpha, F, \tilde{\beta}, \kappa_1$, and κ_2 . Next, in order to bound the last two terms in (5.9), we choose $(\mathbf{v}_h, q_h) = ((d_t \mathbf{u}_h^n, \boldsymbol{\omega}_h^n), p_h^n)$ in (5.1), apply some algebraic manipulation, use the identity (5.5) and the Cauchy–Schwarz and Young’s inequalities, to obtain the discrete version of (3.36):

$$\begin{aligned} & \|d_t \mathbf{u}_h^n\|_{L^2(\Omega)}^2 + \frac{1}{2} d_t \left(\alpha \|\mathbf{u}_h^n\|_{L^2(\Omega)}^2 + \kappa_2 \|\operatorname{div}(\mathbf{u}_h^n)\|_{L^2(\Omega)}^2 + \nu \|\boldsymbol{\omega}_h^n\|_{L^2(\Omega)}^2 \right) + F (|\mathbf{u}_h^n|^{p-2} \mathbf{u}_h^n, d_t \mathbf{u}_h^n)_\Omega \\ & + \frac{1}{2} \Delta t \left(\alpha \|d_t \mathbf{u}_h^n\|_{L^2(\Omega)}^2 + \kappa_2 \|\operatorname{div}(d_t \mathbf{u}_h^n)\|_{L^2(\Omega)}^2 + \nu \|d_t \boldsymbol{\omega}_h^n\|_{L^2(\Omega)}^2 \right) \\ & + \kappa_1 (\operatorname{curl}(\mathbf{u}_h^n) - \boldsymbol{\omega}_h^n, d_t \operatorname{curl}(\mathbf{u}_h^n))_\Omega + \kappa_1 (d_t (\operatorname{curl}(\mathbf{u}_h^n) - \boldsymbol{\omega}_h^n), \boldsymbol{\omega}_h^n)_\Omega \leq \frac{1}{2} \|\mathbf{f}^n\|_{L^2(\Omega)}^2 + \frac{1}{2} \|d_t \mathbf{u}_h^n\|_{L^2(\Omega)}^2, \end{aligned} \tag{5.10}$$

where, using again (5.5), analogously to (3.37), we can obtain the identity

$$\begin{aligned} & \kappa_1 (\operatorname{curl}(\mathbf{u}_h^n) - \boldsymbol{\omega}_h^n, d_t \operatorname{curl}(\mathbf{u}_h^n))_\Omega + \kappa_1 (d_t (\operatorname{curl}(\mathbf{u}_h^n) - \boldsymbol{\omega}_h^n), \boldsymbol{\omega}_h^n)_\Omega \\ & = \frac{\kappa_1}{2} d_t \left(\|\operatorname{curl}(\mathbf{u}_h^n)\|_{L^2(\Omega)}^2 - \|\boldsymbol{\omega}_h^n\|_{L^2(\Omega)}^2 \right) + \frac{\kappa_1}{2} \Delta t \left(\|\operatorname{curl}(d_t \mathbf{u}_h^n)\|_{L^2(\Omega)}^2 - \|d_t \boldsymbol{\omega}_h^n\|_{L^2(\Omega)}^2 \right). \end{aligned} \tag{5.11}$$

In turn, employing Hölder and Young’s inequalities, we are able to deduce (cf. [7, Eq. (5.13)]):

$$(|\mathbf{u}_h^n|^{p-2} \mathbf{u}_h^n, d_t \mathbf{u}_h^n)_\Omega \geq \frac{(\Delta t)^{-1}}{p} \left(\|\mathbf{u}_h^n\|_{L^p(\Omega)}^p - \|\mathbf{u}_h^{n-1}\|_{L^p(\Omega)}^p \right) = \frac{1}{p} d_t \|\mathbf{u}_h^n\|_{L^p(\Omega)}^p. \tag{5.12}$$

Thus, combining (5.10) with (5.11) and (5.12), summing up over the time index $n = 1, \dots, m$, with $m = 1, \dots, N$ and multiplying by Δt , we get

$$\begin{aligned} & \alpha \|\mathbf{u}_h^m\|_{L^2(\Omega)}^2 + \frac{2F}{p} \|\mathbf{u}_h^m\|_{L^p(\Omega)}^p + \gamma_1 \|\nabla \mathbf{u}_h^m\|_{L^2(\Omega)}^2 + \gamma_2 \|\boldsymbol{\omega}_h^m\|_{L^2(\Omega)}^2 + \Delta t \sum_{n=1}^m \|d_t \mathbf{u}_h^n\|_{L^2(\Omega)}^2 \\ & \leq \Delta t \sum_{n=1}^m \|\mathbf{f}^n\|_{L^2(\Omega)}^2 + \alpha \|\mathbf{u}_h^0\|_{L^2(\Omega)}^2 + \frac{2F}{p} \|\mathbf{u}_h^0\|_{L^p(\Omega)}^p + \gamma_1 \|\nabla \mathbf{u}_h^0\|_{L^2(\Omega)}^2 + \gamma_2 \|\boldsymbol{\omega}_h^0\|_{L^2(\Omega)}^2, \end{aligned} \tag{5.13}$$

where γ_1 and γ_2 are defined in (3.17). Then, combining (5.9) and (5.13) yields

$$\begin{aligned} \Delta t \sum_{n=1}^m \|p_h^n\|_{L^2(\Omega)}^2 \leq C_2 \left\{ \left(\Delta t \sum_{n=1}^m \|\mathbf{f}^n\|_{L^2(\Omega)}^2 \right)^{2(p-1)/p} + \Delta t \sum_{n=1}^m \|\mathbf{f}^n\|_{L^2(\Omega)}^2 \right. \\ \left. + \|\mathbf{u}_h^0\|_{L^p(\Omega)}^{2(p-1)} + \|\mathbf{u}_h^0\|_{L^p(\Omega)}^p + \|\mathbf{u}_h^0\|_{\mathbf{H}^1(\Omega)}^{4(p-1)/p} + \|\mathbf{u}_h^0\|_{\mathbf{H}^1(\Omega)}^2 + \|\boldsymbol{\omega}_h^0\|_{L^2(\Omega)}^{4(p-1)/p} + \|\boldsymbol{\omega}_h^0\|_{L^2(\Omega)}^2 \right\}, \end{aligned} \tag{5.14}$$

with $m = 1, \dots, N$ and $C_2 > 0$ depending on $|\Omega|, \|\mathbf{i}_p\|, \nu, \alpha, F, \tilde{\beta}, \kappa_1$, and κ_2 , which combined with (5.7), the fact that $(\mathbf{u}_h^0, \boldsymbol{\omega}_h^0) = (\mathbf{u}_{h,0}, \boldsymbol{\omega}_{h,0})$ and the estimate (4.5), implies (5.3). In addition, (4.5) and (5.13) yields (5.4), which concludes the proof. \square

Remark 5.1. Similarly to Remark 3.6 for the continuous solution, bound (5.7) and the identity (2.7) show that the stability constant for $\|\nabla \mathbf{u}_h\|_{\ell^2(0,T;L^2(\Omega))}$ is linearly dependent on $\frac{1}{\sqrt{\gamma_1}}$, $\gamma_1 = \min\{\kappa_1, \kappa_2\}$, while the one for $\|\boldsymbol{\omega}_h\|_{\ell^2(0,T;L^2(\Omega))}$ is linearly dependent on $\frac{1}{\sqrt{\gamma_2}}$, $\gamma_2 = \nu - \kappa_1$. In addition, bounds (5.7) and (5.14) show that the stability constants for $\|\mathbf{u}_h\|_{\ell^2(0,T;L^2(\Omega))}$ and $\|p_h\|_{\ell^2(0,T;L^2(\Omega))}$ do not depend on $\frac{1}{\nu}, \frac{1}{\kappa_1}$, or $\frac{1}{\kappa_2}$.

Now, we proceed with establishing rates of convergence for the fully discrete scheme (5.1). To that end, we subtract the fully discrete problem (5.1) from the continuous counterparts (2.9) at each time step $n = 1, \dots, N$, to obtain the following error system:

$$\begin{aligned} d_t [\mathcal{E}(\mathbf{e}_u^n), \mathbf{v}_h] + [\mathcal{A}(\mathbf{u}_h^n) - \mathcal{A}(\mathbf{u}_h), \mathbf{v}_h] + [\mathcal{B}(\mathbf{v}_h), \mathbf{e}_p^n] &= (r_n(\mathbf{u}), \mathbf{v}_h)_\Omega, \\ [\mathcal{B}(\mathbf{e}_u^n), q_h] &= 0, \end{aligned} \tag{5.15}$$

for all $\mathbf{v}_h \in \mathbf{H}_h^{\mathbf{a}} \times \mathbf{H}_h^{\omega}$ and $q_h \in H_h^p$, where r_n denotes the difference between the time derivative and its discrete analogue, that is

$$r_n(\mathbf{u}) = d_t \mathbf{u}^n - \partial_t \mathbf{u}(t_n).$$

In addition, we recall from [30, Lemma 4] that for sufficiently smooth \mathbf{u} , there holds

$$\Delta t \sum_{n=1}^N \|r_n(\mathbf{u})\|_{L^2(\Omega)}^2 \leq C(\partial_{tt} \mathbf{u})(\Delta t)^2, \quad \text{with } C(\partial_{tt} \mathbf{u}) := C \|\partial_{tt} \mathbf{u}\|_{L^2(0,T;L^2(\Omega))}^2. \tag{5.16}$$

Then, the proof of the theoretical rate of convergence of the fully discrete scheme (5.1) follows the structure of the proof of Theorem 4.4, using discrete-in-time arguments as in the proof of Theorem 5.1 and the estimate (5.16) (see [7, Theorem 5.4] for a similar approach).

Theorem 5.2. *Let the assumptions of Theorem 4.4 hold, with $p \in [3, 4]$ and $s \in (1/2, k + 1]$. Then, for the solution of the fully discrete problem (5.1) there exists $\widehat{C}(\underline{\mathbf{u}}, p) > 0$ depending only on $C(\underline{\mathbf{u}})$, $C(\partial_t \underline{\mathbf{u}})$, $C(\partial_{tt} \underline{\mathbf{u}})$, $C(p)$, $C(\partial_t p)$, $|\Omega|$, $\|\mathbf{i}_p\|$, $\|\mathbf{i}_{2(p-1)}\|$, ν , α , \mathbf{F} , $\widetilde{\beta}$, κ_1 , κ_2 , and data, such that*

$$\begin{aligned} &\|\mathbf{e}_u\|_{L^\infty(0,T;L^2(\Omega))} + \Delta t \|d_t \mathbf{e}_u\|_{L^2(0,T;L^2(\Omega))} + \|\mathbf{e}_u\|_{L^2(0,T;H^1(\Omega))} \\ &+ \|\mathbf{e}_\omega\|_{L^2(0,T;L^2(\Omega))} + \|\mathbf{e}_p\|_{L^2(0,T;L^2(\Omega))} \leq \widehat{C}(\underline{\mathbf{u}}, p) \left(h^s + h^{s(p-1)} + \Delta t \right). \end{aligned} \tag{5.17}$$

Remark 5.2. For the fully discrete scheme (5.1) we have considered the backward Euler method only for the sake of simplicity. The analysis developed in Section 5 can be adapted to other time discretizations, such as high order BDF schemes or the Crank–Nicholson method.

6. Numerical results

In this section we present some examples illustrating the performance of the augmented mixed formulation. The numerical methods have been implemented using open source finite element libraries: FEniCS [31] and FreeFem++ [32]. We have used FreeFem++ for the 2D test cases, Examples 1, 3, and 4, and FEniCS for the 3D ones, Examples 2 and 5.

Example 1: Verification of spatial convergence

The analysis of convergence established in the previous sections is illustrated numerically using a classical manufactured solution approach. Convergence rates under mesh refinement are computed with respect to the closed-form velocity and pressure

$$\mathbf{u} = \begin{pmatrix} t \cos(\pi x) \sin(\pi y) \\ -t \sin(\pi x) \cos(\pi y) \end{pmatrix}, \quad p = t \sin(\pi x) \sin(\pi y), \tag{6.1}$$

and $\omega = \mathbf{curl}(\mathbf{u})$, defined on the unit square $\Omega = (0, 1)^2$, up to a time $T = 0.05$ and using a fixed time step $\Delta t = 0.01$ (sufficiently small not to interfere with the accuracy verification of the spatial discretization). Non-homogeneous Dirichlet boundary conditions for velocity as well as the forcing term \mathbf{f} are imposed according to the exact manufactured solutions, and the average of the approximate pressure is constrained to match that of the exact pressure (the constraint being imposed through a real Lagrange multiplier). As the Dirichlet boundary conditions depend on time, this needs to be taken into consideration when implementing the initialization of inner Newton–Raphson iterates for each time step.

After backward Euler discretization, the nonlinear algebraic system encountered at each time iteration is solved with a Newton–Raphson algorithm with an absolute incremental tolerance of 10^{-9} (on the ℓ^2 -norm of the finite element incremental vector), and each linear solve of the tangent system is done with the unsymmetric multi-frontal direct solver MUMPS [33]. The finite element family used for these numerical tests is Taylor–Hood–Lagrange (i.e., the three finite dimensional subspaces in (4.2) with $k = 1$).

Table 6.1 illustrates the numerical convergence of the proposed method for this case, which uses the following model parameters values $\alpha = 100$, $\nu = 0.01$, $\mathbf{F} = 10$, and $p = 3.5$. According to Remark 3.3, we take $\kappa_1 = \frac{1}{2}\nu$

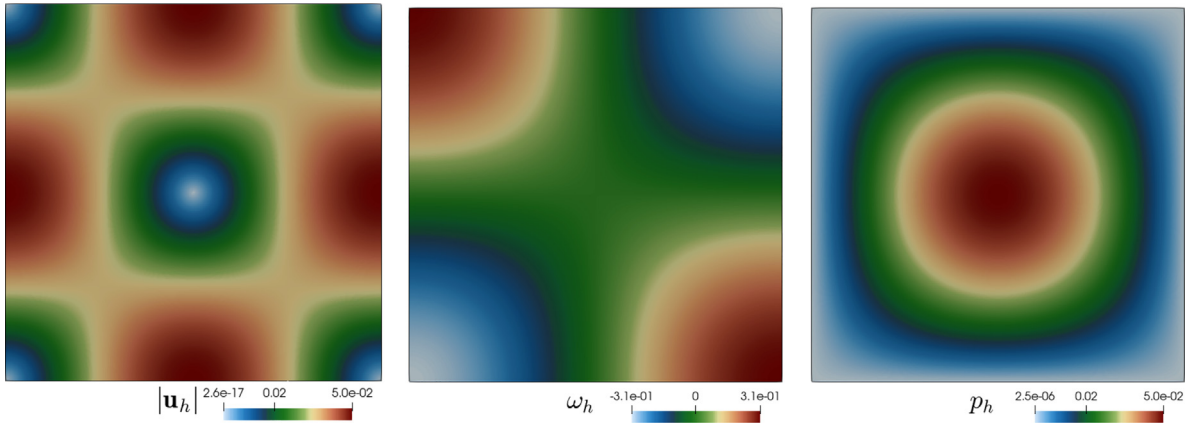


Fig. 6.1. Samples of numerical solutions for the accuracy test up to $T = 0.05$, using the base-line parameters $\alpha = 100$, $\nu = 0.01$, $F = 10$, and $p = 3.5$ and a Taylor–Hood–Lagrange method.

Table 6.1

Example 1. Error history with respect to mesh refinement, computed at $T = 0.05$ using the base-line parameters $\alpha = 100$, $\nu = 0.01$, $F = 10$, and $p = 3.5$ and with a Taylor–Hood–Lagrange method.

DoF	h	e_u	rate	e_ω	rate	e_p	rate	avg_it
69	0.71	3.67e−02	*	3.70e−02	*	9.12e−03	*	3.00
213	0.35	9.97e−03	1.88	8.98e−03	2.04	1.66e−03	2.46	3.00
741	0.18	3.36e−03	1.57	2.08e−03	2.11	3.42e−04	2.28	3.00
2757	0.09	1.12e−03	1.59	5.09e−04	2.03	8.12e−05	2.08	3.00
10629	0.04	2.71e−04	2.05	1.26e−04	2.01	2.01e−05	2.01	3.00
41733	0.02	5.20e−05	2.38	3.16e−05	2.00	5.02e−06	2.00	3.00
165381	0.01	1.05e−05	2.30	7.89e−06	2.00	1.26e−06	2.00	3.00

and $\kappa_2 = \kappa_1$. We display velocity errors in the $\mathbf{H}^1(\Omega)$ –norm, vorticity in the $L^2(\Omega)$ –norm and pressure in the $L^2(\Omega)$ –norm, computed at the final time

$$e_u := \|\mathbf{u} - \mathbf{u}_h\|_{\mathbf{H}^1(\Omega)}, \quad e_\omega := \|\boldsymbol{\omega} - \boldsymbol{\omega}_h\|_{L^2(\Omega)}, \quad e_p := \|p - p_h\|_{L^2(\Omega)}, \tag{6.2}$$

together with experimental rates of convergence

$$\text{rate} := \frac{\log(e_{(\cdot)})/e'_{(\cdot)}}{\log(h/h')},$$

where h and h' denote two consecutive mesh sizes with errors $e_{(\cdot)}$ and $e'_{(\cdot)}$, respectively. We also tabulate the average of Newton–Raphson iterates (avg_it) needed through all time steps on each refinement level. Approximate solutions for this case are plotted in Fig. 6.1.

Next we perform similar tests but now varying the Forchheimer exponent p and the Forchheimer number F (Table 6.2). In Table 6.2 (top) very slight differences (with respect to the error history reported in Table 6.1) in absolute individual errors are observed for coarser meshes, but after the first two mesh refinements the convergences are identical for all cases, showing the optimal $\mathcal{O}(h^{k+1})$ rate as predicted by the theory. In Table 6.2 (bottom) the iteration count increases due to the strength of the nonlinearity (for $F = 10000$) but the convergence rates remain optimal.

The next set of runs focuses on varying the Darcy number ($\alpha = 10^{-4}, 10^4$) and the viscosity ($\nu = 10^{-3}, 10^{-4}, 10^{-5}$), taking $\kappa_1 = \frac{\nu}{2}$ and $\kappa_2 = \kappa_1$ (see Table 6.3). Optimal convergence rates are observed independently of the chosen Darcy number (see top table). Regarding the variation in viscosity, Table 6.3 (bottom) indicates an optimal convergence for vorticity and pressure, whereas for velocity a clear sub-optimal convergence is attained for the case of smaller viscosities. The latter is consistent with Remark 4.1, which indicates that for $\kappa_1 = \kappa_2 = O(\nu)$ the convergence constant for $\|\nabla \mathbf{e}_u\|_{\mathbb{L}^2(0,T;L^2(\Omega))}$ depends linearly on $\frac{1}{\nu}$. According to Remark 4.1, we expect to recover

Table 6.2

Example 1. Error history with respect to mesh refinement, computed at $T = 0.05$ using the base-line parameters $\alpha = 100$, $\nu = 0.01$, and varying p with $F = 10$ fixed (top) and varying F with $p = 3.5$ fixed (bottom).

DoF	h	e_u	rate	e_ω	rate	e_p	rate	avg_it
p = 3								
69	0.71	3.67e-02	*	3.70e-02	*	9.17e-03	*	3.00
213	0.35	9.97e-03	1.88	8.98e-03	2.04	1.66e-03	2.47	3.00
741	0.18	3.36e-03	1.57	2.08e-03	2.11	3.42e-04	2.28	3.00
2757	0.09	1.12e-03	1.59	5.09e-04	2.03	8.12e-05	2.08	3.00
10629	0.04	2.71e-04	2.05	1.26e-04	2.01	2.01e-05	2.01	3.00
41733	0.02	5.20e-05	2.38	3.16e-05	2.00	5.02e-06	2.00	3.00
165381	0.01	1.05e-05	2.30	7.89e-06	2.00	1.26e-06	2.00	3.00
p = 4								
69	0.71	3.67e-02	*	3.70e-02	*	9.17e-03	*	3.00
213	0.35	9.97e-03	1.88	8.98e-03	2.04	1.66e-03	2.47	3.00
741	0.18	3.36e-03	1.57	2.08e-03	2.11	3.42e-04	2.28	3.00
2757	0.09	1.12e-03	1.59	5.09e-04	2.03	8.12e-05	2.08	3.00
10629	0.04	2.71e-04	2.05	1.26e-04	2.01	2.01e-05	2.01	3.00
41733	0.02	5.20e-05	2.38	3.16e-05	2.00	5.02e-06	2.00	3.00
165381	0.01	1.05e-05	2.30	7.89e-06	2.00	1.26e-06	2.00	3.00
DoF	h	e_u	rate	e_ω	rate	e_p	rate	avg_it
F = 10⁻⁴								
69	0.71	3.67e-02	*	3.70e-02	*	9.11e-03	*	2.00
213	0.35	9.97e-03	1.88	8.98e-03	2.04	1.66e-03	2.46	2.60
741	0.18	3.37e-03	1.57	2.08e-03	2.11	3.42e-04	2.28	2.80
2757	0.09	1.12e-03	1.59	5.09e-04	2.03	8.12e-05	2.08	3.00
10629	0.04	2.71e-04	2.05	1.26e-04	2.01	2.01e-05	2.01	3.00
41733	0.02	5.20e-05	2.38	3.16e-05	2.00	5.02e-06	2.00	3.00
165381	0.01	1.05e-05	2.30	7.89e-06	2.00	1.26e-06	2.00	3.00
F = 10⁴								
69	0.71	3.68e-02	*	3.70e-02	*	2.64e-02	*	4.00
213	0.35	9.54e-03	1.95	8.98e-03	2.04	2.31e-03	3.52	4.20
741	0.18	2.76e-03	1.79	2.08e-03	2.11	3.63e-04	2.67	4.00
2757	0.09	8.57e-04	1.69	5.09e-04	2.03	8.16e-05	2.15	4.00
10629	0.04	2.31e-04	1.89	1.26e-04	2.01	2.01e-05	2.02	4.20
41733	0.02	4.98e-05	2.21	3.16e-05	2.00	5.02e-06	2.00	4.60
165381	0.01	1.05e-05	2.25	7.89e-06	2.00	1.26e-06	2.00	4.60

Table 6.3

Example 1. Error history with respect to mesh refinement at $T = 0.05$, computed using the base-line parameters $p = 3.5$, $F = 10$, and varying α with $\nu = 0.01$ fixed (top) and varying ν with $\alpha = 100$ fixed (bottom). Here we have used $\kappa_1 = \kappa_2 = \frac{\nu}{2}$. A sub-optimal convergence in the velocity is observed for small viscosity.

DoF	h	e_u	rate	e_ω	rate	e_p	rate	avg_it
$\alpha = 10^{-4}$								
69	0.71	3.73e-02	*	3.70e-02	*	4.98e-03	*	3.00
213	0.35	1.52e-02	1.29	9.07e-03	2.03	1.53e-03	1.71	3.00
741	0.18	7.27e-03	1.07	2.09e-03	2.12	3.35e-04	2.19	3.00
2757	0.09	1.94e-03	1.91	5.09e-04	2.04	8.10e-05	2.05	3.00
10629	0.04	3.29e-04	2.56	1.26e-04	2.01	2.01e-05	2.01	3.00
41733	0.02	5.40e-05	2.61	3.16e-05	2.00	5.02e-06	2.00	3.00
165381	0.01	1.06e-05	2.35	7.89e-06	2.00	1.26e-06	2.00	3.00

(continued on next page)

Table 6.3 (continued).

DoF	h	$e_{\mathbf{u}}$	rate	e_{ω}	rate	e_p	rate	avg_it
$\alpha = 10^{-4}$								
$\alpha = 10^4$								
69	0.71	3.67e-02	*	3.70e-02	*	6.46e-01	*	3.00
213	0.35	9.36e-03	1.97	8.98e-03	2.04	5.09e-02	3.67	3.00
741	0.18	2.39e-03	1.97	2.08e-03	2.11	4.57e-03	3.48	3.00
2757	0.09	5.98e-04	2.00	5.09e-04	2.03	3.37e-04	3.76	3.00
10629	0.04	1.50e-04	2.00	1.26e-04	2.01	2.93e-05	3.53	3.00
41733	0.02	3.76e-05	1.99	3.16e-05	2.00	5.20e-06	2.49	3.00
165381	0.01	9.48e-06	1.99	7.89e-06	2.00	1.26e-06	2.05	3.00
DoF	h	$e_{\mathbf{u}}$	rate	e_{ω}	rate	e_p	rate	avg_it
$\nu = 10^{-5}$								
69	0.71	3.67e-02	*	3.70e-02	*	9.13e-03	*	3.00
213	0.35	1.00e-02	1.87	8.98e-03	2.04	1.67e-03	2.45	3.00
741	0.18	3.64e-03	1.46	2.09e-03	2.11	3.44e-04	2.27	3.00
2757	0.09	1.69e-03	1.11	5.09e-04	2.03	8.13e-05	2.08	3.00
10629	0.04	8.41e-04	1.00	1.26e-04	2.01	2.01e-05	2.01	3.00
41733	0.02	4.21e-04	1.00	3.16e-05	2.00	5.02e-06	2.00	3.00
165381	0.01	2.05e-04	1.04	7.89e-06	2.00	1.26e-06	2.00	3.00
$\nu = 10^{-4}$								
69	0.71	3.67e-02	*	3.70e-02	*	9.13e-03	*	3.00
213	0.35	1.00e-02	1.87	8.98e-03	2.04	1.67e-03	2.45	3.00
741	0.18	3.64e-03	1.46	2.09e-03	2.11	3.44e-04	2.27	3.00
2757	0.09	1.68e-03	1.12	5.09e-04	2.03	8.13e-05	2.08	3.00
10629	0.04	8.21e-04	1.03	1.26e-04	2.01	2.01e-05	2.01	3.00
41733	0.02	3.82e-04	1.10	3.16e-05	2.00	5.02e-06	2.00	3.00
165381	0.01	1.48e-04	1.37	7.89e-06	2.00	1.26e-06	2.00	3.00
$\nu = 10^{-3}$								
69	0.71	3.67e-02	*	3.70e-02	*	9.13e-03	*	3.00
213	0.35	1.00e-02	1.88	8.98e-03	2.04	1.66e-03	2.45	3.00
741	0.18	3.61e-03	1.47	2.09e-03	2.11	3.44e-04	2.27	3.00
2757	0.09	1.59e-03	1.18	5.09e-04	2.03	8.13e-05	2.08	3.00
10629	0.04	6.66e-04	1.26	1.26e-04	2.01	2.01e-05	2.01	3.00
41733	0.02	2.06e-04	1.69	3.16e-05	2.00	5.02e-06	2.00	3.00
165381	0.01	4.12e-05	2.32	7.89e-06	2.00	1.26e-06	2.00	3.00

the optimal convergence by either setting the augmentation constants κ_1 and κ_2 independent of ν or by modifying the velocity norm to

$$e_{\mathbf{u}}^* := \|\mathbf{u} - \mathbf{u}_h\|_{\mathbb{L}^2(\Omega)} + \nu \|\nabla \mathbf{u} - \nabla \mathbf{u}_h\|_{\mathbb{L}^2(\Omega)}$$

when $\kappa_1 = O(\nu)$ or $\kappa_2 = O(\nu)$. This is verified by the results reported in Table 6.4, where in the top part we take $\kappa_1 = \kappa_2 = 0.5$ and in the bottom part we take $\kappa_1 = \kappa_2 = \frac{\nu}{2}$. The first remedy indicates that the κ_1 and κ_2 augmentation terms may be explored to improve the robustness of the method for small viscosity values. We note that while the choice of $\kappa_1 = 0.5$ does not align with Remark 3.3, it is consistent with Remark 3.1 about the case $\kappa_1 > \nu$.

As usual for grad-div type stabilizations, the divergence-free property of the approximate solutions is modulated by the parameter κ_2 . This is exemplified in Table 6.5 where the effect of increasing κ_2 is tested. We denote by $\mathcal{P}_0(\text{div}(\mathbf{u}_h))$ the L^2 -projection of $\text{div}(\mathbf{u}_h)$ into the space of piecewise constant functions. As the mesh is refined, the ℓ^∞ norm of the coefficient vector associated with $\mathcal{P}_0(\text{div}(\mathbf{u}_h))$ decreases down to 5.03e-11.

Table 6.4

Example 1. Error history with respect to mesh refinement at $T = 0.05$, computed using the base-line parameters $p = 3.5$, $F = 10$, $\alpha = 100$, varying ν and using $\kappa_1 = \kappa_2 = 0.5$ (top), and $\kappa_1 = \kappa_2 = \nu/2$ with a different velocity norm (bottom).

DoF	h	e_u	rate	e_ω	rate	e_p	rate	avg_it
$\nu = 10^{-5}$								
69	0.71	3.48e-02	*	3.71e-02	*	4.82e-03	*	3.00
213	0.35	9.67e-03	1.85	8.99e-03	2.04	1.51e-03	1.68	3.00
741	0.18	2.43e-03	1.99	2.09e-03	2.11	3.36e-04	2.17	3.00
2757	0.09	6.01e-04	2.01	5.10e-04	2.03	8.11e-05	2.05	3.00
10629	0.04	1.50e-04	2.00	1.27e-04	2.01	2.01e-05	2.01	3.00
41733	0.02	3.76e-05	2.00	3.18e-05	2.00	5.02e-06	2.00	3.00
165381	0.01	9.44e-06	1.99	8.01e-06	1.99	1.26e-06	2.00	3.00
$\nu = 10^{-4}$								
69	0.71	3.48e-02	*	3.71e-02	*	4.82e-03	*	3.00
213	0.35	9.67e-03	1.85	8.99e-03	2.04	1.51e-03	1.68	3.00
741	0.18	2.43e-03	1.99	2.09e-03	2.11	3.36e-04	2.17	3.00
2757	0.09	6.01e-04	2.01	5.10e-04	2.03	8.11e-05	2.05	3.00
10629	0.04	1.50e-04	2.00	1.27e-04	2.01	2.01e-05	2.01	3.00
41733	0.02	3.75e-05	2.00	3.18e-05	2.00	5.02e-06	2.00	3.00
165381	0.01	9.42e-06	1.99	7.99e-06	1.99	1.26e-06	2.00	3.00
$\nu = 10^{-3}$								
69	0.71	3.48e-02	*	3.71e-02	*	4.82e-03	*	3.00
213	0.35	9.67e-03	1.85	8.99e-03	2.04	1.51e-03	1.68	3.00
741	0.18	2.43e-03	1.99	2.09e-03	2.11	3.36e-04	2.17	3.00
2757	0.09	6.01e-04	2.01	5.10e-04	2.03	8.11e-05	2.05	3.00
10629	0.04	1.50e-04	2.00	1.27e-04	2.01	2.01e-05	2.01	3.00
41733	0.02	3.75e-05	2.00	3.17e-05	2.00	5.02e-06	2.00	3.00
165381	0.01	9.36e-06	2.00	7.92e-06	2.00	1.26e-06	2.00	3.00
DoF	h	e_u^*	rate	e_ω	rate	e_p	rate	avg_it
$\nu = 10^{-5}$								
69	0.71	1.87e-03	*	3.70e-02	*	9.13e-03	*	3.00
213	0.35	2.74e-04	2.77	8.98e-03	2.04	1.67e-03	2.45	3.00
741	0.18	5.51e-05	2.32	2.09e-03	2.11	3.44e-04	2.27	3.00
2757	0.09	1.30e-05	2.09	5.09e-04	2.03	8.13e-05	2.08	3.00
10629	0.04	3.23e-06	2.01	1.26e-04	2.01	2.01e-05	2.01	3.00
41733	0.02	8.06e-07	2.00	3.16e-05	2.00	5.02e-06	2.00	3.00
165381	0.01	1.96e-07	2.04	7.89e-06	2.00	1.26e-06	2.00	3.00
$\nu = 10^{-4}$								
69	0.71	1.87e-03	*	3.70e-02	*	9.13e-03	*	3.00
213	0.35	2.74e-04	2.77	8.98e-03	2.04	1.67e-03	2.45	3.00
741	0.18	5.51e-05	2.32	2.09e-03	2.11	3.44e-04	2.27	3.00
2757	0.09	1.29e-05	2.09	5.09e-04	2.03	8.13e-05	2.08	3.00
10629	0.04	3.16e-06	2.03	1.26e-04	2.01	2.01e-05	2.01	3.00
41733	0.02	7.38e-07	2.10	3.16e-05	2.00	5.02e-06	2.00	3.00
165381	0.01	1.45e-07	2.35	7.89e-06	2.00	1.26e-06	2.00	3.00
$\nu = 10^{-3}$								
69	0.71	1.87e-03	*	3.70e-02	*	9.13e-03	*	3.00
213	0.35	2.74e-04	2.77	8.98e-03	2.04	1.66e-03	2.45	3.00
741	0.18	5.47e-05	2.33	2.09e-03	2.11	3.44e-04	2.27	3.00
2757	0.09	1.24e-05	2.14	5.09e-04	2.03	8.13e-05	2.08	3.00
10629	0.04	2.68e-06	2.21	1.26e-04	2.01	2.01e-05	2.01	3.00
41733	0.02	4.54e-07	2.56	3.16e-05	2.00	5.02e-06	2.00	3.00
165381	0.01	7.80e-08	2.57	7.89e-06	2.00	1.26e-06	2.00	3.00

Table 6.5

Example 1. Decay of $\text{div}(\mathbf{u}_h)$ (projected into the space of piecewise constants) with respect to mesh refinement at $T = 0.05$, computed using the base-line parameters $p = 3.5$, $F = 10$, $\alpha = 100$, $\nu = 0.01$, using $\kappa_1 = \nu/2$ and increasing κ_2 .

DoF	h	$\ \mathcal{P}_0(\text{div}(\mathbf{u}_h))\ _{\ell^\infty}$			
		$\kappa_2 = 0.005$	$\kappa_2 = 1$	$\kappa_2 = 100$	$\kappa_2 = 50000$
69	0.71	2.81e-03	3.47e-03	8.30e-04	2.00e-06
213	0.35	3.43e-03	8.91e-04	1.14e-04	2.64e-07
741	0.18	2.28e-03	1.40e-04	1.10e-05	2.44e-08
2757	0.09	1.13e-03	1.91e-05	1.57e-06	3.55e-09
10629	0.04	4.66e-04	2.50e-06	3.23e-07	8.50e-10
41733	0.02	1.34e-04	3.20e-07	8.44e-08	1.27e-10
165381	0.01	3.82e-05	9.01e-08	7.39e-09	5.03e-11

Table 6.6

Example 2. Error history with respect to mesh refinement in 3D, computed up to the final time $T = 0.03$ using the parameters $\alpha = 100$, $\nu = 0.01$, $F = 10$, and $p = 4$ and with three different discretizations. In all cases we take overall continuous and piecewise linear vorticity approximations.

DoF	h	$e_{\mathbf{u}}$	rate	$e_{\boldsymbol{\omega}}$	rate	e_p	rate	avg_it
Taylor–Hood–Lagrange								
484	0.87	4.81e-01	–	4.22e-01	–	7.81e-02	–	3.00
2688	0.43	1.32e-01	1.86	1.26e-01	1.74	1.30e-02	2.58	3.00
17656	0.22	3.98e-02	1.73	2.93e-02	2.11	2.45e-03	2.41	3.00
127464	0.11	1.19e-02	1.74	7.12e-03	2.04	5.39e-04	2.19	3.00
967624	0.05	2.85e-03	2.06	1.76e-03	2.01	1.32e-04	2.02	2.67
MINI Element–Lagrange								
334	0.87	2.56e+00	–	5.32e-01	–	7.79e-02	–	2.67
2028	0.43	1.45e+00	0.82	1.67e-01	1.68	2.23e-02	1.52	3.00
14320	0.22	4.93e-01	1.56	4.94e-02	1.75	1.41e-02	1.19	3.00
108120	0.11	1.96e-01	1.33	1.66e-02	1.57	5.92e-03	1.25	3.00
841384	0.05	9.15e-02	1.10	5.60e-03	1.57	1.76e-03	1.61	3.67
Crouzeix–Raviart–Lagrange								
490	0.87	7.64e-01	–	6.46e-01	–	7.52e-02	–	3.00
3352	0.43	4.05e-01	0.92	2.14e-01	1.59	3.07e-02	0.77	3.00
24844	0.22	2.15e-01	0.91	6.06e-02	1.82	1.74e-02	0.94	3.00
191380	0.11	1.04e-01	0.99	1.94e-02	1.64	8.94e-03	0.95	3.00
1502500	0.05	5.03e-01	0.99	7.43e-03	1.47	4.50e-03	0.96	3.67

Example 2: Verification of spatial convergence in 3D

We also test the implementation and the accuracy of the method in 3D. This constitutes Example 2, where we consider the exact solutions

$$\mathbf{u} = \begin{pmatrix} t \sin(\pi x) \cos(\pi y) \cos(\pi z) \\ -2t \cos(\pi x) \sin(\pi y) \cos(\pi z) \\ t \cos(\pi x) \cos(\pi y) \sin(\pi z) \end{pmatrix}, \quad p = t \sin(\pi x) \sin(\pi y) \sin(\pi z),$$

and $\boldsymbol{\omega} = \text{curl}(\mathbf{u})$, defined on the unit cube $\Omega = (0, 1)^3$, and now up to a time $T = 0.03$ and using a fixed time step $\Delta t = 0.01$. We also use different discretizations, but in all of them the discrete space \mathbf{H}_h^ω consists of overall continuous piecewise linear elements. For this case we have used the parameters $\alpha = 100$, $\nu = 0.01$, $F = 10$, $p = 4$ and tabulate the results in Table 6.6, which indicate an optimal convergence.

Table 6.7

Example 3. Error history with respect to time step refinement, computed up to the final time $T = 1$ using the parameters $\alpha = 1$, $\nu = 0.1$, $F = 1$, and $p = 4$.

Δt	$E_{\mathbf{u}}$	rate	E_{ω}	rate	E_p	rate	avg_it
0.5	2.82e-02	–	2.80e-02	–	2.80e-02	–	3.00
0.25	1.35e-02	1.06	1.34e-02	1.06	1.35e-02	1.05	3.00
0.125	6.62e-03	1.03	6.57e-03	1.03	6.63e-03	1.03	3.00
0.0625	3.28e-03	1.02	3.25e-03	1.02	3.28e-03	1.02	3.00
0.0312	1.63e-03	1.01	1.62e-03	1.01	1.63e-03	1.01	3.00
0.0156	8.15e-04	1.00	8.05e-04	1.00	8.20e-04	0.99	3.00

Example 3: Verification of temporal convergence

To close the verification of convergence, we conduct a test to illustrate the convergence in time. The time interval is subdivided, and instead of (6.1) we consider the following manufactured solutions

$$\mathbf{u} = \begin{pmatrix} \sin(t)xy \\ -\sin(t)(\frac{1}{2}y^2 + x) \end{pmatrix}, \quad p = \exp(-t)(x^4 - y^4),$$

and $\omega = \text{curl}(\mathbf{u})$. A fixed structured mesh of 40 elements per side is used to discretize the unit square, and the parameters are $\alpha = 1$, $\nu = 0.1$, $F = 1$, and $p = 4$. The time interval $(0, 1)$ is discretized into successively refined segments and the convergence history is displayed in Table 6.7. There we show the errors in the $\ell^2(0, T; V)$ norm (cf. (5.2)), denoted as

$$E_{\mathbf{u}} := \left(\sum_{n=1}^N \Delta t \|\mathbf{u} - \mathbf{u}_h^n\|_{\mathbf{H}^1(\Omega)}^2 \right)^{1/2}, \quad E_{\omega} := \left(\sum_{n=1}^N \Delta t \|\omega - \omega_h^n\|_{L^2(\Omega)}^2 \right)^{1/2}, \quad E_p := \left(\sum_{n=1}^N \Delta t \|p - p_h^n\|_{L^2(\Omega)}^2 \right)^{1/2},$$

and the corresponding rates of convergence are

$$r := \frac{\log(E_{(c)}/E'_{(c)})}{\log(\Delta t/[\Delta t]')},$$

where Δt and $[\Delta t]'$ denote two consecutive time steps with errors $E_{(c)}$ and $E'_{(c)}$, respectively. The expected linear convergence is observed for all fields. For this case it suffices to take $\kappa_2 = \kappa_1 = 0.05$ to achieve optimal convergence.

Example 4: Flow in fractured porous media

Next we focus on two problems of application relevance, where closed-form solutions are not available. We consider as computational domain a regularization of the upper-right quarter of the well-known five spot geometry (see, e.g., [34]), that is, $\Omega = (0, 1)^2 \setminus (B_{0.05}(0, 0) \cup B_{0.05}(1, 1))$, where $B_r(\mathbf{x}^c)$ denotes the ball of radius r centered at a given point $\mathbf{x}^c = (x^c, y^c)$. We generate a simple network of relatively large fractures and generate a relatively coarse unstructured mesh made of 16954 triangles. The bottom left circle arc is an inlet section (or injection well) Γ_{in} on which we impose a constantly increasing inflow velocity $\mathbf{u}_{\text{in}} = \frac{t\mathbf{x}}{4|\mathbf{x}|}$. On the walls we set no-slip velocity, and on the outlet Γ_{out} (the producer well, located at the top-right circle arc) we prescribe a zero traction condition. For this we use a condition on the pseudo-stress, as the formulation does not easily allow for exact stress reconstruction. More precisely, we set $\tilde{\sigma}\mathbf{n} = \mathbf{0}$ on Γ_{out} by imposing

$$\langle \tilde{\sigma}\mathbf{n}, \mathbf{v} \rangle_{\Gamma_{\text{out}}} = \langle \omega, \mathbf{v} \times \mathbf{n} \rangle_{\Gamma_{\text{out}}} + \langle p, \mathbf{v} \cdot \mathbf{n} \rangle_{\Gamma_{\text{out}}} = 0.$$

For this example the external force is zero, the Forchheimer exponent is $p = 3.2$, the viscosity is $\nu = 0.0001$, the final time is $T = 3$ and the fixed time step is $\Delta t = 0.2$. In order to illustrate the ability of the model to capture the Stokes and Darcy regimes, the Forchheimer and Darcy coefficients are taken heterogeneous in the following manner: On the bulk domain we use a normal random field $\eta(\mathbf{x})$ between -0.1 and 0.1 , and take case A

$$\alpha(\mathbf{x}) = \begin{cases} \alpha_{\max}(0.9 + \eta(\mathbf{x})) & \text{in the rock,} \\ \alpha_{\min} & \text{in the fractures,} \end{cases} \quad \mathbf{F}(\mathbf{x}) = \begin{cases} F_{\max}(0.9 + \eta(\mathbf{x})) & \text{in the rock,} \\ F_{\min} & \text{in the fractures,} \end{cases}$$

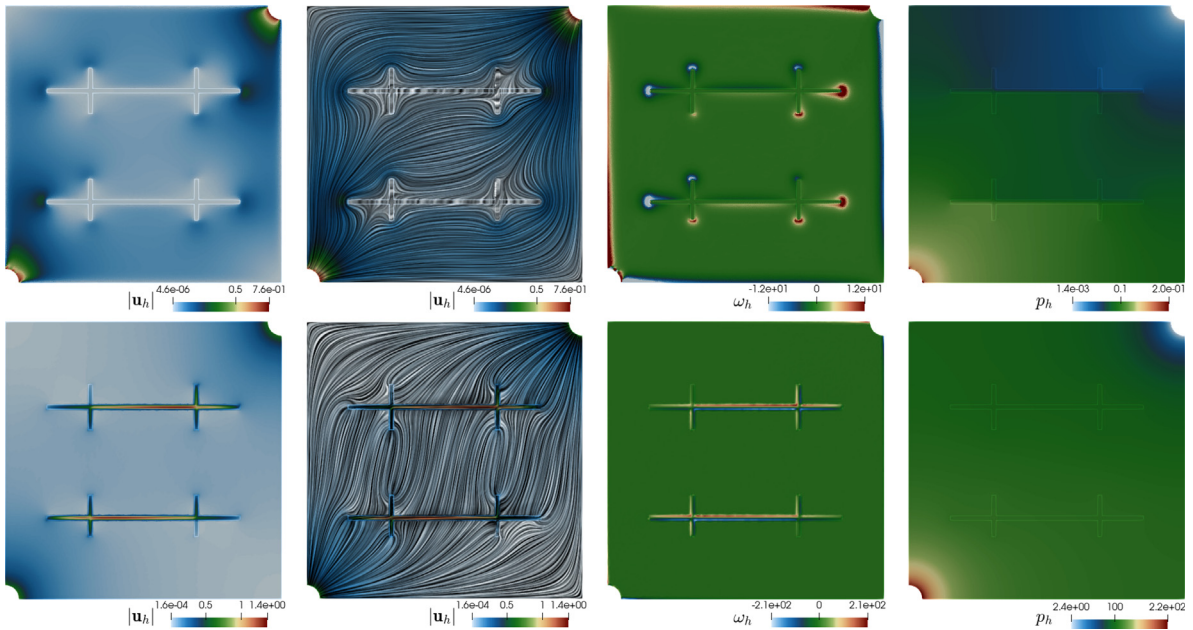


Fig. 6.2. Example 4. Samples at $t = 3$, of numerical solutions for the quarter five-spot filtration problem with embedded fractures. Velocity magnitude (left) velocity line integral convolution (center left), vorticity (center right) and pressure (right) for fractures much less permeable than rock (top row) and fractures much more permeable than rock (bottom).

and case B as

$$\alpha(\mathbf{x}) = \begin{cases} \alpha_{\min}(0.9 + \eta(\mathbf{x})) & \text{in the rock,} \\ \alpha_{\max} & \text{in the fractures,} \end{cases} \quad \mathbf{F}(\mathbf{x}) = \begin{cases} \mathbf{F}_{\min}(0.9 + \eta(\mathbf{x})) & \text{in the rock,} \\ \mathbf{F}_{\max} & \text{in the fractures.} \end{cases}$$

That is, case A has fractures that are much less permeable than the rest of the domain while case B follows the opposite arrangement. Here we have considered the constants $F_{\max} = 5000$, $F_{\min} = 1$, $\alpha_{\min} = 0.1$, $\alpha_{\max} = 500$. Note that we do not impose any transmission conditions as the same set of equations is solved on both subdomains defined simply by the discontinuous parameters indicated above. In Fig. 6.2 we show line convolution integrals of velocity, pressure, and vorticity profiles at the final time for both permeability distributions. A steep pressure gradient is observed near the injection wells in both cases. We also see from the different velocity and vorticity patterns in case B, that the flow avoids the region with lowest permeability. Both cases required almost the same average number of Newton–Raphson iterations (3.73 vs 3.86) to reach the prescribed tolerance of 10^{-7} .

Example 5: Lid-driven heterogeneous cubic cavity

Finally, we conduct a simulation of the 3D lid-driven cavity flow within an inhomogeneous unit cube $\Omega = (0, 1)^3$. On the top lid $z = 1$ we set the tangential velocity $\mathbf{u} = (1, 0, 0)$ whereas the remainder of the boundary has no-slip conditions. The fluid inside the cavity is initially at rest. With this configuration, high pressure gradients are expected to develop near the discontinuity of the Dirichlet data. We use a tetrahedral mesh of 82944 elements, a time step of $\Delta t = 0.05$ and run the test until $T = 1$. The velocity–pressure pair is approximated with the MINI element. The body force is $\mathbf{f} = \mathbf{0}$ and the model parameters are $\nu = 0.015$, $p = 4$, $\alpha = \{1 \text{ if } x \leq 0.5, \text{ or } 100 \text{ otherwise}\}$, and $\mathbf{F} = \{100 \text{ if } x \leq 0.5, \text{ or } 1 \text{ otherwise}\}$. The numerical results are represented in Fig. 6.3 showing velocity and vorticity streamlines. A large-scale recirculation influenced by the transfer of momentum from the top surface to the rest of the fluid is observed, but the usually expected symmetric flow structure (when projecting the solution into the xz plane) is disrupted by the discontinuity of the Darcy and Forchheimer numbers across the mid-plane $x = 0.5$.

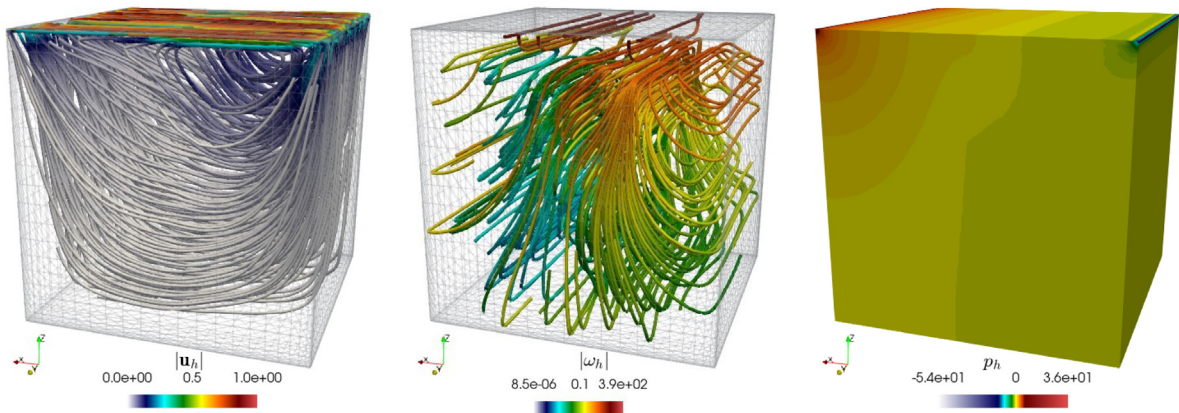


Fig. 6.3. Example 5. Samples of velocity streamlines (left), vorticity streamlines (center) and pressure distribution (right) at $T = 1$ for the lid-driven cavity test with discontinuous Darcy and Forchheimer coefficients.

Declaration of competing interest

The authors declare that they have no known competing financial interests or personal relationships that could have appeared to influence the work reported in this paper.

Data availability

No data was used for the research described in the article.

References

- [1] A.O. Celebi, V.K. Kalantarov, D. Ugurlu, On continuous dependence on coefficients of the Brinkman–Forchheimer equations, *Appl. Math. Lett.* 19 (2006) 801–807.
- [2] L.E. Payne, B. Straughan, Convergence and continuous dependence for the Brinkman–Forchheimer equations, *Stud. Appl. Math.* 102 (1999) 419–439.
- [3] M. Louaked, N. Seloula, S. Sun, S. Trabelsi, A pseudocompressibility method for the incompressible Brinkman–Forchheimer equations, *Differential Integral Equations* 28 (2015) 361–382.
- [4] M. Louaked, N. Seloula, S. Trabelsi, Approximation of the unsteady Brinkman–Forchheimer equations by the pressure stabilization method, *Numer. Methods Partial Differential Equations* 33 (2017) 1949–1965.
- [5] J. Kou, S. Sun, Y. Wu, A semi-analytic porosity evolution scheme for simulating wormhole propagation with the Darcy–Brinkman–Forchheimer model, *J. Comput. Appl. Math.* 348 (2019) 401–420.
- [6] S. Caucao, I. Yotov, A Banach space mixed formulation for the unsteady Brinkman–Forchheimer equations, *IMA J. Numer. Anal.* 41 (2021) 2708–2743.
- [7] S. Caucao, R. Oyarzúa, S. Villa-Fuentes, I. Yotov, A three-field Banach spaces-based mixed formulation for the unsteady Brinkman–Forchheimer equations, *Comput. Methods Appl. Mech. Engrg.* 394 (2022) 114895.
- [8] L. Zhao, M.F. Lam, E. Chung, A uniformly robust staggered DG method for the unsteady Darcy–Forchheimer–Brinkman problem, *Commun. Appl. Math. Comput.* 4 (2022) 205–226.
- [9] P.H. Cocquet, M. Rakotobe, D. Ramalingom, A. Bastide, Error analysis for the finite element approximation of the Darcy–Brinkman–Forchheimer model for porous media with mixed boundary conditions, *J. Comput. Appl. Math.* 381 (2021) e113008.
- [10] S. Caucao, G.N. Gatica, J.P. Ortega, A fully-mixed formulation in Banach spaces for the coupling of the steady Brinkman–Forchheimer and double-diffusion equations, *ESAIM Math. Model. Numer. Anal.* 55 (2021) 2725–2758.
- [11] V. Anaya, G.N. Gatica, D. Mora, R. Ruiz-Baier, An augmented velocity–vorticity–pressure formulation for the Brinkman equations, *Internat. J. Numer. Methods Fluids* 79 (2015) 109–137.
- [12] V. Anaya, R. Caraballo, B. Gómez-Vargas, D. Mora, R. Ruiz-Baier, Velocity–vorticity–pressure formulation for the Oseen problem with variable viscosity, *Calcolo* 58 (2021) e44(1–25).
- [13] M.O.L. Hansen, J.N. Sørensen, W.Z. Shen, Vorticity–velocity formulation of the 3D Navier–Stokes equations in cylindrical coordinates, *Internat. J. Numer. Methods Fluids* 41 (2003) 29–45.
- [14] C.G. Speziale, On the advantages of the vorticity–velocity formulations of the equations of fluid dynamics, *J. Comput. Phys.* 73 (1987) 476–480.
- [15] V. Anaya, B. Gómez-Vargas, D. Mora, R. Ruiz-Baier, Incorporating variable viscosity in vorticity-based formulations for Brinkman equations, *C. R. Math. Acad. Sci. Paris* 357 (2019) 552–560.

- [16] R.E. Showalter, *Monotone Operators in Banach Space and Nonlinear Partial Differential Equations*, in: *Mathematical Surveys and Monographs*, vol. 49, American Mathematical Society, Providence, RI, 1997.
- [17] A. Quarteroni, A. Valli, *Numerical Approximation of Partial Differential Equations*, in: *Springer Series in Computational Mathematics*, vol. 23, Springer-Verlag, Berlin, 1994.
- [18] J.K. Djoko, P.A. Razafimandimby, Analysis of the Brinkman–Forchheimer equations with slip boundary conditions, *Appl. Anal.* 93 (2014) 1477–1494.
- [19] V. Girault, P.A. Raviart, *Finite Element Methods for Navier–Stokes Equations. Theory and Algorithms*, in: *Springer Series in Computational Mathematics*, vol. 5, Springer-Verlag, Berlin, 1986.
- [20] S. Caucao, M. Discacciati, G.N. Gatica, R. Oyarzúa, A conforming mixed finite element method for the Navier–Stokes/Darcy–Forchheimer coupled problem, *ESAIM Math. Model. Numer. Anal.* 54 (2020) 1689–1723.
- [21] J.W. Barrett, W.B. Liu, Finite element approximation of the p-Laplacian, *Math. Comp.* 61 (1993) 523–537.
- [22] A. Ern, J.-L. Guermond, *Theory and Practice of Finite Elements*, in: *Applied Mathematical Sciences*, vol. 159, Springer-Verlag, New York, 2004.
- [23] D. Boffi, F. Brezzi, M. Fortin, *Mixed Finite Element Methods and Applications*, in: *Springer Series in Computational Mathematics*, vol. 44, Springer, Heidelberg, 2013.
- [24] F. Brezzi, M. Fortin, *Mixed and Hybrid Finite Element Methods*, in: *Springer Series in Computational Mathematics*, vol. 15, Springer-Verlag, New York, 1991.
- [25] C. Taylor, P. Hood, A numerical solution of the Navier–Stokes equations using the finite element technique, *Int. J. Comput. Fluids* 1 (1973) 73–100.
- [26] D. Boffi, Stability of higher order triangular Hood–Taylor methods for stationary Stokes equations, *Math. Models Methods Appl. Sci.* 4 (1994) 223–235.
- [27] M. Crouzeix, P.-A. Raviart, Conforming and nonconforming finite element methods for solving the stationary Stokes equations I, *Rev. Fr. Autom. Inform. Rech. Oper.* 7 (1973) 33–75.
- [28] C. Carstensen, S. Sauter, Crouzeix–Raviart triangular elements are inf-sup stable, *Math. Comp.* 91 (2022) 2041–2057.
- [29] G.N. Gatica, *A Simple Introduction to the Mixed Finite Element Method. Theory and Applications*, in: *Springer Briefs in Mathematics*, Springer, Cham, 2014.
- [30] M. Bukač, I. Yotov, P. Zunino, An operator splitting approach for the interaction between a fluid and a multilayered poroelastic structure, *Numer. Methods Partial Differential Equations* 31 (2015) 1054–1100.
- [31] M.S. Alnæs, J. Blechta, J. Hake, A. Johansson, B. Kehlet, A. Logg, C. Richardson, J. Ring, M.E. Rognes, G.N. Wells, The FEniCS project version 1.5, *Arch. Numer. Softw.* 3 (2015) 9–23.
- [32] F. Hecht, New development in FreeFem++, *J. Numer. Math.* 20 (2012) 251–265.
- [33] P.R. Amestoy, I.S. Duff, J.-Y. L’Excellent, Multifrontal parallel distributed symmetric and unsymmetric solvers, *Comput. Methods Appl. Mech. Engrg.* 184 (2000) 501–520.
- [34] K.B. Nakshatrala, K.R. Rajagopal, A numerical study of fluids with pressure-dependent viscosity flowing through a rigid porous medium, *Internat. J. Numer. Methods Fluids* 67 (2011) 342–368.